PRODUCTION AND CHARACTERIZATION OF BORON CONTAINING FLAME RETARDANT POLYAMIDE-6 AND POLYPROPYLENE COMPOSITES AND FIBERS

A THESIS SUBMITTED TO
THE GRADUATE SCHOOL OF NATURAL AND APPLIED SCIENCES
OF
MIDDLE EAST TECHNICAL UNIVERSITY

BY

MEHMET DOĞAN

IN PARTIAL FULFILLMENT OF THE REQUIREMENTS
FOR
THE DEGREE OF DOCTOR OF PHILOSOPHY
IN
POLYMER SCIENCE AND TECHNOLOGY

MAY 2011

Approval of the thesis:

PRODUCTION AND CHARACTERIZATION OF BORON CONTAINING FLAME RETARDANT POLYAMIDE-6 AND POLYPROPYLENE COMPOSITES AND FIBERS

submitted by **MEHMET DOĞAN** in partial fulfillment of the requirements for the degree of **Doctor of Philosophy in Polymer Science and Technology, Middle East Technical University** by,

Prof. Dr. Canan Özgen
Dean, Graduate School of **Natural and Applied Sciences**

Prof. Dr. Necati Özkan
Head of Department, **Polymer Science and Technology**

Prof. Dr. Erdal Bayramlı
Supervisor, **Chemistry Dept., METU**

Examining Committee Members:

Prof. Dr. Teoman Tinçer
Chemistry Dept., METU

Prof. Dr. Erdal Bayramlı
Chemistry Dept., METU

Prof. Dr. Göknur Bayram
Chemical Engineering Dept., METU

Prof. Dr. Ülkü Yılmazer
Chemical Engineering Dept., METU

Prof. Dr. Mehmet Saçak
Chemistry Dept., Ankara University

Date: May 25, 2011

I hereby declare that all information in this document has been obtained and presented in accordance with academic rules and ethical conduct. I also declare that, as required by these rules and conduct, I have fully cited and referenced all material and results that are not original to this work.

Name, Last name : Mehmet Doğan

Signature:

ABSTRACT

PRODUCTION AND CHARACTERIZATION OF BORON CONTAINING FLAME RETARDANT POLYAMIDE-6 AND POLYPROPYLENE COMPOSITES AND FIBERS

Doğan, Mehmet
Ph.D., Department of Polymer Science and Technology
Supervisor: Prof. Dr. Erdal Bayramlı

March 2011, 195 pages

The main objective of this study was to produce flame retardant polyamide-6 (PA-6) and polypropylene (PP) composites and fibers containing boron compounds. The synergistic effect on flame retardancy of boron compounds (boron silicon containing oligomer (BSi), zinc borate (ZnB), boron phosphate (BPO_4), metal oxide doped BPO_4 and lanthanum borate (LaB)) with conventional flame retardants were investigated. The synergistic effect of nano-clay with commercial flame retardants was also investigated in order to reduce the total amount of flame retardant that is essential for fiber applications. The UL-94, limiting oxygen index (LOI), differential scanning calorimeter (DSC), thermal gravimetric analysis (TGA), fourrier transform infrared spectroscopy (FTIR) and cone calorimeter tests were conducted on composite materials in order to investigate the effect of synergy agents on the flame retardant and thermal properties of conventional flame retardant containing PA-6 and PP composites.

According to the results from composite materials, boron compounds and clay showed synergistic effect with phosphorus based commercial flame retardants by acting generally with a condensed phase mechanism by increasing the char formation and/or by increasing the barrier effect of the final char residue.

Inspired from the previous studies, firstly, only nano-sized BPO_4 containing flame retardant fibers were produced and characterized. In the view of the results obtained from the composite trials, the boron compounds and organo clay were used with phosphorus based flame retardants to produce flame retardant fibers. The characterization of fiber samples were made with mechanical testing, melt flow index measurements (MFI), TGA, DSC, SEM and Micro Combustion Calorimeter (MCC) tests.

According to the results from fiber samples, the inclusion of BPO_4 reduced the peak heat release rate of the pure PA-6 and PP fiber. The reduction for PA-6 is higher than the PP fiber due to char forming character of PA-6. The usage of boron compounds and clay with phosphorus based flame retardants caused further reduction of peak heat release rate (PHRR) and total heat release values and increased the char formation. The amount of reduction of PHRR and total heat release (THR) is not so much due to the thermally thin character of fiber samples of nearly 40 microns. It is evident that a fabric made with these fibers will show better flame retardant behavior than single fiber tests due to its thick character with respect to the fiber samples.

Keywords: boron compounds, flame retardancy, nanocomposites, polypropylene, polyamide-6, fiber

ÖZ

BOR İÇEREN GÜÇ TUTUŞUR POLAMİD-6 VE POLİPROPİLEN KOMPOZİTLERİN VE LİFLERİN ÜRETİLMESİ VE KARAKTERİZASYONU

Doğan, Mehmet
Doktora, Polimer Bilimi ve Teknolojisi Bölümü
Tez Yöneticisi: Prof. Dr. Erdal Bayramlı

Mart 2011, 195 sayfa

Bu çalışmanın ana amacı borlu bileşik içeren güç tutuşur poliamid-6 (PA-6) ve polipropilen (PP) kompozitlerin ve liflerin üretilmesiydi. Borlu bileşiklerin (bor ve silicon içeren oligomer (BSi), çinkoborat (ZnB), borfosfat (BPO_4), metal doplanmış BPO_4 ve lantan borat (LaB)) geleneksel güç tutuşurluk maddeleriyle yanmazlık üzerine sinerjik etkileri incelenmiştir. Nano-kilin geleneksel güç tutuşurluk maddeleriyle olan sinerjik etkileri de lif uygulamalarında önemli olan güç tutuşurluk madde miktarını azaltmak için incelenmiştir. UL-94, sınırlayıcı oksijen indeksi (LOI), diferansiyel taramalı kalorimetre (DSC), termal gravimetrik analiz (TGA), fourier dönüşümlü kızılötesi spektrometre (FTIR) ve konik kalorimetre testleri sinerjik etki için kullanılan maddelerin ticari güç tutuşurluk maddesi içeren PA-6 ve PP kompozitlerin termal ve güç tutuşurluk özelliklerini incelemek için değişik şekillerdeki kompozit malzemelere uygulanmıştır.

Kompozit malzeme denemelerinden çıkarılan sonuçlara göre, borlu bileşikler ve kil, oluşan kül tabakasının koruyucu etkisini artırarak ve/veya külleşme miktarını artırarak kondens faz üzerinden etki göstererek, fosfor esaslı güç tutuşurluk maddeleri ile sinerjik etki göstermiştir.

Geçmişte yapılan çalışmalardan esinlenerek, ilk başta sadece nano boyuta sahip BPO_4 içeren lifler üretilmiş ve karakterize edilmiştir. Kompozit malzeme denemelerinden elde edilen sonuçların ışığında, borlu bileşikler ve kil, güç tutuşur lif üretmek için fosfor esaslı güç tutuşurluk maddeleriyle birlikte kullanılmıştır. Lif numunelerinin karakterizasyonu mekanik test, erime akış indeksi ölçümleri (MFI), TGA, DSC, SEM and Mikro Yanma Kalorimetre (MCC) testleri ile yapılmıştır.

Lif numunelerinden elde edilen sonuçlara göre, BPO_4 ilavesi saf PA-6 ve PP liflerinin maksimum ısıl salınım değerini (PHRR) düşürmüştür. PA-6'daki düşüş miktarı külleşme yeteneğinden dolayı PP'e göre daha yüksek olmuştur. Borlu bileşikler ve kilin fosfor esaslı güç tutuşurluk maddeleriyle kullanılması maksimum (PHRR) ve toplam ısıl salınım (THR) değerlerinin daha da düşmesine ve külleşme miktarının artmasına neden olmuştur. PHRR ve THR değerlerindeki düşme yaklaşık 40 micron kalınlığındaki liflerin termal olarak ince olmasından dolayı çok yüksek olmamıştır. Üretilen bu liflerden kumaş yapıldığında lif numunelerine göre daha kalın olduğundan daha iyi güç tutuşur özellik göstereceği aşikardır.

Anahtar Kelimeler: borlu bileşikler, güç tutuşurluk, nanokompozit, polipropilen, poliamid-6, lif

Dedicated to my family

ACKNOWLEDGEMENTS

I would like to express my deepest gratitude to my thesis supervisor Prof. Dr. Erdal Bayramlı for his guidance, understanding, kind support, encouraging advices, criticism, and valuable discussions throughout my thesis. His approach to the students and solving the problems will sure help me in my future academic life.

I am greatly indebted to Assoc. Prof. Dr. Ayşen Yılmaz and her students for synthesizing different boron phosphates and lanthanum borate and their characterization. I am very greatful to Prof. Dr. Cevdet Kaynak, Prof. Dr. Ülkü Yılmazer, Prof. Dr. Göknur Bayram and Prof. Dr. Teoman Tinçer for providing me every opportunity to use the instruments in their laboratories.

This study was supported by BOREN Institute with a project number of BOREN 2009 Ç0209. I express special thanks to BOREN employees, especially Poyraz Uzun for her help during the whole project. Thank you for the materialistic support of TÜBİTAK during my PhD studies.

I would also like to thank to Faculty Development Program (ÖYP) for the financial support during my thesis and Erciyes University for providing me the opportunity to work and stay at METU.

I express my special thanks to Nihat Ali Işıtman for conducting cone calorimeter studies and for all his help during my experiments. I would sincerely thank to Ali Sinan Dike and Selahattin Erdoğan for their endless friendship, support and help in all parts of my life, making my stay in METU happy and memorable and being always right beside me.

I would also like to thank to my friends Osman Yaşlıtaş, Ümit Tayfun, Güralp Özkoç, Yasin Kanbur, Yasemin Altun, and Serdal Kaya for cooperation and friendship, and helping me in all the possible ways.

This thesis could not be written without the patience, support and understanding of my wife Ş. Dilem Doğan. I express my sincerest love and thanks to her for contributions in every single step of this study. Last but not the least; I wish to express my sincere thanks to my family for supporting, encouraging, and loving me all through my life.

TABLE OF CONTENTS

CHAPTERS

LIST OF TABLES

TABLES

LIST OF FIGURES

FIGURES

ABBREVIATIONS

AlPi	Aluminium diethyl phosphinate
APP	Ammoniumpolyphosphate
ASTM	American Society for Testing and Materials
BSi	Boron and Silicon Containing Oligomer
BPO_4	Boron Phosphate
DSC	Differential Scanning Calorimeter
FTIR	Fourier Transform Infrared Spectroscopy
GPC	Gel Permeation Chromatography
HRR	Heat Release Rate
IFR	Intumescent Flame Retardant
ISO	International Organization for Standardization
LaB	Lanthanum borate
m-APP	Surface Modified APP
MC	Melamine Cyanurate
MCC	Micro Combustion Calorimeter
MFI	Melt Flow Index
MLR	Mass Loss Rate
PA-6	Polyamide-6
PER	Pentaerythritol
PHRR	Peak Heat Release Rate
PP	Polypropylene
PP-g-Ma	Polypropylene grafted maleic anhydride
P-red	Red Phosphorus
SEM	Scanning Electron Microscopy
SAXS	Small Angle X-ray Scattering

TEM	Transmission Electron Microscopy
TGA	Thermal Gravimetric Analysis
THE	Total Heat Evolved
TML	Total Mass Loss
TOF	Time of Combustion
UL-94	Underwriters laboratory UL-94 test
XRD	X-ray Diffraction
WAXS	Wide Angle X-ray Scattering
ZnB	Zinc Borate
ZnPi	Zinc bis-diethyl phosphinate

CHAPTER 1

INTRODUCTION

Turkey has the largest and highest quality reserves and is the second largest producer of boron after the USA. Boron compounds found a lot of usage from the manufacture of starch additives, ceramics, paints, soaps and detergents, fiber glass, flame proofing, gasoline additives to the production of fuel cells. To find new application areas and to increase the amount of usage of boron compounds is very important in terms of the economical and the strategical benefit of Turkey. In this study, both commercial and newly synthesized boron compounds were used as flame retardant agents with conventional flame retardants to improve the flame retardant properties of composite materials. This point is important to increase the usage of boron compounds. Secondly boron compounds were used for the first time in the production of flame retardant fibers. This point is important to find new application areas for boron compounds.

A flame retardant polymeric or textile material means that it does not continue to burn or glow once the source of ignition has been removed, although there are some changes in the physical and chemical characteristics. The need for flame retardant polymeric materials increased in the last years due to the increase of the usage of plastic materials in our daily life, not only in bulk parts but also as films, fibers, coatings and foams. The regulations made by developed countries, especially by European countries, also increased the need for flame retardant polymeric materials in new application areas.

A flame retardant polymeric material can be obtained using different methods or approaches. A flame retardant co-monomer is used during polymerization and the synthesized polymer itself gains inherent flame retardant property. This is called “reactive approach”. Flame retardant additives can be added into polymer melt during mixing. This is called “additive approach”. Flame retardant polymeric materials can also be obtained by surface modification i.e. by grafting flame retardant substances. This is called “surface approach”. Reactive, additive and surface approaches can be applied both to polymers and textiles. The last approach is the flame retardant finishing which is widely used for obtaining flame retardant textiles. In this study, the flame retardant composites and fibers were produced by additive approach.

In additive approach, flame retardants are incorporated in polymer either prior to, during or more frequently, following polymerization. This approach is widely used for the production of flame retardant thermoplastic materials used in bulk form. Numerous commercial flame retardant additives are available for polymers. They can be classified as halogen, phosphorus, nitrogen, silicon, boron containing flame retardants and miscellaneous inorganic additives. Although the halogenated compounds are known as the most effective flame retardants for polymers, they have limited usage because of the toxic nature of their combustion products and their effect on the ozone layer. In this study, phosphorus, nitrogen, silicon and boron containing flame retardants are used instead of halogenated ones.

Fiber specialists have tried to produce flame retardant fiber by additive approach for years since the fiber production by additive approach is likely to be cheaper and has higher wash fastness than conventionally produced flame retarded textile articles. To produce a flame retardant fiber, higher amounts of flame retardants are needed than composites of the same matrix material due to its thin character with high surface area. The total amount of flame retardant must be below 15 wt % to minimize its adverse effect on fiber textile properties. For these reasons, the nanotechnology and synergy between different flame retardants gain importance for the production of flame retardant fibers. Generally, nanoparticles (layered silicates, carbon nanotubes, polyhedral oligomeric silsesquioxanes), boron compounds and metal oxides are used with conventional flame retardants for their synergistic effect. If a synergy is found among different flame retardants, less flame retardant additive can be used to obtain the same flame retardant effect.

Polyamide-6 (PA-6) and polypropylene (PP) are widely used polymers for their excellent properties in a variety of forms such as fiber, film and composite. To widen their application areas, the flammability of these polymers must be increased. The main objective of this study was to produce flame retardant PA-6 and PP fiber containing boron compounds by melt spinning method. The synergistic effect of clay with conventional flame retardants were also investigated in order to reduce the total amount of flame retardant which is an important parameter for fiber applications. Initially in this study, the synergistic effect of boron compounds and clay with conventional flame retardants were investigated as a composite material with various dimensions depending on the test made. In the view of the test results obtained from the composite materials, formulations were chosen for the production of flame retardant PA-6 and PP fibers.

Melamine, Melamine Cyanurate (MC), red phosphorus and organic phosphinates were used as main flame retardant agents for PA-6 composites. Ammonium polyphosphate (APP) / pentaerythritol (PER) combination and surface modified APP (m-APP) were used as main flame retardant agents for PP composites. Boron silicon containing oligomer (BSi), zinc borate (ZnB), boron phosphate (BPO_4), metal oxide doped BPO_4 and lanthanum borate (LaB) were used as boron compounds. Two different commercial layered silicates, namely, Cloisite 30B and Cloisite 15A were used for their synergistic effect. The former was used with PA-6, the latter was used with PP. The dispersion of clay platelets were characterized with the X-ray diffraction method (XRD).

The characterization of the composite materials was made with UL-94, Limiting Oxygen Index (LOI), Differential Scanning Calorimeter (DSC), Thermal Gravimetric Analysis (TGA), Fourier Transform Infrared Spectroscopy (FTIR) and Cone Calorimeter tests in order to investigate the effect of synergy agents on the flame retardancy and thermal properties of conventional flame retardant containing PA-6 and PP composites. The characterization of fiber samples was made with mechanical testing, melt flow index measurements (MFI), TGA, SEM, DSC, and Micro Combustion Calorimeter (MCC) tests.

CHAPTER 2

BACKGROUND INFORMATION

2.1 Boron Minerals in Turkey and in the World

Boron ores in Turkey are among the most important mineral sources. These minerals are called tincal, kernite, colemanite, ulexite and probertite. Turkey is the second largest producer of boron minerals after the USA. Eight percent of boron minerals produced are used domestically, and 92 % are exported. Turkey has the largest and highest quality reserves, ranking first in the world [1, 2].

Boron minerals contain different amounts of B_2O_3 in their structures. The important factor for industrial application of boron minerals is B_2O_3 content and boron deposits in Turkey are rich in B_2O_3. Three major boron mineral in Turkey are colemanite, ulexite-probertite and tincal ores [1].

Boron compounds are used in the manufacture of starch additives, ceramics, paints, soaps and detergents, fiber glass, flame proofing, gasoline additives, electrolytic condensers, glass, nuclear reactor control rods, photographic chemicals and porcelain enamels. Boron compounds are also used in fungus control, herbicides and agriculture. In agriculture usage, boron compounds have been generally used as essential micronutrients for all plants. In construction and cement, they are used for strength and insulation purposes. In detergents and soaps, they are used for various purposes, for example, they act as a Ph buffer. Boron compounds are also considered as the most promising candidates among the metal hydrates for the safe storage of hydrogen which is an impediment to the commercial use of hydrogen as fuel in fuel cells [1, 2]

2.2 The Definition of Flame Retardant Polymeric Materials

The terms flame resistant, flame retardant, fire retardant and fire resistant are all similar terms and can be used interchangeably. The terms “flammable” and “nonflammable” are rarely used by fire researchers as regards to polymer based compounds. A polymeric material that is flame or fire resistant does not continue to burn or glow once the source of ignition has been removed, although there are some changes in the physical and chemical characteristics. An ideal flame retardant polymeric material must have some special characteristics; high resistance to ignition and flame propagation, a low rate of combustion and smoke generation, low combustibility and toxicity of combustion gases, acceptability in appearance and properties for specific uses and little or no economic penalty [3-5].

2.3 The Need for Flame Retardant Polymeric Materials

The need for flame retardant polymeric materials increases in the last years due to the increase of the usage of plastic materials in our daily life, not only in bulk parts but also as films, fibers, coatings and foams. The regulations made by developed countries, especially by European countries, also increased the need for flame retardant polymeric materials in new areas [3, 4].

2.4 General Concepts of Polymer Combustion

Polymers are the long-chain molecules that constitute most of our environment, both natural and synthetic. The combustion of polymeric materials, like the combustion of any other fuel material, is a combination of complex physical and chemical processes, which include the transformation of initial products. This whole conversion process may be divided into stages, with specific physical and chemical processes occurring in each of these stages [6]. There are four individual stages involving polymer flammability; heating of flammable substrate (pre-heating), degradation and decomposition, the ignition of flammable gases evolved and combustion and propagation. Four individual stages involved in polymer flammability are shown in Figure 2.1 [7].

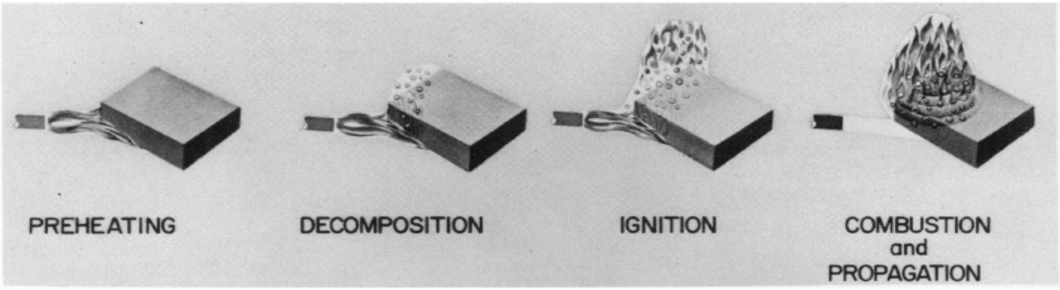

Figure 2.1 Four individual stages involved polymer flammability [6]

Preheating involves heating of the material by means of an external source which raises the temperature of the material at a rate dependent upon the thermal intensity of the ignition source, thermal conductivity of the material, specific heat of the material and latent heat of fusion and vaporization of the material. When sufficiently heated, the material begins to degrade and it loses its original properties as the weakest bonds begin to break. Gaseous combustion products may be formed that depend on such factors as intensity of external heat, temperature required for decomposition and rate of decomposition. By the effect of ignition source (heat, flame and etc.), the gaseous products can be ignited and combustion starts. Ignitability depends on how quickly the surface can be raised to the ignition temperature. If the heat evolved is larger than the heat consumed during combustion, combustion propagates when the heat source is removed [7, 8].

2.5 Strategies for Obtaining Flame Retardant Polymers and Textiles

The flame retardation of a polymeric material is normally developed on the basis of information regarding; chemical and physical properties of a polymer, phases of polymer degradation, combustion of the polymer and chemical and physical properties of flame retardant compositions and their interactions with polymeric substance [8]. In order to understand which flame retardant strategy will be chosen to obtain flame retardant polymeric material, degradation mechanism of the polymer must be known. Four general mechanisms which are random chain scission, end chain scission, chain stripping and crosslinking are important pathways for the thermal decomposition of polymers [9].

2.5.1 Thermal Behavior of Polypropylene

Polypropylene (PP) is easily flammable and burns in air with a very hot and clean flame by dripping without giving any char residue. The flammable nature of PP is understandable because of its saturated long chain hydrocarbon structure which is responsible for the excellent physical, chemical and electrical properties [4, 8, 10]. PP yields low molecular weight volatile fuel fragments that undergo free radical and oxidation reactions in the pre-ignition zone and flame zone. PP pyrolizes at relatively high temperature and the pyrolsis temperature of PP depends critically on the oxygen concentration [4, 8, 10]. Thermal properties of i-PP are given in Table 2.1 [10,11].

2.5.2 Thermal Behavior of Polyamide-6

Polyamide-6 (PA-6) softens and melts prior to thermal degradation. It burns slowly, drips and may self-extinguish due to extensive shrinkage and dripping during combustion. First and second order transitions, Tm and Tg, and the percent crystallinity of PA-6 are contributing factors to thermal stabilization of PA-6. A high degree of crystallinity will decrease the rate of oxygen diffusion through the polymer and thus show an improved thermal-oxidative stability [4, 11, 12]. The main degradation products of PA-6 are water, carbondioxide, carbonmonoxide, methanol, formaldehyde, ammonia, acetaldehyde and numerous other aliphatic and aromatic hydrocarbons [12]. Thermal properties of PA-6 are given in Table 2.1 [10, 11].

Table 2.1 Thermal properties of i-PP and PA-6 [10, 11]

POLYMER	**Tg (°C)**	**Tm (°C)**	**Tp (°C)**	**Tc (°C)**	**LOI**	**Cp (cal/g°C)**	**K (cal/sec.cm^2)**
PA-6	50	215	431	450	20-22	0.38	6.0
i-PP	-20	165	470	550	17-18	0.46	2.8

2.5.3 General Approaches to Obtain Flame Retardancy in Polymers and Textiles

A flame retardant polymeric article can be obtained during polymerization by using flame retardant co-monomers. This is called reactive approach. Flame retardant additive can be added into the polymer. This is called additive approach. Flame retardant polymeric articles can also be obtained by surface modification by grafting flame retardant substances. This is called surface approach. Reactive, additive and surface approaches can be applied both to polymers and textiles. The last approach is the flame retardant finishing which is widely used to obtain flame retardant textiles. The schematic representation of these approaches is shown in Figure 2.2 [13].

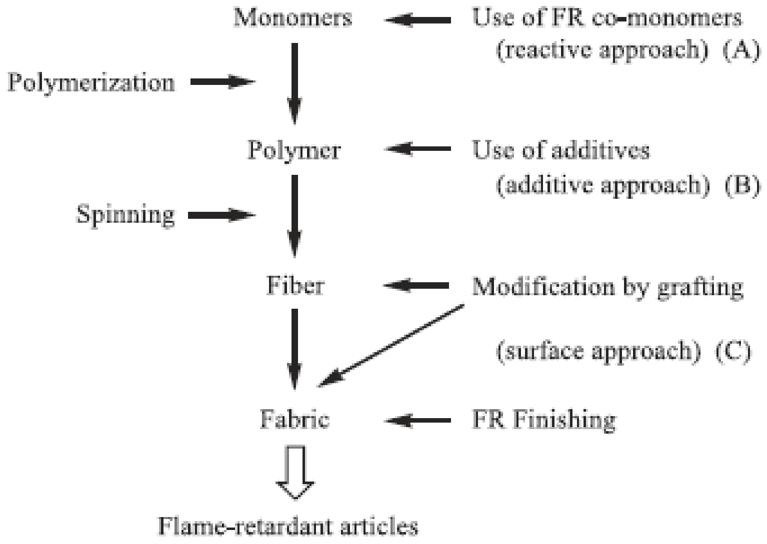

Figure 2.2 Schematic representation of general flame retardancy approaches [13]

Although additive approach is widely used for the production of flame retardant polymeric composites, it is not preferred for flame retardant textile (fiber) production. Detailed information is given about additive approach and why it is not preferred for the production of flame retardant fibers. A modified form of this approach is used to obtain both flame retardant polymer composites and textile fibers throughout this study.

2.6 Additive Approach

In this approach, flame retardants are incorporated in polymer either prior to, during or more frequently, following polymerization. They are used especially in thermoplastics. If they are compatible with the polymer they act as plasticizer, otherwise they can be considered as fillers. They are sometimes volatile and tend to bleed so their flame retardancy may be gradually lost. The development of high molecular weight products enables polymers to be made permanently fire retardant by the additive method. Additive type flame retardants are generally incorporated by compounding and are useful in variety of polymer systems [6].

2.6.1 Advantages and Drawbacks of Additive Approach for Fiber Production

Fiber specialists have tried to produce flame retardant fiber by additive approach for years. It is an economical method to incorporate flame retardant substance in molten polymer before fiber spinning. The produced fiber is cheaper and has higher wash fastness than conventionally produced flame retarded textile articles. An acceptable flame retardant filler for fiber production is hard to find. It should be thermally stable up to the processing temperature. Most of the phosphorus, metal and halogen additives are not stable at fiber spinning temperature. It should be compatible with polymer and have no leaching and migratory properties. The additive should retain its flame retardant properties when present in the fiber. It should be present at a relatively low level (typically less than 15 % w/w) to minimize its effect on fiber textile properties as well as cost. Recent applications of nanotechnology opened a new opportunity for the production of both flame retardant fiber and polymer composites. Detailed information about nanocomposites and its benefits on flame retardant properties of fibers and polymer composites are given in further sections [9-11, 14-16].

2. 7 Flame Retardant Additives

A wide range of flame retardant materials have been developed for polymers, around 150 to 200 different compounds being commercially available. Flame retardants can be classified as additive or reactive compounds. Additive compounds are mixed into polymer during processing, but do not chemically react with polymer. Reactive compounds are polymerized with a resin during processing to become integrated into the molecular network structure. In this study, all flame retardants used are in the class of additive compounds so detailed information is given about additive compounds [17]. Flame retardant additives can be classified as halogen, phosphorus, nitrogen, silicon, and boron containing flame retardants and miscellaneous inorganic additives [6, 12, 17, 18]. Phosphorus, nitrogen, silicon and boron containing flame retardants are used in this study. Accordingly, information is given only about these flame retardants in the following sections.

2.7.1 General Mechanism of Flame Retardant Additives

Flame retardant additives differ from each other in terms of chemical structure and certain general mechanisms of action. All flame retardants act chemically and/or physically in the condensed phase and/or in the gas phase by interfering with at least one of the individual stages of burning process [18-19]. Normally an efficient flame retardant additive will affect more than one of these steps either in physical or in chemical way. The end result in the presence of flame retardant additive is the retardation and final elimination of burning process mechanism [8].

Gas phase active flame retardants act through scavenging free radicals responsible for the branching of radical chain reactions in the flame. This is the chemical action mechanism in the gas phase. Some of the flame retardants produce large amounts of noncombustible gases that dilute the combustible gases, decompose endothermically, and decrease the temperature by absorbing heat. This is the physical action mechanism in the gas phase [9, 19].

In condensed phase mechanism, flame retardant additives act in two different modes of action. First, flame retardants accelerate the degradation of polymer and increase the dripping of the polymer. By increasing the dripping behavior of the polymer, fuel source is removed from the combustion zone. Second, flame retardants can leave a layer of carbon (charring) on the polymer surface [19]. The formed intumescent char acts as a physical barrier to reduce the heat and mass (fuel, oxygen) transfer between the gas and condensed phases so it protects the underlying material from the effect of flame. The amount and the properties (integrity, stability and foam structure) of the char determine the flame retarding effect of an intumescent system. The major advantage of this system is the decrease in the heat generated during the combustion due to the formation of carbon rather than formation of CO and CO_2 [20-23]. The schematic representation of general mechanisms of flame retardant additives is given in Figure 2.3 [24].

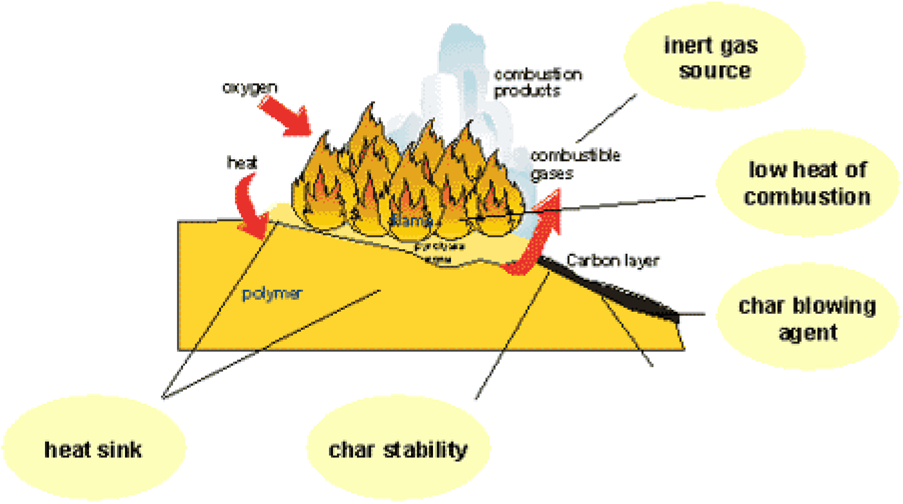

Figure 2.3 General mechanisms of flame retardant additives [24].

When individual stages of burning process are considered, in the initial heating stage the presence of an effective flame retardant can result by the formation of a glassy layer. This coating is of low thermal conductivity and/or high reflectivity which enables to repel radiant heat from the external source before extensive decomposition of the substrate. Additives that swell on heating to yield an intumescent coating are examples of flame retardants yielding a surface layer with poor thermal conductivity [8, 19].

During the degradation and decomposition stages of the burning process, the flame retardant additive can chemically alter the thermo-oxidative decomposition of the flammable substrate. The desired result would be a lower concentration of combustible gases. This can be accomplished by promoting char formation, by hydrogenation or by dehydration, thus limiting the production of combustible hydrocarbon gases [8].

In the ignition stage of burning process, the candidate additive can be effective in a number of ways. Basically, any mechanism that tends to increase the concentration of noncombustible decomposition gases or decreases the production of combustible gases moieties will result in inhibiting the burning process at the ignition process. Besides these routes the flame retardant agent may also produce, by its own degradation or interaction with the substrate, free radical terminating species. These gaseous inhibitors reduce the flame speed by their interaction with the highly energetic chain-propagating species, such as OH radicals. An additive can also produce a very dense gas that can blanket the surface of the flammable substrate and exclude oxygen needed for the ignition process [8].

Even after the ignition of the substrate has occurred, the combustion and the propagation stages of the burning process can be inhibited by decreasing the heat transfer rate at the surface of the burning substrate. One notable way of achieving this would be from a flame retardant additive that on decomposing generates particulate matter in the pre-flame zone. These smoke particles provide a surface that attenuates the radiative thermal energy from the flame zone [8].

2.7.2 Synergism and Antagonism of Flame Retardant Additives

The term synergism is defined as an effect greater than the addition of individual effects. Antagonism can be unequivocal if two flame retardants, each producing a positive result when used separately, produce, when added together, a result less than the result which would have been obtained from either one alone at the same total concentration [4].

The studies made on flame retardancy, generally, focused on finding synergy among different flame retardants. Generally, nanoparticles (clay, carbon nanotubes, polyhedral oligomeric silsesquioxanes), boron compounds and metal oxides are used with conventional flame retardants for their synergistic effect. If a synergy is found among different flame retardants, less flame retardant additive can be used to obtain same flame retardant effect. For this reason, to find synergy between different flame retardant additives is also important for the production of flame retardant fibers by additive approach [4, 10]. There are numerous synergisms seen among different flame retardants such as antimony- halogen, nitrogen- halogen, phosphorus- phosphorus, nitrogen- phosphorus, silicon- phosphorus, boron- phosphorus, etc. [4]. While a substance can show synergistic effect with a flame retardant additive, the same substance can show antagonistic effect with different flame retardant additives. Isıtman et al. showed that the inclusion of nanoclay into PA-6 in the presence of phosphorus containing flame retardant shows synergistic effect by increasing the barrier effect of intumescent char [25]. Kiliaris et al. showed that the inclusion nanoclay into PA-6 in the presence of nitrogen containing flame retardants shows antagonistic effect by hindering the dripping behavior of PA-6 [26].

2.8 Types of Flame Retardant Additives

2.8.1 Nitrogen Containing Flame Retardants

Nitrogen containing flame retardants are considered as environmentally friendly because they are less toxic, do not add additional elements to those already present in the polymer and are suitable for recycling [6, 18]. The most important type of nitrogen containing flame retardants are melamine and its derivates. Melamine and melamine cyanurate (MC) are widely used with unfilled polyamides. Melamine phosphate and melamine polyphosphate are used with polyolefins. Melamine and its derivates show their flame retardant effect by acting both in condensed and gas phase [6, 12, 18]. In this study, melamine and MC are used with PA-6 for their flame retarding effect.

2.8.1.1 Melamine Cyanurate

MC which is a salt of melamine and cyanuric acid is used primarily with unfilled polyamides. The molecular structure of MC is shown in Figure 2.4 [27]. Above 320 °C, it undergoes endothermic decomposition to melamine and cyanuric acid and acts as a heat sink during the burning process [6, 11, 12, 18, 28]. Cyanuric acid which strongly contributes to the degradation and dripping of polyamides causes the drips to be smaller and extinguish when they reach the cotton. The vaporized melamine acts as an inert gas and dilutes the oxygen and the fuel gases present at the point of combustion. Further degradation of melamine into ammonia and thermally stable condensates absorbs the generated heat and cools the substrate [9, 26, 28, 29].

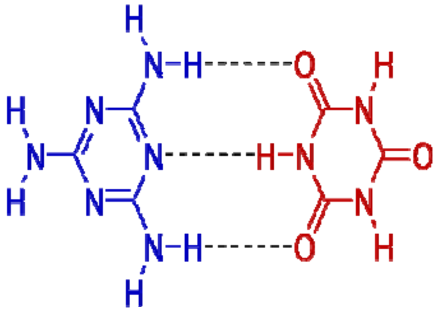

Figure 2.4 Molecular structure of melamine cyanurate [27].

2.8.1.2 Melamine

Melamine, a white crystalline solid, has a melting point of approximately 350 ºC [6]. The molecular structure of melamine is shown in Figure 2.5 [30]. Melamine has three effects on the individual stages of burning process. At its melting point, melamine is known to vaporize or sublime rather than go through a traditional melting phase change. During sublimation, it absorbs significant amount of heat (1965 kJ/mole), thus acting as a heat sink during burning process. The vaporized melamine also acts as an inert gas and dilutes the oxygen and the fuel gases present at the point of combustion.

Melamine destabilizes the PA-6 and increases the dripping behavior of polymer so fuel source is removed from combustion zone [6, 9, 12, 31].

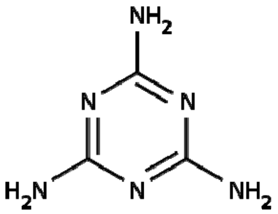

Figure 2.5 Molecular structure of melamine [30].

2.8.2 Phosphorus Containing Flame Retardants

Phosphorus containing flame retardants are the second most widely used flame retardant additives for thermoplastics, thermosets, textiles, paper and coatings [4, 9]. Phosphorus is found in both organic and inorganic materials which have flame retardant properties [19]. The range of phosphorus containing flame retardants that exist in several oxidation states are extremely wide. Phosphines, phosphine oxides, phosphonium compounds, phosphonates, elemental red phosphorus, phosphites and phosphates are all used as flame retardants [18].

The flame retardant mechanism of phosphorus containing flame retardants depends on the type of phosphorus compound and the chemical structure of the polymer. They are more effective in oxygen or nitrogen containing polymers [9]. They can function both in the condensed phase and gas phase [4]. It is believed to perform most of its flame retardant function in the condensed phase mechanism [10, 12, 18].

Phosphorus compounds show the flame retarding effect in the condensed phase, such as the following: (1) They may redirect the chemical reactions involved in decomposition in favor of reactions yielding carbon rather than CO or CO_2, and the end result is the promotion of char formation. (2) Phosphoric and related acids act as a heat sink since they retard the oxidation of carbon monooxide to carbon dioxide; this will decrease the heating process. (3) The acids may form a thin glassy or liquid protective coating on the condensed phase, thus lowering the oxygen diffusion and heat and mass transfer between the gas and the condensed phase. This barrier disturbs the oxidation process of carbon at the carbon monoxide stage, thus reducing the exothermic heat of combustion. (4) They may reduce the melt viscosity to favor a melt drip mode of flame extinction [6, 10, 12, 18].

Phosphorus compounds also show the flame retarding effect in the gas phase, such as the following; (1) They form reactive phosphorus based species such as $PO^{\cdot}$, $P^{\cdot}$, PO_2, $HPO^{\cdot}$, $HPO_2^{\cdot}$ which are capable of reacting with the free radicals that can drive combustion [19]. Volatile phosphorus compounds are the most effective inhibitors of combustion [9]. The proposed radical trap theory is shown in Figure 2.6 [4]. (2) They may dilute the combustible pyrolysates by a less combustible vapor [10].

$$H_3PO_4 \longrightarrow HPO_2 + HPO + PO$$

$$H + PO \longrightarrow HPO$$

$$H + HPO \longrightarrow H_2 + PO$$

$$OH + PO \longrightarrow HPO + H_2O$$

$$OH + H_2 + PO \longrightarrow HPO + H_2O$$

Figure 2.6 The proposed radical trap theory of phosphorus compounds [4].

In this study, red phosphorus, organic phosphinates and ammonium polyphosphate are used as flame retardant additives. The detailed information is given about these additives.

2.8.2.1 Red Phosphorus

The term red phosphorus (P-red) is used for describing one of the allotropic forms of phosphorus, a largely amorphous inorganic polymer described as a complex three dimensional polymer [32]. The chemical structure of P-red is shown in Figure 2.7 [33].

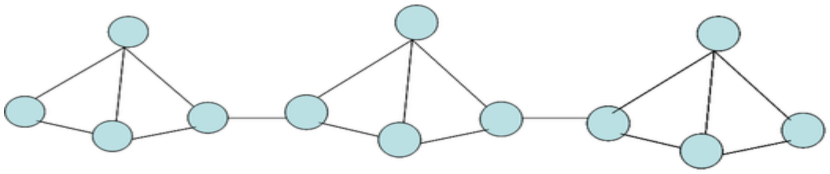

Figure 2.7 Chemical structure of P-red [33].

P-red that is the most concentrated source of phosphorus for flame retardancy has been known as a highly effective flame retardant for many polymers, especially nitrogen and/or oxygen containing ones [4, 9]. P-red shows relatively weak flame retarding effect in polyolefins and polystyrene. P-red is an effective flame retardant additive at a concentration ranging from 2-15 wt% based on the polymer [4, 9]. Table 2.2 shows the concentration of P-red required for V0 rating for UL-94 testing for different polymers [4].

Table 2.2 The concentration of P-red required for V0 rating for UL-94 testing for different polymers [4].

POLYMER	% wt
Polystyrene	15
Polyethylene	10
Polyamide	7
Filled phenolic	3
Polycarbonate	1
Polyethylene terephthalate	3

P-red has some advantages and drawbacks in practical usage. The advantages include high phosphorus content, low cost and good flame retardant properties at lower percentages [32, 34]. Nonetheless, P-red has several drawbacks including thermal instability (forms highly toxic phosphine gas), strong moisture absorption and reddish brown color, thus restricting extensive commercial applications [4, 9, 12, 29, 32, 34]. To reduce the drawbacks of P-red, it needs surface treatments including inorganic and polymeric coating or microencapsulation. Various thermosetting resins such as epoxy, melamine formaldehyde, urea formaldehyde and phenol formaldehyde resins are preferred to encapsulate P-red [4, 12, 29, 32, 34, 35].

The flame retardant mechanism of P-red is not completely understood. The mechanism is believed to be through the formation of phosphoric acid, although some evidence also suggests free radical scavenging. P-red shows its flame retarding action in condensed phase in PA-6. P-red reacts with PA-6 and phosphoric esters are formed [4, 9, 35- 37]. Zinc borate, zinc oxide and iron oxide help to retard the corrosive effect of phosphine and may also enhance the flame retarding action [29, 38, 39].

2.8.2.2 Organic Phosphinates

Organic phosphinates are a novel class of phosphorus flame retardants for engineering thermoplastics, especially for polyamides and polyesters [40, 41]. They are commercialized as metal salts of phosphinates. Aluminium diethylphosphinate (AlPi) and Zinc bis-diethylphosphinate (ZnPi) are the most widely used ones for polyamides and polyesters, respectively. The molecular structures of AlPi and ZnPi are shown in Figure 2.8 [42].

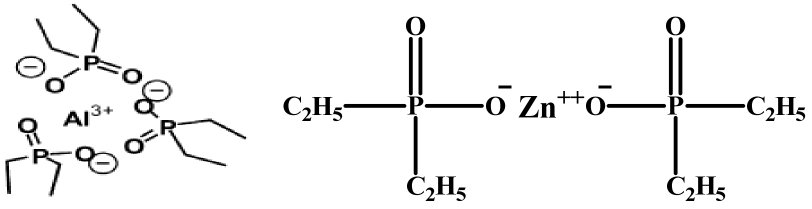

Figure 2.8 The molecular structures of AlPi and ZnPi [42].

Although the usage of these flame retardants increases, there must be much more mechanistic study to be made for better understanding of their fire retardant mechanisms with different kinds of polymers. Like other phosphorus compounds, it is believed that organic phosphinates show their flame retarding effect through the condensed and gas phase mechanism. The previous studies showed that the predominant mechanism changes with the type of polymer and synergy agents. Braun et al. showed that the flame retardant mechanism of AlPi in poly(1,4-butylene terephthalate) is not clear and both condensed and predominantly gas phase mechanism of AlPi was observed [42]. Braun et al, Laachachi et al. and Isıtman et al. showed that the flame retardant mechanism of AlPi in polyamide 6,6, poly(methyl methacrylate) and PA-6 is based on predominantly condensed phase mechanism, respectively [25, 43, 44]. Previous studies showed that although organic phosphinates show strong flame retardant activity on their own, they show synergism with different substances such as; melamine cyanurate, melamine phosphate, metal oxides, zinc borate, polyhedral oligomeric silsesquioxanes (POSS) and nanoclay [25, 42-47].

2.8.2.3 Ammonium Polyphosphate

Ammonium polyphosphate (APP), an inorganic salt of polyphosphoric acid and ammonia, is commonly used as flame retardant in polymers, especially with polyolefins. APP also found application area to obtain flame retardant textiles [48, 49]. APP has two main crystal types; crystal phases I and II. Phase I is characterized by a variable linear chain length, showing a lower decomposition temperature and higher water solubility than phase II. Phase II which has crosslinked and branched structure is more preferred for flame retardant activities [19]. The molecular structure of APP is shown in Figure 2.9 [50]. APP shows its flame retardant effect in condensed phase by the formation of intumescent char. For better understanding of flame retardant effect of APP, the detailed information is given about the intumescent system and how APP forms intumescent char.

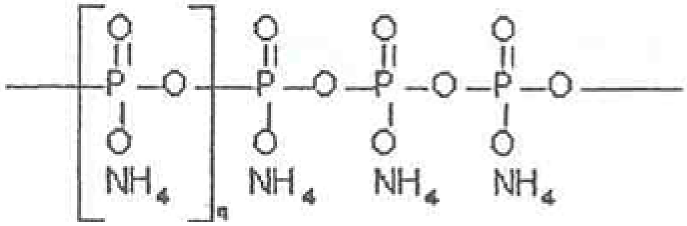

Figure 2.9 The molecular structure of APP [50].

Intumescent system was reported in literature in 1938. Intumescent system protects the underlying material by the formation of highly porous, thick and thermally stable char layer [17]. This layer acts as a physical barrier to reduce the heat and mass (fuel, oxygen) transfer between the gas and condensed phases so it protects the polymer from the effect of flame. The amount and the properties (integrity, stability and foam structure) of the char determine the flame retardant effect of an intumescent system. The major advantage of this system is the decrease in the heat generated during the combustion due to the formation of carbon rather than formation of CO and CO_2 [20-23]. The flame retardant effect of intumescent char is shown in Figure 2.10 [51].

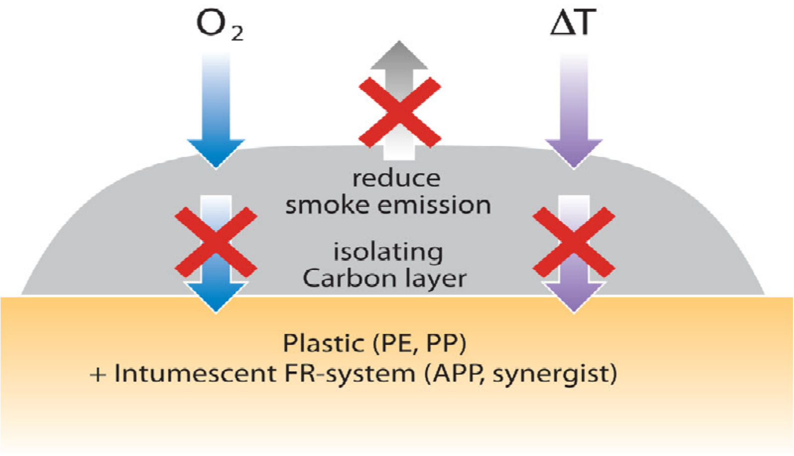

Figure 2.10 The flame retardant effect of intumescent char [51].

An intumescent system is commonly composed of three components which are an acid source, a char forming agent (carbonific) and a blowing agent (spumific). By a series of decomposition reactions and physical processes of these compounds, intumescent char is formed [17, 52]. The sequence of intumescent reaction processes is shown in Figure 2.11 [17].

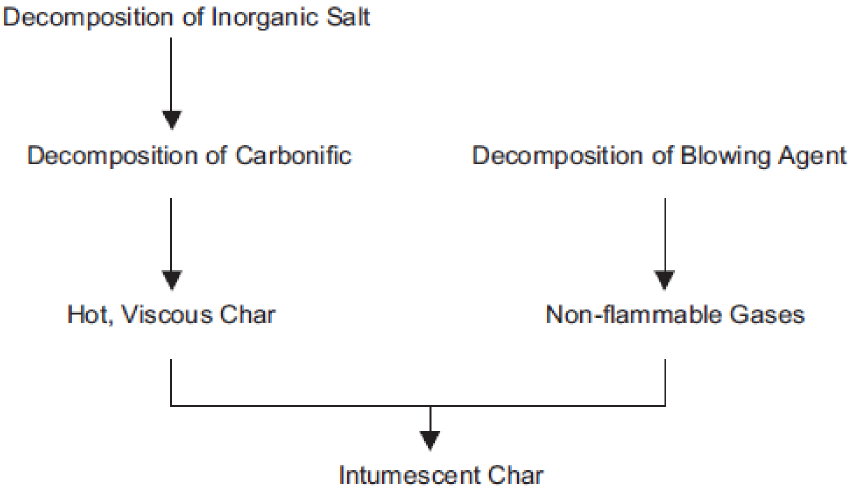

Figure 2.11 The sequence of intumescent reaction processes [17].

In the case of APP, it acts both as an acid source and blowing agent during combustion. The thermal degradation of APP gives polyphosphoric acid, orthophosphates, phosphoric acid, ammonia and water [20-23, 52-55]. The schematic representation of the thermal degradation of APP is shown in Figure 2.12 [4].

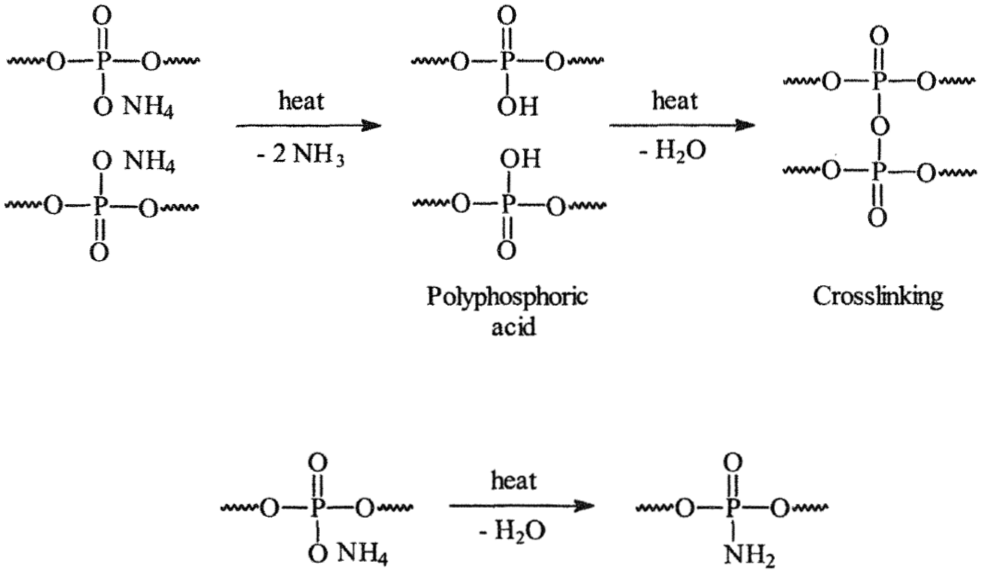

Figure 2.12 The schematic representation of thermal degradation of APP [4].

Polyphosphoric acid, phosphoric acid and orthophosphates acting as an acid source undergo esterification reaction with carbonizing agent. Ammonia and water act as blowing source. In order to increase the barrier effect of intumescent char, different blowing agents can be used with APP. Generally, nitrogen containing compounds such as; urea, dicyandiamide, melamine and polyamides are used as blowing agent [52-55]. Starch, dextrins, sorbitol, mannitol, pentaerythritol (PER) and char former polymers can be used as carbonizing agent. APP and PER combination is widely used with PP as intumescent flame retardant [52-59]. The schematic representation of esterification reaction between APP and PER is shown in Figure 2.13 [4]. Newly developed APPs are coated with the carbonizing source with reduced water solubility. The esterification reaction takes place between coating material and APP. Previous studies showed that these systems are much more effective than the APP/PER combination [21, 60, 61].

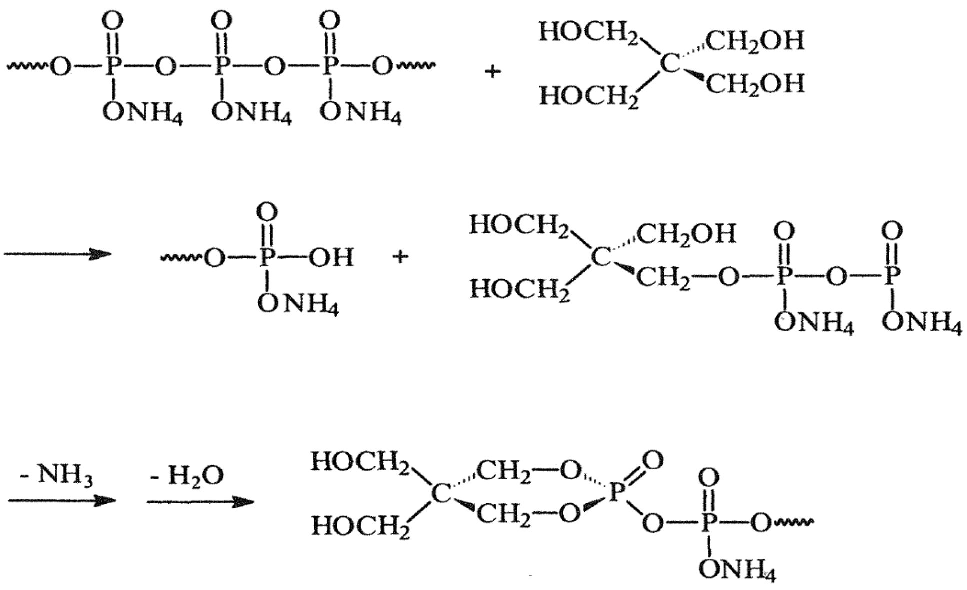

Figure 2.13 The schematic representation of esterification reaction between APP and PER [4]

The addition of nitrogen, metal, silicon and boron containing substances shows synergistic effect with intumescent flame retardant (IFR) and increases the limiting oxygen index value of PP composites [61-72].

2.8.3 Boron Containing Flame Retardants

Numerous boron compounds are used for their flame retarding effect and synergistic effect to obtain flame retardant textiles and plastics. Water soluble boron compounds, borax and boric acid, are widely used with cellulosic materials (paper, wood, cotton, etc.). On the other hand, water insoluble and thermally more stable boron compounds are used to obtain flame retardant plastic materials [6, 9, 18, 73-75]. Reactive boron compounds also find application area to obtain flame retardant thermosetting polymers [76-79]. Table 2.3 shows the widely used boron containing flame retardants and their application areas [73].

Table 2.3 The widely used boron containing flame retardants and their application areas [73].

Chemical Name	Applications
Borax pentahydrate	Wood/cellulose/cotton, coating
Borax decahydrate	Wood/cellulose
Boric acid	Wood/cellulose/cotton, polymer, coating
Boric oxide	Engineering plastics
Calcium borate	Rubber modified roofing membrane
Zinc borate	Polymer, elastomers, coating, sealants
Ammonium pentaborate	Epoxy, urethane, coating
Melamine diborate	Epoxy intumescent coating, cotton fabric
Boron phosphate	PPE/Polyamide, PPE/HIPS, PO

The boron containing flame retardants used with polymers act generally in the condensed phase by redirecting the decomposition process in favor of carbon formation rather than CO and CO_2 and by the formation of protective char on the burning surface which prevents the oxidation of carbon by limiting the accessible oxygen. In both cases a char is formed [6, 9, 73].

2.8.3.1 Zinc Borates

Zinc borate (ZnB) is an inorganic fire retardant with different chemical compositions of $xZnO.yB_2O_3.zH_2O$. The major commercially used ZnBs are given in Table 2.4 [73]. The molecular structure of $2ZnO.3B_2O_3.3.5H_2O$ is shown in Figure 2.14 [73]. ZnB functions as smoke suppressant, afterglow suppressant and anti-arcing agent in addition to its flame retardant effect. In halogen free flame retardant systems, ZnB reduces the rate of heat release and promotes char formation by the catalytic effect of Zn atom and the formation of B_2O_3 glassy layer which hinders the thermo oxidative degradation of carboneous char [73].

Table 2.4 The major commercially used ZnBs [73].

Formula	Dehydration Temperature
$2ZnO.3B_2O_3.7H_2O$	170
$2ZnO.3B_2O_3.3H_2O$	200
$2ZnO.3B_2O_3.3.5H_2O$	290
$2ZnO.3B_2O_3$	None
$4ZnO.B_2O_3.H_2O$	>415

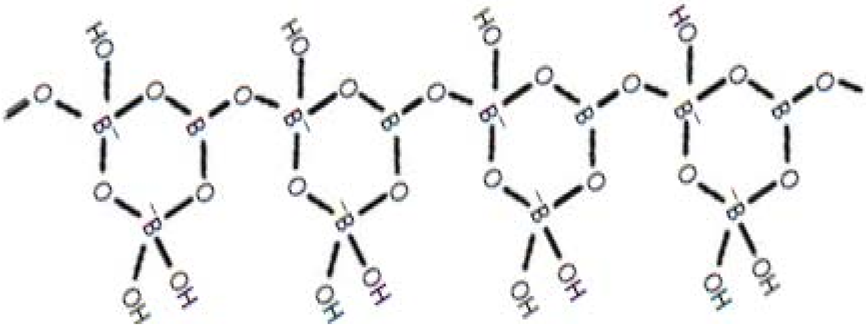

Figure 2. 14 The molecular structure of $2ZnO.3B_2O_3.3.5H_2O$ [73]

2.8.3.2 Boron Phosphate

Boron phosphate (BPO_4) is an inorganic polymer that consists of boron, phosphate and oxygen atoms. The chemical structure of BPO_4 is given in Figure 2.15 [73]. BPO_4 can be synthesized by dry, wet and microwave techniques. In this study, BPO_4 is synthesized by using microwave technique. In this technique, boric acid and diammonium phosphate are taken in stoichiometric ratios and urea is used to initiate the reaction. The reactants are mixed in a ceramic crucible and are placed in microwave. The BPO_4 produced is ground and put into oven to remove the residual urea [80-83]. BPO_4 shows its flame retarding effect in the condensed phase by increasing the char yield and reinforcing the char. Kılınç et al. also showed that BPO_4 has flame retarding effect in the gas phase by increasing the CO_2 formation [83].

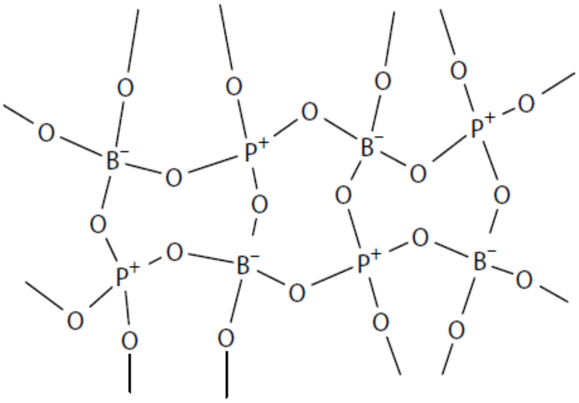

Figure 2. 15 The chemical structure of BPO_4

2.8.4 Silicon Containing Flame Retardants

Many types of silicon containing compounds have been used as potential flame retardants with polymers. Silicones, silanes, silsesquioxane, silica, and silicates are widely used silicon based materials for their flame retarding and synergistic effect. Their flame retardant effect changed with the type of polymer and the flame retardant used [4, 10, 14, 18, 73]. Previous studies showed that the inclusion of small amount of silicon compounds can significantly improve the flame retardancy by both char forming in the condensed phase and the trapping of active radicals in the gas phase [4, 10, 14, 18, 73, 84-86]. In this study, organo modified silicates are used for their synergistic effect. Detailed information about the flame retardant effect of organo modified silicates is given in nanocomposites section.

2.9 Nanocomposites

Nanocomposites are a new class of composites that are particle filled polymers in which at least one dimension of the dispersed particles in the nanometer range [87]. Nanocomposites have several advantages such as improved mechanical properties, barrier properties, thermal stability, flame retardancy and processability when compared to conventional composites. Different types of fillers can be used to produce polymer nanocomposites and they can be classified into three groups according to their particle shapes [87, 91]. The particle shapes of fillers are given in Figure 2.16 [90]. The first group including nano calcium carbonate, silica beads and nano zinc borate is isodimensional nanoparticles in which three dimensions are in the order of nanometers. When two dimensions of the particles are in the nanometer scale and the third dimension is larger, the structure is an elongated structure and includes carbon nanotubes, titanium nanotube and cellulose whiskers. The third group including polymer layered silicates is characterized by only one dimension in the nanometer range [87, 91].

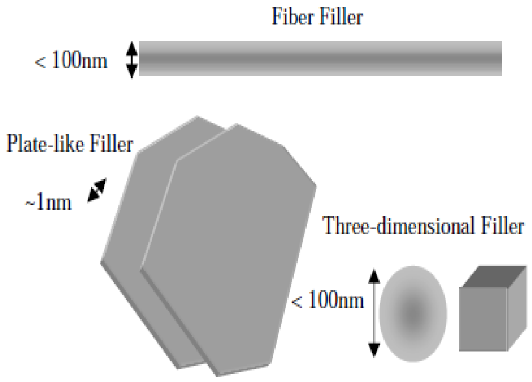

Figure 2.16 The different shapes of nanoparticles

In this study, layered silicates are used as nanoparticules so the detailed information is given about layered silicates and polymer layered silicate nanocomposites.

2.9.1 Layered Silicates

Montmorillonite, hectorite and saponite are the most commonly used layered silicates. Layered silicates have two different structural units. The simplest structure is the 1:1 structure (e.g. in kaolinite) where a silica tetrahedral sheet is fused to an aluminum octahedron, sharing the oxygen atoms. 2:1 phyllosilicates (e.g. montmorillonite) are the second type of layered silicates commonly used for the preparation of nanocomposites. Their crystal structure consists of stacked layers made of two silica tetrahedrons fused to an edge- shared octahedral sheet of alumina. The layer thickness of the crystal structure is around 1 nm, and the lateral dimensions of these layers may be in the range of 30 nm to several microns or larger [87-92]. The structure of layered silicates is shown in Figure 2.17 [73].

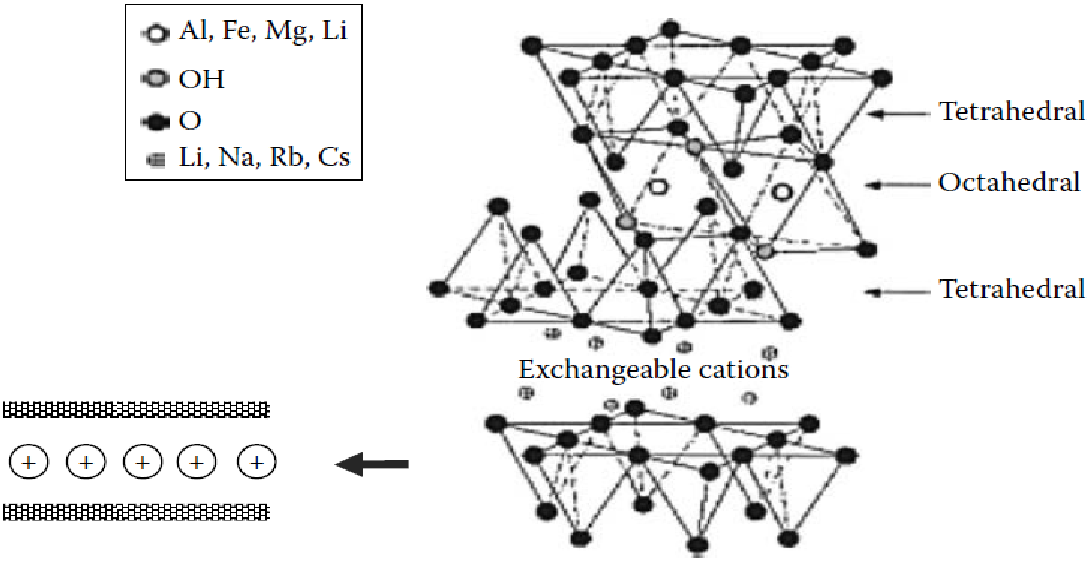

Figure 2.17 The structure of layered silicates [73].

The silicate layers are separated by a regular van der Waals gap called the interlayer or the gallery. Isomorphic substitution within the layers generates negative charges that are generally counterbalanced by sodium and calcium cations. The negative charge gives clays highly hydrophilic nature. The hydrophilic nature of clay and the narrow distance between the silicate layers limit their usage for obtaining nanocomposite structures with different polymers, especially hydrophobic ones. In order to reduce the hydrophilic character of clay and to increase the interlayer spacing between silicates layers, hydrated cations of the interlayer can be exchanged with cationic surfactants such as alkylammonium or alkylphosphonium (onium) [87-93]. This process is schematically illustrated in Figure 2.18 [93].

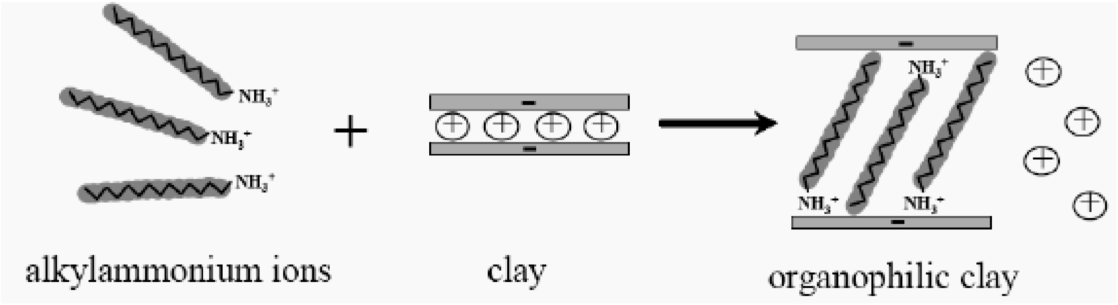

Figure 2.18 The cation-exchange process [93].

Three different methods used for preparing polymer layered silicate nanocomposites are; In-Situ Intercalative Polymerization Method, Solution Intercalation Method and Melt Intercalation Method [87-93]. In this study, melt intercalation method is used for obtaining nanocomposite structure. Detailed information is given about only the melt intercalation method.

2.9.2 Melt Intercalation Method

During melt intercalation method, the layered silicate and the polymer are mixed in the molten state. During mixing, the polymer chains can diffuse into the clay galleries and either an intercalated or an exfoliated nanocomposite structure is formed. The schematic representation of melt intercalation method is shown in Figure 2.19 [93].

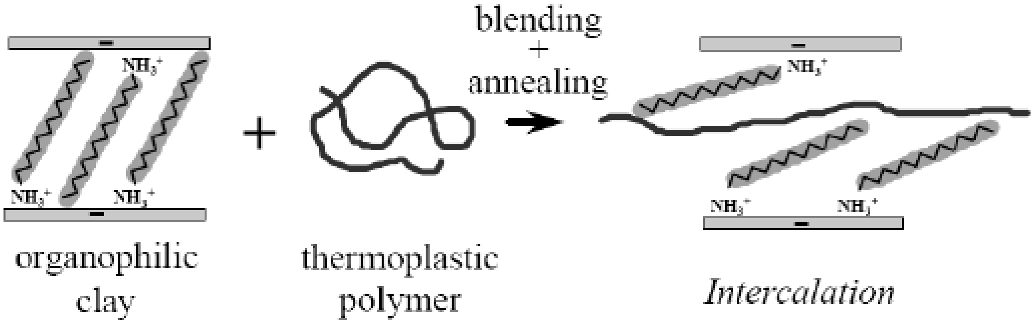

Figure 2.19 The schematic representation of melt intercalation method [93].

By melt intercalation method, three different types of nano-composite structures which are conventional, intercalated and exfoliated can be obtained. If the silicate layers are not separated, conventional structure is obtained. If the polymer chains swell the galleries of the silicate layers but preserve the stacking of layers, intercalated structure is obtained. If the silicates are completely and uniformly dispersed in the continuous polymer matrix, exfoliated structure is obtained [87- 93]. The schematic representation of three different types of nanocomposite structure is shown in Figure 2.20 [87]. The entropic and enthalphic factors determine the state of dispersion. Dispersion of organoclay in a polymer matrix requires favorable enthalphic contributions to overcome any entropic penalties. Favorable enthalpy of mixing for the polymer and layered silicates is achieved when the polymer layered silicate interactions are more favorable compared to the surfactant-layered silicate interactions [87-93]. For most polar polymers like PA-6, an alkyl ammonium surfactant is adequate to offer sufficient excess enthalpy and promotes the nanocomposite formation [88, 94]. For apolar polymers like PP, an alkyl ammonium surfactant is not sufficient to obtain nanocomposite structure (intercalated or exfoliated). In the case of PP, the polymeric compatibilizers such as maleic anhydride grafted PP must be used to favor the enthalpic contributions [88].

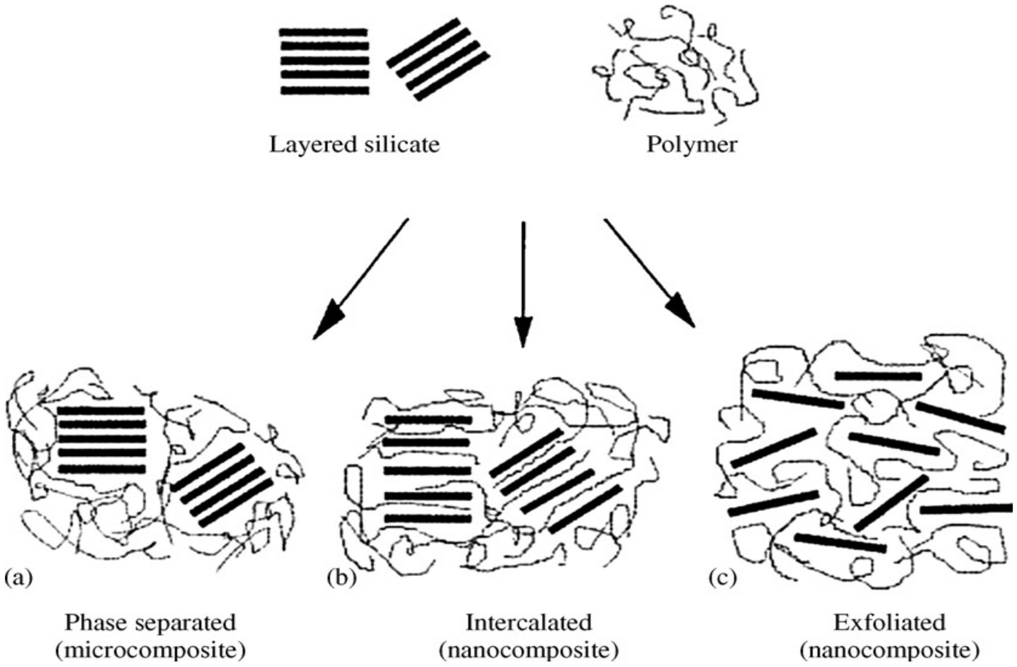

Figure 2.20 The schematic representation of three different types of nanocomposite structure [87].

The state of dispersion in nanocomposites can be determined by Transmission Electron Microscopy (TEM) and X Ray Diffraction (XRD) Methods. In this study, only the XRD method is used for understanding the state of dispersion. The detailed information is only given about XRD method.

2.9.3 X Ray Diffraction Method

XRD is one of the two primary tools to characterize the structure or morphology of nanocomposites. Wide Angle X-ray Scattering (WAXS) and Small Angle X-ray Scattering (SAXS) are two kinds of typically used XRD, but the use of WAXS is much more common. WAXS is usually used to determine the d-spacing of the clay layers less than 6-8 nm, while SAXS is used to obtain the d-spacing larger than this, which WAXS is unable to detect. However, WAXS is enough in most cases to determine if intercalation has occurred [73]. The principle of XRD method is shown in Figure 2.21

[95]. The structure of the nanocomposites can be understood from Bragg's equation ($n\lambda = 2d \sin\theta$), where, n is the degree of diffraction, λ is the wavelength, θ is the measured diffraction angle, and d refers to the interlayer spacing [95]. From Bragg's equation, the *d*-spacing of clay platelets can be found. When an intercalated structure is obtained, *d*-spacing increases from the value in the virgin organically-modified clay to some larger value. When an exfoliated structure is obtained, the registry between the clay layers is lost and no peak should be observed in XRD. In some cases, disorderness of clay leads to the absence of a peak. The smaller *d*-spacing value with respect to that of the virgin organically-modified clay is the indication of the silicate layer collapse [17].

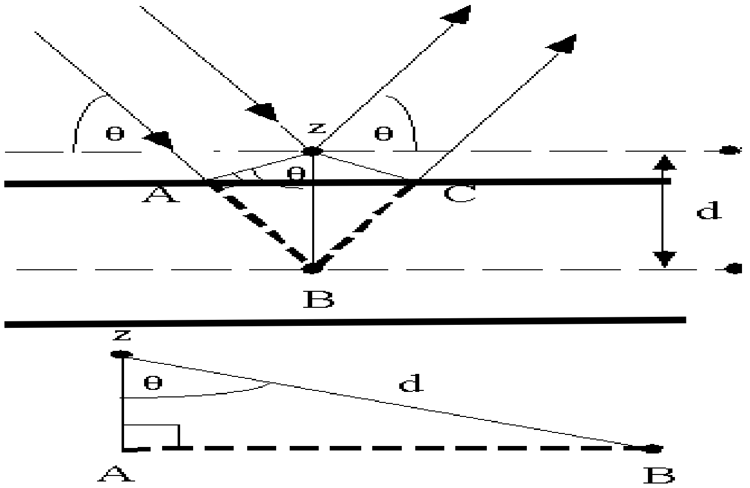

Figure 2.21 The principles of XRD method [95].

2.9.4 Fire Retardancy of Polymer/ Layered Silicate Nanocomposites

The most significant effect of the addition of layered silicates in polymers by the formation of nanocomposites structure (intercalated and exfoliated) is the reduction of peak heat release rate (PHRR) with respect to neat polymer matrix [92, 96-106]. In addition to the reduction of PHRR, the layered silicates increase the thermal stability and the char formation in a variety of polymers [97, 107-111]. Besides the aforementioned advantages of layered silicates on flame retardancy, total heat release rate (THR), time to ignition (TTI), UL-94, Limiting Oxygen Index (LOI) are not influenced much by the presence of layered silicates [9, 105, 106, 113]. Accordingly, recent publications focused on the synergistic effect of layered silicates with conventional flame retardants [9, 58, 72, 84 100, 114-117].

Previous studies showed that the formation of multilayered carbonaceous-silicate layer, a combination of physical and chemical processes, is the most important reason for the reduction of PHRR. Demixing, silicate phase formation, charring, migration and bubbles of decomposition products favor the formation of multilayered carbonaceous-silicate layer on the burning surface [87, 88, 96, 103, 118-123]. The schematic view of the migration of the layered silicates is shown in Figure 2.22 [73]. This layer acts as a barrier for mass and heat transport and slows down the escape of the flammable volatiles generated during combustion. By the barrier effect of carbonaceous-silicate layer, the heat release rate of flammable fuel is reduced but the total amount of fuel source does not change, so the combustion continues until almost all the carbon mass has been pyrolized and combusted. Accordingly, although the average HRR and PHRR decrease significantly by the formation of carbonaceous-silicate layer, THR is not influenced much [9, 105,106]. TTI is not influenced much or worsened by the presence of layered silicates due to the release of volatiles evolved by the decomposition of the organic modifier (e.g. alkyl ammonium surfactant) [99, 124-127].

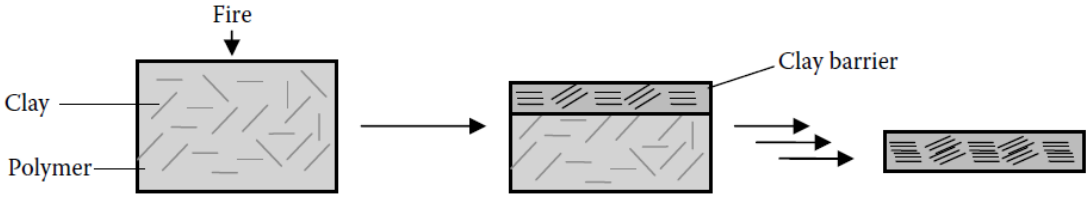

Figure 2.22 The schematic view of the migration of the layered silicates during burning [73].

Layered silicates also increase the char formation of polymers. Vaia et al. and Zanetti et al. showed that the layered silicates promote char formation of PA-6 and PP [97, 107]. Previous studies proposed different reasons for the increase in char yield. (1) The acid sites formed on silicates due to the degradation of organic moieties make catalytic effect on crosslinking and charring reactions. (2) Bronsted and Lewis acid sites present on the clay lattice catalyze the char formation. (3) Layered silicates provide a confined, superheated environment where the trapped decomposing polymer chains obtain the opportunity to undergo additional intermolecular reactions leading to the formation of complex compounds (Cage Effect) [97, 107-111].

The last proposed mechanism of layered silicates is the gas phase mechanism by radical scavenging due to the adsorption of radical species to the Lewis acid sites of the silicates. All proposed flame retardant mechanisms of layered silicates are shown in Figure 2.23 [99].

The flame retardant effect of nanocomposites is related with the sample thickness. When the composites gets thinner, the flame retardant behavior of nanocomposites gets poorer due to the competition between the formation of a surface carbonaceous silicate layer and the volatilization of fuel. In thin composites, volatilization is favored [103]. Although fiber scientists made numerous studies in order to produce nanocomposite fibers with reduced flammability, they observed only a small reduction of PHRR and average HRR. During the last years, scientists focused on the usage of nanoparticles with conventional flame retardants for their synergistic effect to produce flame retardant fiber. In that way, the total amount of flame retardant is reduced and desirable textile properties can be obtained [15, 16, 128-137].

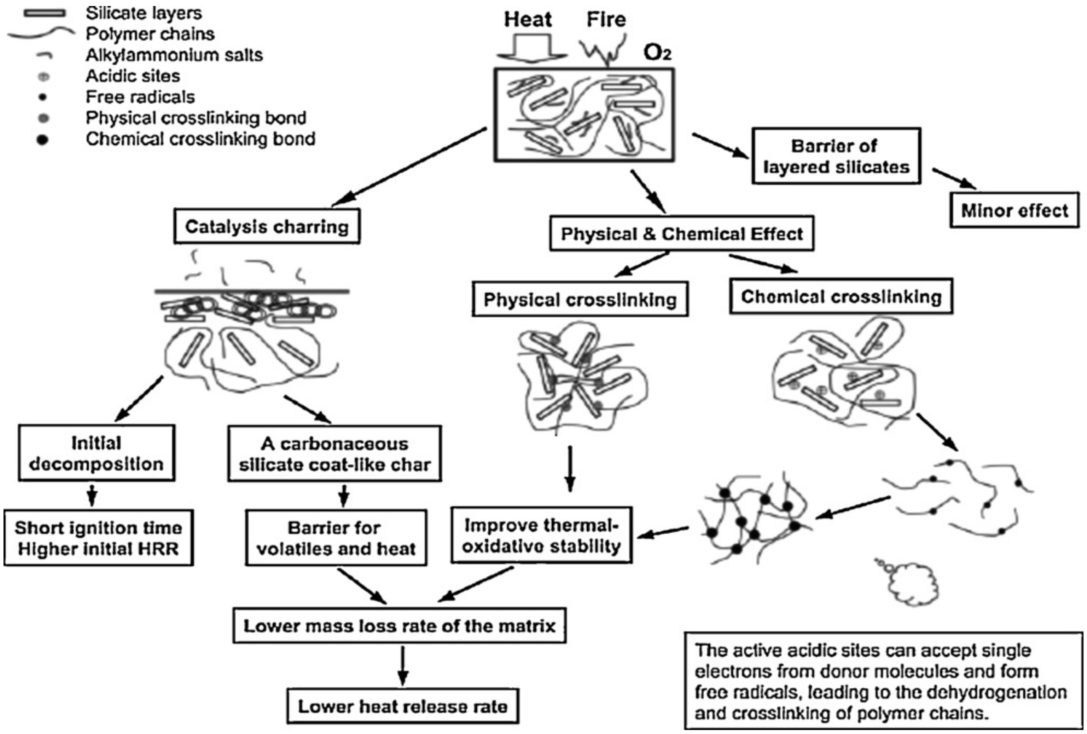

Figure 2.23 Proposed flame retardant mechanisms of layered silicates [99].

2.10 Characterization Methods

Numerous test methods are used for evaluating the fire retardant and thermal properties of polymers and textiles. In this study, Underwriters Laboratory UL 94 Test (UL-94), Limiting Oxygen Index (LOI), Thermal Gravimetric Analysis (TGA), Differential Scanning Calorimeter (DSC) and Cone Calorimeter tests are used for polymer composite materials. For the characterization of flame retardant behavior of fibers, Micro Combustion Calorimeter (MCC) test is the only one used due to the amount of fiber produced which is not enough for the production of a fabric sample. Melt Flow Index (MFI) and Tensile Test are also used for understanding the flow and tensile properties of fibers.

2.10.1 UL-94

UL-94 is the most commonly used test method for measuring the ignitability and the flame spread of polymeric materials exposed to a small flame at vertical position which is practical and easy to apply. The schematic view of the UL-94 test is shown in Figure 2.24 [138].

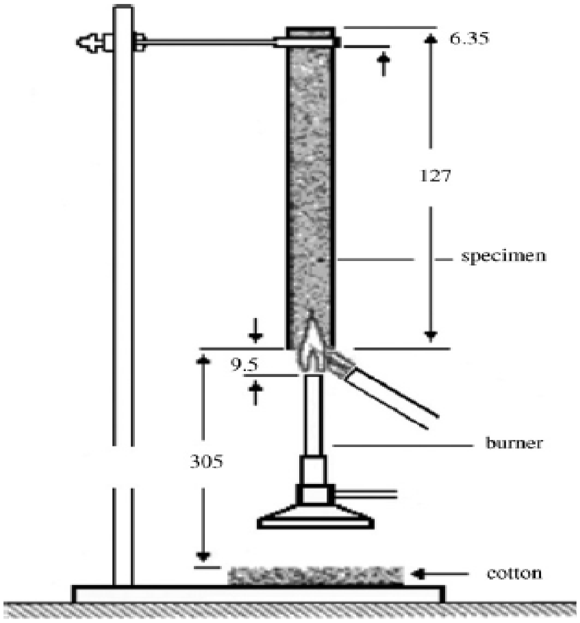

Figure 2.24 The schematic view of the UL-94 test [138].

The flame is applied to the bottom of the specimen and the top of the burner has to be located at 10 mm from the bottom edge of the specimen. The flame is applied for 10 seconds and removed. The after flame time t_1 (the time required for the flame to extinguish) is noted. After extinction, the flame is applied for another 10 second. The after flame time t_2 is noted, together with the afterglow time t_3 (the time required for the fire glow to disappear). During the test, the presence of burning drops, causing a piece of cotton located under the sample to ignite, must be noted. In view of these data, the flammability of material is classified into three categories (V0, V1, V2) depending on their performance regarding the individual duration of burning for each specimen, total burning time for all specimens and the presence or absence of burning drips [92, 138, 139]. Criteria for UL-94 Classifications are shown in Table 2.5 [138, 139].

Table 2.5 Criteria for UL-94 classifications

	V0	**V1**	**V2**
t_1	<10	<30	<30
t_2	<10	<30	<30
t_1+ t_2(for five samples)	<50	<250	<250
t_2+t_3	<30	<60	<60
Cotton ignited by burning drips	No	No	Yes
Afterglow or afterflame up to the holding clamp	No	No	No

2.10.2 Limiting Oxygen Index (LOI)

LOI is widely used to quantify the flammability of polymers. LOI test was proposed in 1966 and was standardized as NF T 51-071 (in France), ASTM D 2863 (in the United States), ISO 4589 (international standard) [92, 138, 139]. The schematic representation of LOI test is shown in Figure 2.25 [92]. Slow stream of oxygen/nitrogen mix is supplied from the bottom of the tube. The ratio of oxygen and nitrogen is changed throughout the test to determine the oxygen concentration that will support the combustion of the material for at least 3 minutes or the combustion of 50 mm of the sample. The LOI value is calculated as $[O_2/(O_2+N_2)]*100$. As air contains 21% oxygen, material with an LOI below 21 are classified as combustible, LOI above 21 are classified as self-extinguishing. The higher the LOI is the better the flame retardant property [92, 138, 139]. Despite its widespread use, the LOI method has several deficiencies; (1) The test condition has never been correlated to any aspect of full size fires, (2) The use of downward flame spread for a distance of 50 mm to define the oxygen index of a material. In real fires, the downward spread of flame is of little importance, (3) LOI test is conducted at oxygen concentration usually above the normal oxygen content of air, which again does not occur in most fires [17].

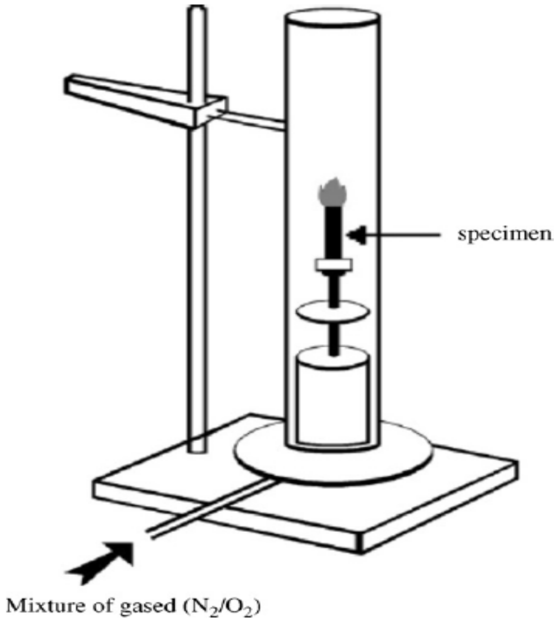

Figure 2.25 The schematic representation of LOI test [92].

2.10.3 Thermal Gravimetric Analysis

TGA is a test method in which changes in the weight of a specimen are monitored as the specimen is progressively heated. The components of polymer and additives evaporate or decompose at different temperatures. This leads to be seen a series of weight loss steps in TGA curve. TGA analysis can yield important information on a polymer system, such as the volatile content, the onset of thermal decomposition, inorganic filler content, the volatility of additives and the effectiveness of flame retardants. TGA instrument can be coupled with Fourier Transform Infrared Spectroscopy (FTIR) or Mass Spectroscopy (MS) to obtain additional information about the thermal degradation of polymers [140,141].

2.10.4 Differential Scanning Calorimeter

DSC is a widely used technique for the thermal analysis of polymeric materials. DSC has two small metal containers, one is for the polymer sample which is tested and the other one is for the reference sample. Sample and reference containers are maintained at the same temperature throughout the experiment by individual electric heaters. The difference in electrical power supplied to the two cups is measured as a function of temperature and hence time. It is possible to determine the heats of transition, heat capacity, melting temperature, glass transition temperature, crystallization temperature and heats of reaction for polymeric materials by DSC instruments [140,141].

2.10.5 Cone Calorimeter

The name of cone calorimeter comes from the conical shape heater used to heat specimen during testing. Cone calorimeter has the ability to determine large number of fire reaction properties in a single test using a small specimen and the burning environment during test is a good representation of majority of actual fire conditions. For these reasons, cone calorimeter test gained popularity among the scientists and is standardized as ASTM E 1354 (in the United State) and ISO 5660 (International Standard) [17].

The principle of the cone calorimeter is based on exposing the specimen to an incident heat flux by a heating element. The schematic view of cone calorimeter is shown in Figure 2.26 [92]. By heating, the material starts to decompose and flammable gases evolve from the sample. These gases are ignited by an electric spark. The combustion gases pass through the heating cone and are captured by an exhaust duct system with centrifugal fan and hood. The measurement of gas flow and oxygen concentration is used to quantify fire properties of the samples. HRR, PHRR, THR, Mass Loss Rate (MLR), TTI, Time of Combustion (TOF), mass loss quantities of CO and CO_2 and total smoke released values can be obtained from cone calorimeter [17, 92, 139, 142, 143].

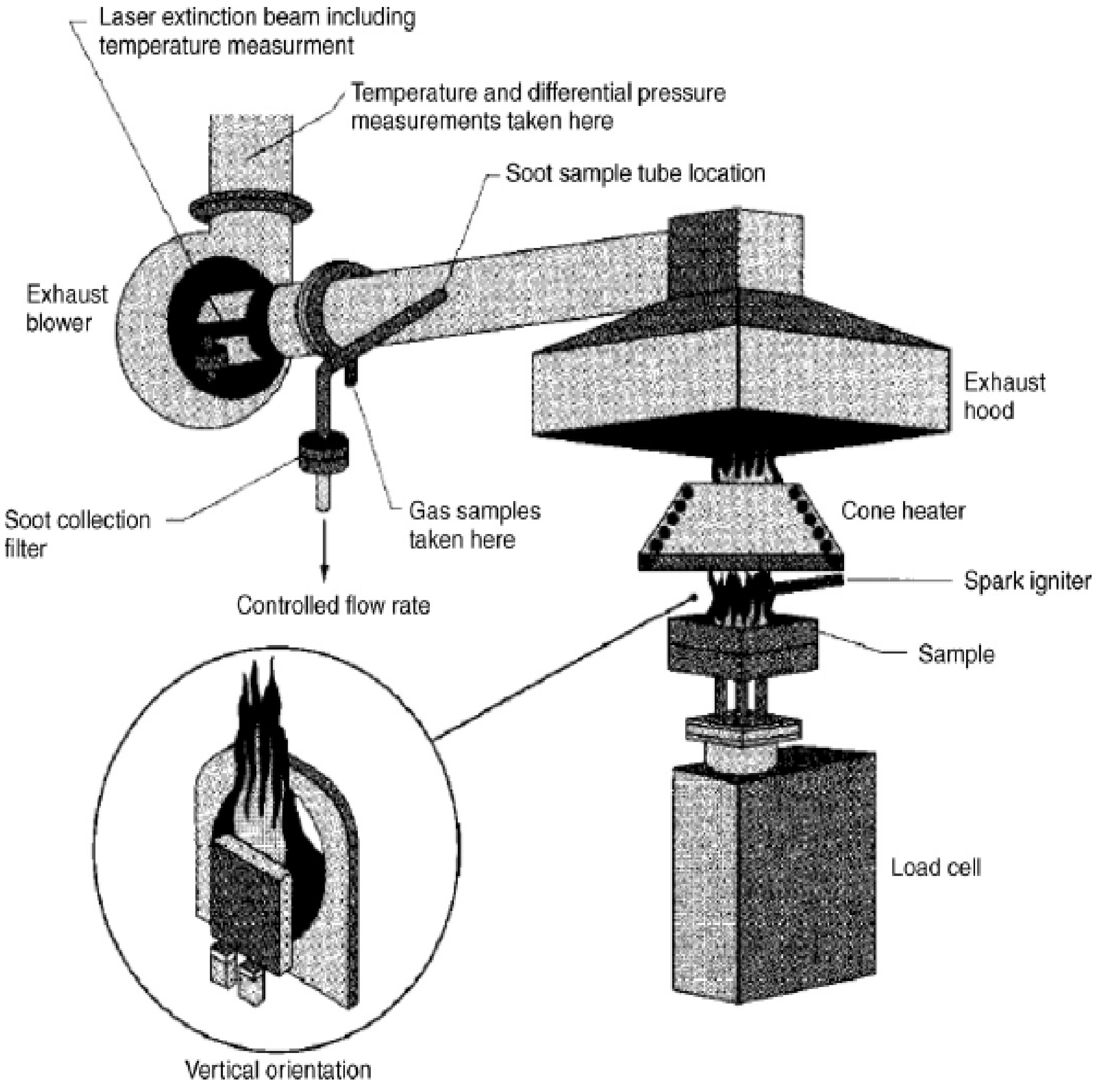

Figure 2.26 The schematic view of cone calorimeter [92].

The heat flux used in cone calorimeter test can be varied between 10-100 kWm^{-2}. The heat fluxes 35 and 50 kWm^{-2} corresponding to heat fluxes found in developing fires are most widely used in cone calorimeter test. The position of the sample can either be in a horizontal or vertical direction. Tests are usually performed in the horizontal direction because the convective component of heat transfer is almost negligible. The sample is positioned 2.5 cm below the heater in horizontal direction. Samples with 10 x 10 cm^2 with varying thickness up to 50 mm can be tested. The cone calorimeter results are strongly dependent on the sample thickness. Thermally thin sample shows lower TTI and higher PHRR values than same sample with higher thickness [17, 92, 139, 142, 143].

Different polymers and polymer composites exhibiting different types of burning behavior and give different types of HRR versus time curve. The shape of this curve also gives valuable information about the burning characteristics of polymers and polymer composites. Some of HRR versus time curves are shown in Figure 2.27 [143].

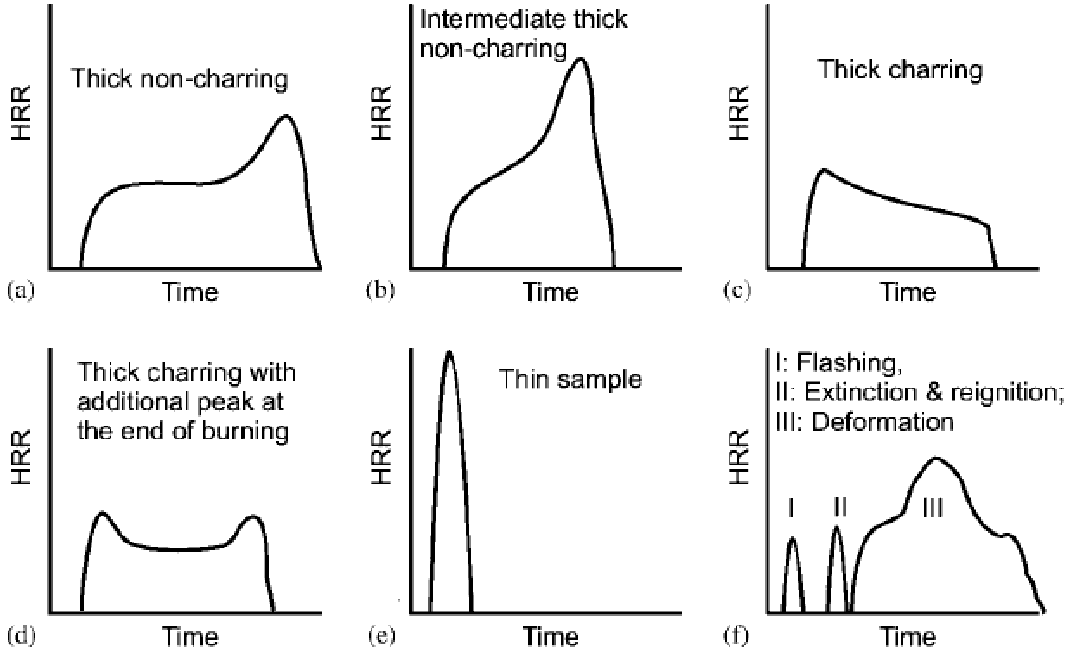

Figure 2.27 Typical HRR curves for various characteristic burning behaviors [143].

2.10.6 Micro Combustion Calorimeter

MCC is a new small-scale instrument which measures the heat release of a material by oxygen consumption calorimeter. Oxygen consumption calorimeter works via Thornton's Rule, which is an empirical relationship that gives the average heat of combustion of oxygen with typical organic (C, H, N, O) gases, liquids, and solids. Specifically, an average 1 g of oxygen gives off 13.1 +/- 0.7 kJ of heat when it reacts with typical organic materials to produce water, carbon dioxide and N_2. Polymers containing a large mole fraction of oxygen (POM, ethylene oxide, etc.) are outside of this standard deviation, as are silicones that consume oxygen to make silica instead of CO_2 and H_2O. Despite these limitations for these particular polymers, oxygen consumption calorimetry serves as a useful technique for assessing the heat release and flammability of many polymeric and organic materials [144-147].

The way the MCC operates is to expose a small sample (5-50mg) to very fast heating rates to mimic fire conditions. The sample can be pyrolyzed under an inert gas (nitrogen) at a fast heating rate, and the gases from the thermally decomposed product are then pushed into a 900 °C combustion furnace where they are mixed with oxygen, or, the sample can be thermally decomposed under oxidizing conditions (such as air, or a mixture of N_2 and O_2 up to 50%/50%) before going to the combustion furnace. After the gases from the pyrolyzed/thermally decomposed sample are combusted in the 900 °C furnace, they are then sent to an oxygen sensor, and the amount of oxygen consumed during that combustion process equals the heat release for the material at that temperature using Thornton's rule as described above. A general schematic representation of the instrument function and a picture of the instrument are shown below in Figure 2.28. This instrument is a standardized technique, ASTM D7309-07, and is referred to both MCC and as the "pyrolysis combustion flow calorimeter" (PCFC) [144-147].

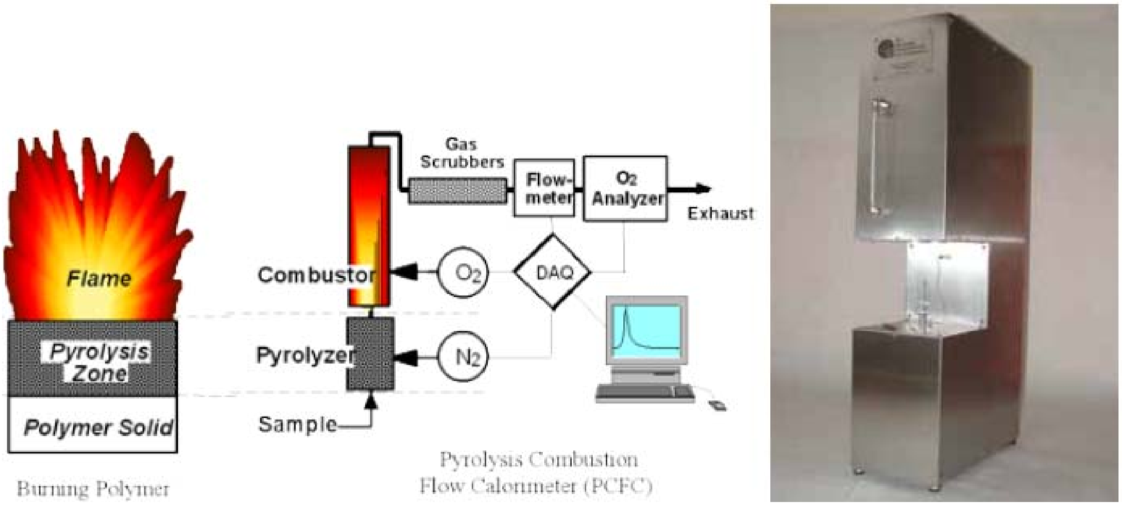

Figure 2.28 A general schematic representation of the instrument function and a picture of MCC [148].

2.10.7 Melt Flow Index

Melt flow index (MFI) is a conventional property of a polymer for expressing important flow characteristics. MFI test measures the rate of extrusion of a thermoplastic material through an orifice of specific length and diameter under prescribed conditions of temperature and load. The weight of the material extruded during the specified time is the melt index expressed in g/10 min [140].

2.10.8 Tensile Test of Fibers

Textile fibers must have a tensile strength over a critical value which depends on further processes such as spinning, weaving, knitting, chemical treatment and where they are used. Generally, the zero strength temperature should be above 215 °C except for certain applications such as carpets, blankets, upholstery and curtains. The tensile strength should be around 5 g/den, higher values are rarely needed. The elongation to break should not be below 10 %. Flexibility permits the fibers to be spun and woven, and gives to a textile its unique draping characteristics. In addition to properties such as strength and flexibility, a textile fiber should be elastic. There should be some completely reversible elongation in the range up to 5 % strain; in general, the more the better. Tensile strength, elongation at break, flexibility and elasticity limit can be understood from the tensile test. Tensile test of a fiber is one of the most important test methods for understanding whether it can find application areas in textile industry [149-151].

Tensile properties of single textile fibers are determined according to the ASTM D 3822 01. According to the test method, single-fiber specimens are broken on a constant-rate-of extension type tensile testing machine at a predetermined gage length and rate of extension. Using the force extension curve, the breaking force and the elongation at break are determined. The force-elongation curve and linear density are used to calculate breaking tenacity, initial modulus, chord modulus, tangent modulus, tensile stress at specified elongation, and breaking toughness [152].

2.11 Production Methods of Polymer Composites and Fibers

In this study, the additives are mixed into polymer by twin screw extruder for the production of both polymer composites and fibers. Polymer pellets obtained after extrusion were compression molded in order to give desired shape for flammability testings. Fibers are directly produced by melt spinning method after extrusion process. Therefore, the detailed information is given about extrusion, compression molding and melt spinning method.

2.11.1 Extrusion

Extrusion is the most efficient and widely used method for melting plastic resin as a part of the process of adding or mixing fillers, colorants and other additives into molten plastic. Although the thermoplastics are the most common plastics to be extruded, some thermosets (especially rubber) can also be extruded. At the end of the extrusion process, plastics can be produced in different shapes such as pipes, sheets, fibers coating on wire, cable and long thin rods that are chopped into pellets [153-154].

During extrusion process, plastic granules or pellets and any other materials to be mixed with them are fed into hopper. The materials in the hopper come through a hole in the top of the extruder screw. This screw both conveys the plastic forward until it exits through a hole at the end of the extruder barrel called as die and melts the polymer by the combination of external heating and heat formed from the friction of polymer melts. The die imparts a shape to the molten plastic stream which is immediately cooled to solidify the plastic, thus retaining the shape created by the die [153-154].

2.11.2 Compression Molding

Compression molding is a widely used method for molding of polymeric materials (especially thermosets). The principle of compression molding is quite simple. The molding material is generally preheated in an open, heated mold cavity. After the mold is closed, pressure is applied to force the material into contact with all mold areas, while heat and pressure are maintained until the molding material is finished. In this study, stainless steel plates, of which the inner parts are cut out into desired shape, are used as mold. Teflon film is used to prevent the adhesion of polymer melts onto the heated upper and lower plates of the hydraulic press [154].

2.11.3 Fiber Spinning

The conversion of polymer into fiber form requires solubility in suitable solvents or a melting point below the decomposition temperature to permit extrusion. Three different methods are used for the production of man made fibers as wet spinning, dry spinning and melt spinning. Among the three methods, the melt spinning is the most economic and the easiest one because it lets us high spinning speeds and it does not require any solvent and precipitating agents [150, 151, 155, 156].

2.11.3.1 Melt Spinning Process

In melt spinning process, polymer pellets are fed into extruder. The extrusion process involves melting and mixing of spinnable polymer and ingredients. The screw of the extruder delivers the mixed and the molten polymer to the multihole capillary die called spinneret. The molten material is extruded from spinneret. A tensile force is usually applied to the extrudate in order to draw the filaments down to a desired diameter while they are simultaneously being cooled by air blowing across the filament bundle. The filament velocity increases along the spinning path until it reaches a final velocity called spinning speed. The spinning speed used in fiber formation from polymer melts ranges from 100 m/min to several thousand meters per minute. Attenuation and molecular orientation are achieved by taking up fiber many times, perhaps 100 times faster than of extrusion. The resulting filaments are either wound onto a bobbin or they are directly passed to another drawing procedure [150, 151, 155, 156]. The schematic representation of melt spinning process is shown in Figure 2.29 [151]

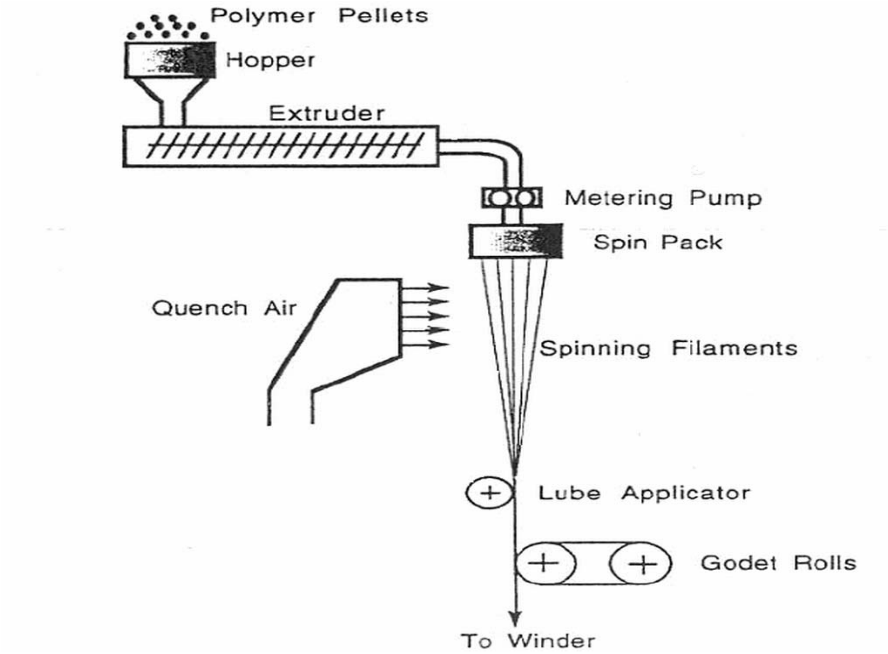

Figure 2.29 The schematic representation of melt spinning process [151].

The major parameters affecting the spinning process and final fiber properties are extrusion temperature, mass flow rate of polymer, spinning speed, spinline cooling conditions, the spinneret orifice shape and dimensions and the length of the spinline. These variables are not independent of each other [150, 151, 155, 156].

The extrusion temperature of polymers must be below its degradation temperature, and the viscosity of the polymer melt should let them to be extruded from the spinneret. From the rheological point of view, three groups of polymers are used for melt spinning; polycondensation polymers (polyamides, polyurethanes, polyesters), polyolefins (PP, polyethylene) and vinyl polymers. Polycondensation polymers with moderate molecular weights (10,000-25,000) are suitable for melt spinning process. Linear polyolefines and vinyl polymers with high molecular weights (30,000- 400,000) are suitable for melt spinning process [150, 151, 155, 156].

Spinnability of polycondensation polymers is very good. When melted, the materials of the first group form liquids with rather low viscosity with very slight non- newtonian viscosity properties and elasticity and with rather short relaxation times. Short relaxation times make rapid elongation of molten jets of polycondensates possible. The spinning speeds reach up to 4000-5000 m/min. Generally, melt fracture does not appear in the spinning of polycondensates, except for extremely low extrusion temperatures, close to the solidification temperature. When the extrusion temperature is too high, capillary breakup is observed [150, 151, 155, 156].

When polyolefins are melted, they form liquids with very strong non-Newtonian behavior and long relaxation times. High pressures are required because of high viscosities. The spinnability of molten polyolefins is usually limited by melt fracture. Long relaxation times lead to serious limitation of elongation rates and deformation ratios [150, 151, 155, 156].

The mass flow rate is the second parameter that affects the fiber properties. The variation of output causes non uniformity at resulting fiber, so a metering pump is put before spin pack. The metering pump controls and ensures a steady flow of polymer to the spin pack [150, 151, 155, 156].

The most important variable of the melt spinning process is the spinning speed. The spinning speed controls the productivity of the spinline. Drawing along the spin line gives rise to parallelization and extension of structural units along the fiber axis. Structural characteristics measured along the spinning path give evidence for the fact that fiber orientation is developed gradually in the course of free jet flow at both amorphous and crystalline parts. Orientation can be due to either of two further mechanism, streaming orientation in the elongational flow or deformational orientation. The degree of orientation affects the mechanical, optical and dyeability properties of fibers [150, 151, 155, 156].

The length of the spinline will generally be controlled by the efficiency of the cooling conditions along the spinline. More efficient cooling conditions allow shorter spinlines. Spinline cooling conditions are largely controlled by the velocity, temperature and the distribution of the cooling air, spinneret configuration and mass throughput. The cooling conditions show most of their effects on crystal structure and percent crystallinity of the fiber. Increasing cooling rate decreases the amount of time available for crystallization at any given temperature. Thus, increasing cooling rates tend to suppress the amount of crystallization that can occur. Ultimately, if we cool sufficiently fast, crystallization does not have time to occur, and the material simply vitrifies into noncrystalline glass when cooled below its glass transition temperature. The change of crystallinity of as spun fibers sometimes may also proceed during the conditioning before drawing. If the surrounding temperature is lower than the glass transition of the polymer, the phase transition is negligible. When surrounding temperature is larger than the glass transition of the polymer, the phase structure of fibers is not stable.

Crystal structure and the degree of crystallinity affect tensile strength, maximum draw ratio, elongation, density and dyeability of the fibers [150, 151, 155, 156].

The cross-sectional shape of the melt spun fibers is determined by the shape of spinnerets and volume change accompanying the spinning process. In melt spinning, volume contraction is only about 10 %. To improve handle, luster, dyeability and other properties of melt spun fibers, spinnerets with noncircular orifices were developed. Melt spinning of non-cylindrical filaments requires not only the presence of special spinnerets but also careful choosing of the spinning conditions [150, 151, 155, 156].

2.11.3.2 Melt Spinning of Polyamide-6

PA-6 can generally be produced from Є caprolactam by ring opening reaction. Water, acids or bases can initiate the reaction. Water is preferred in industry. In the presence of water, the caprolactam ring scission is of hydrolytic type and gives aminocaproic acid. Polymerization can proceed either by polycondensation or polyaddition mechanism. During polymerization, polyaddition mechanism is prevalent, polycaprolactam follows the rules of polycondensation at equilibrium [157, 158].

PA-6 is a partially crystalline material. Therefore, it is characterized by both an unordered amorphous state and ordered crystalline state. The crystal structure of PA-6 results from the conformation of the macromolecules and their lateral packing. Generally, the packing of polymer chains will be such that the occupied volume is at a minimum, thereby minimizing the potential energy of the structure, but maintaining appropriate distances for intermolecular forces between adjacent chain segments. In PA-6, these intermolecular forces are both van der Waals bonds and hydrogen bonds. The latter involving the NH and CO moieties, causes the formation of sheetlike arrangements between adjacent chains. The stacking of these hydrogen-bonded sheets controls the size and the shape of the unit cell [157-159].

The crystal structure of PA-6 is very complex compared to other polyamides, the following different phases have been discovered by X-ray diffraction; amorphous, γ (pseudohexagonal), β (hexagonal), α (paracrystalline monoclinic). α- monoclinic crystal structure is comprised of stacks of sheets of planar hydrogen bonded extended chain segments. The hydrogen bonded sheets of the α-form are characterized by an antiparallel alignment of the extended chain segments [157-159]. The unit cell of the α-form of PA-6 is shown in Figure 2.30 [158]. In undrawn fiber, immediately after spinning, there is no crystallinity at all but after a short time crystallization begins with a large amount of γ phase and small amount of α and β phases. After drawing, especially after hot drawing, the more stable α form is prevalent. In direct spinning, the predominant crystalline phase is the γ form. Fibers with a prevalent γ structure have a lower tenacity than those with α structure [158-159].

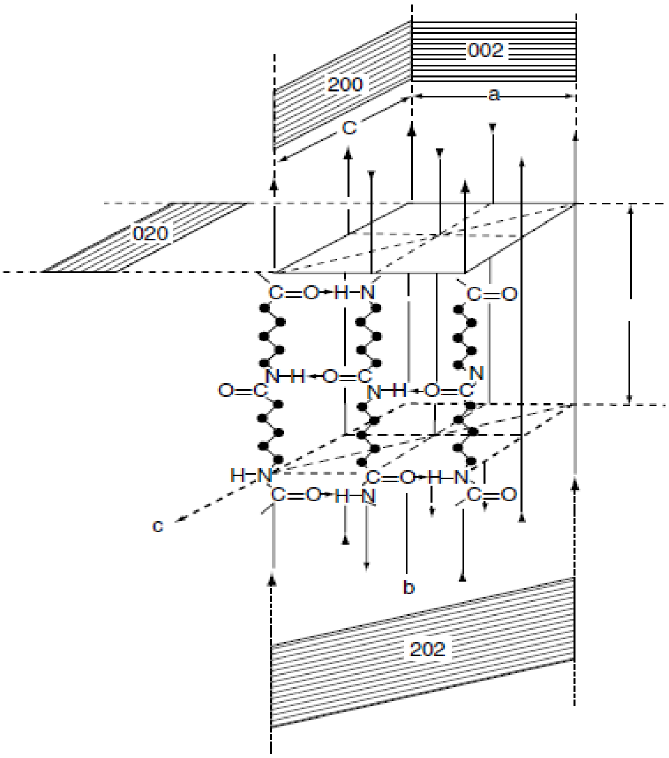

Figure 2.30 Unit cell of the α-form of PA-6 [158]

The melt spinning process for the production of textile fibers from PA-6 is very similar to that of PA 6.6. It is very important to dry PA-6 chips to consistent moisture level (about % 0.12) for successful spinning. Generally, PA-6 is extruded at 250-260 °C. During spinning process, the heating of the polymer has tended to bring about regeneration of some free caprolactam. The formation of caprolactam must not exceed 3% so as to avoid difficulties at fiber processing stage [156-159].

In melt extrusion, the polymer chips are melted by a heated grid, or by an extruder. Alternatively, the polymer may be supplied directly from continuous polymerization. The molten polymer is fed to a metering pump, which is very important for adjusting the linear density of fiber. The molten polymer is then filtered by passing it through a bed of fine sand supported on a metal mesh or though a series of sintered metal screens. The filters remove from the polymer melt any particulate matter or gels that could block the spinneret holes. The filter material also subjects the molten polymer to a high shear that affects the rheological behavior by inducing some molecular orientation. The molten polymer then passes though the spinneret, which has a number of small holes, typically 100- 400 μm in diameter. The spinneret is a stainless steel plate 5 mm or more in thickness. Each hole is made up of a counter-bore, a conical transition zone, and the capillary. The capillaries must be consistent not only in their diameter but also in length: L/D ratios of 2-5 are typical. Some orientation is induced in the polymer by shear as it passes though the filter and the capillary. The PA-6 emerges from spinneret holes into air; immediately the orientation imparted in filaments tends to relax and post extrusion swelling is observed [156-159].

Following this post extrusion swelling, the polymer stream is drawn down by the take-up reel and undergoes a considerable acceleration. It also enters the quenching air stream. The accelerated filaments solidify in cool air and there is some orientation of the molecules along the fiber axis and some crystallization [156-159]. The effects of spinning speed on mechanical properties of PA-6 fiber are seen at Figure 2.31 [159].

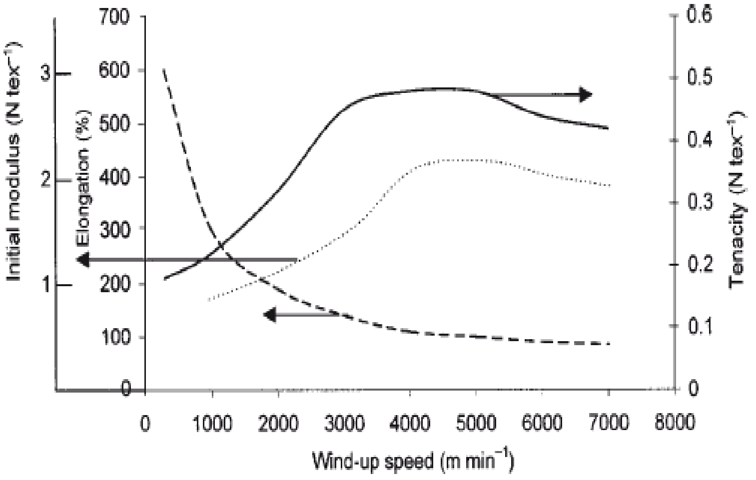

Figure 2.31 Effect of take-up speed on the tenacity (-), extension at break (---) and initial modulus (.....) of PA-6 fibers [159].

Following the extrusion process the polymer is in a fibrous form, but lacks adequate tensile properties. The tensile strength and modulus are low, extension at break is high; in use the product would have poor dimensional stability and would stretch by a factor of up to 3.5- 4 times. The draw ratios commonly used in practice range from 3.5-3.9 depending on the pre-orientation at spinning [156-159]. Dependence of the residual draw ratio of PA-6 on the take-up speed is shown in Figure 2.32 [159].

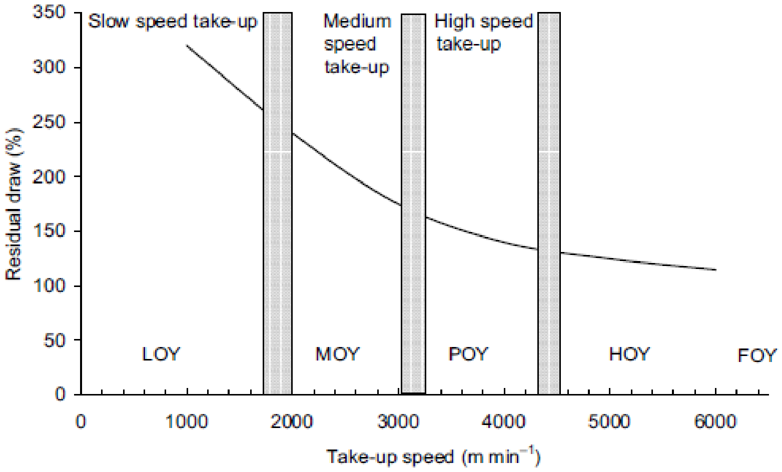

Figure 2.32 Dependence of the residual draw ratio of nylon on the take-up speed [159].

The objective of the fiber drawing process is to yield a yarn with acceptable fiber properties. For apparel and carpet end uses the PA-6 are drawn cold, while for high tenacity industrial applications the yarns are heated before drawing. After drawing, the yarn is again wound onto a bobbin. To obtain very high tensile strength, it is necessary to have high molecular weight, orientation and crystallinity. Hot drawing is used with fibers with molecular weights of 20,000-25,000. Hot drawing facilitates the drawing process due to the higher molecular mobility, drawing tensions decrease and crystallinity is increased. Hot-drawing usually follows normal cold drawing with a low draw ratio; both operations can be carried out either on one machine or on two different machines. Tenacities above 8 g/den and elongation at break below 12% can be obtained by correct hot drawing [156-159]. Tensile properties of typical PA-6 fibers are shown in Table 2.6 [159].

Table 2.6 Tensile properties of typical polyamide- 6 fibers [159]

Tenacity (N/tex)	Normal	0.4-0.6
	High tenacity	0.6-0.9
Breaking Extension (%)	Normal	20-40
	High tenacity	15-20
Initial modulus (N/tex)	Normal	1.5-3.5
	High tenacity	4-5
Work of rupture(mN/tex)	Normal	70-80
	High tenacity	60-70

2.11.3.3 Melt Spinning of Polypropylene

PP can be used in many different forms such as composite, sheet and fiber. PP fibres have a wide range of end uses, and these uses are expected to increase over the coming years. PP fibres are to be found in ropes, fishing gears, carpets, sewing thread, blankets, upholstery, filtration fabrics, tire cord, geotextiles, sacks, cables and conveyor belting [156-159]. Some physical properties of commercial polypropylene fiber are shown in Table 2.7 [159].

Table 2.7 Physical properties of commercial polypropylene fiber [159].

Properties	**Values**
Specific Gravity (g/cm^3)	0.9-0.91
Tenacity (g/den)	4.5-8.5
Elongation to rupture (%)	15-25
Shrinkage % of original length at 212 °F	10-15
Moisture regain (20°C, 65% relative humidity)	<0.04%
Melting temperature (°C)	175
Glass transition temperature (°C)	-18

Propylene is catalytically polymerized to form PP. The molecule of PP consists of a long chain of carbon atoms, with methyl groups forming appendages which stand out from the sides of the chain. PP chains adopt a three dimensional helical configuration, as shown in Figure 2.33 [159].

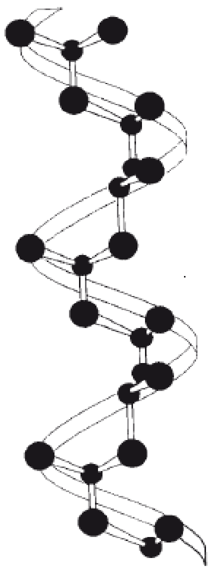

Figure 2.33 Helical configuration of an isotactic PP polymer chain [159].

PP fiber is a partially crystalline material. Therefore, it is characterized by both an amorphous state and crystalline state. In the amorphous regions, an assembly of random interpenetrating chains may be considered. In crystalline regions, the segments of the polymer chains exist in well-defined lattice structures. PP has three different crystalline forms: α- monoclinic, β-hexagonal and γ- orthorhombic. The common feature of these crystalline forms is the helical conformation of the constituent PP chains. The α-form is the most stable and also the most important in the context of PP fibers. Crystals of the β-form can be obtained with the use of special nucleating agents. The orthorhombic γ-form can be obtained by the crystallization of PP at high pressure or of PP with a small proportion of comonomer at low pressure. The degree of crystallinity depends on the average molecular weight, molecular weight distribution and conditions of fiber spinning process. The normal commercial polymer has a degree of crystallinity of about 65 to 75 % [157-159].

PP fiber is produced by melt spinning technique. The extrusion of PP and the processing of the fiber, do not present any basic difficulties. General procedure resembles the PA-6 fiber production. The average molecular weights of PP used in fiber manufacture are commonly higher than 300,000. Due to the high molecular weight, their melt viscosity is too high. For this reason, the melt spinning is made at 100 °C higher than the melting temperature of PP [157-159].

Melt fracture is the most important problem for spinning of the PP. High molecular weight, molecular weight distribution and draw resonance are reasons of melt fracture. Draw resonance can be seen as periodic fluctuations in diameter in the filament melt. The presence of additives can also promote draw resonance.

The rate of crystallization and the extent of crystallinity in as-spun fibers depend both on the grade of polymer extruded and the extrusion processing conditions. When the magnitude of spinline stress is increased, the crystallization rate and the overall crystallinity of as spun fibers are also increased. Spinline stress can be increased by raising cooling rate and winding speed and by lowering metering pump speed and spinning temperature. Fast cooling leads to the formation of small crystallites and low degree of crystallinity. On the other hand, slow cooling rates control a high degree of crystallization with heavy agglomerations of densely packed crystallized region.

Drawing under carefully controlled conditions can markedly improve the mechanical performance of PP fibers. Generally, higher draw ratios give rise to higher tensile strength and modulus and lower elongation at break of the drawn fibers. Draw ratio, drawing temperature, drawing speeds and the number of drawing stages are important factors affecting final fiber properties. Drawing temperature influences the mobility of the structural units during deformation. Drawing at ambient temperatures converts as-spun PP fibers with α- monoclinic crystalline structures into more oriented structure with reduced crystallite size, increased lattice strains and defects that are similar to paracrystalline form. Drawing at low temperature can induce the formation of microvoids, which elongate in the direction of fiber axis as a result of tensile force applied. The presence of these micro voids lowers the modulus of the fibers. Drawing at more elevated temperature can be considered to be similar to a combination of cold drawing followed by annealing fibers in which highly ordered and oriented structures are formed.

More than one drawing stage is often needed to achieve the desirable mechanical properties in the final fiber. Two stage drawing can provide a route to filaments of high tenacity, where the first stage utilizes a high draw ratio at low temperature (60 °C) and the second stage utilizes a low draw ratio at high temperature (140 °C). The as-spun fiber should be in the paracrystalline state. With this two stage approach, a high orientation of the PP chains could be obtained in the first stage before transformation from paracrystalline to the α- monoclinic form in the second stage.

.

CHAPTER 3

EXPERIMENTAL

Experimental part of this dissertation is divided into four parts. In the first and second parts, the materials and experimental procedures used to prepare and characterize flame retardant polyamide-6 (PA-6) and polypropylene (PP) composites are mentioned, respectively. In the third and fourth parts, the materials and experimental procedures used to prepare flame retardant PA-6 and PP fibers are mentioned, respectively. For providing integrity throughout the dissertation, the compositions of the composites are given in results and discussion part.

3.1 Production of Flame Retardant PA-6 composites

For the production of flame retardant PA-6 composites, four different commercial flame retardants, melamine cyanurate (MC), melamine, red phosphorus (P-red) and aluminum diethylphosphinate (AlPi), were used with different boron containing compounds and organoclay (Cloisite 30B). Zinc borate (ZnB), borophosphate (BPO_4), and boron and silicon containing oligomer (BSi) were used with MC and melamine for their synergistic effect. For the composites that contain P-red, only ZnB and BPO_4 were used. For the composites containing AlPi, Cloisite 30B, ZnB and BPO_4 were used. For MC and melamine containing composites, the combustion and the thermal degradation characteristics were investigated by using limiting oxygen index (LOI), UL-94, thermogravimetric analysis-Fourier transform infrared spectroscopy (TGA-FTIR), differential scanning calorimeter (DSC) and scanning electron microscopy (SEM). For

P-red containing composites, UL-94, LOI, TGA and cone calorimeter tests were done. For AlPi containing composites, X Ray Diffraction (XRD), FTIR, UL-94, LOI, TGA and cone calorimeter tests were done.

3.1.1 Materials

PA-6, Bergamid B65 Natur- TP, was obtained from Polyone. The properties of commercially available flame retardants used in these studies are specified in Table 3.1.

Table 3.1 The properties of the commercially available flame retardants.

Material	Trade Name and Supplier	Specifications
MC	Ciba® MELAPUR® MC25, Ciba	Appearance: White Powder Molecular weight: 255.2 g/mol Density: 1.7 g/cm^3 Bulk density: 150-200 g/l Particle size: D_{98} max. 25µm
Melamine	Melafine, DSM	Appearance: White Powder Molecular weight: 126.13 g/mol Density: 1.574 g/cm^3 Melting point: 350 ^{o}C
P-red	Phosphorus (red), Merck	Appearance: Brownish Powder Molecular weight: 30.97 g/mol P content ≥ 97% (w/w)
AlPi	OP 1230, Clariant	Appearance: White powder Molecular weight: 390.3 g/mol Density: 1.35 g/cm^3 Bulk density: 400-600 kg/m^3 Particle Size: D50 20-40 µm P content: 23.3-24 % (w/w)
ZnB	Firebrake ZB, Luzenac	Appearance: White powder Density: 2.77 g/cm^3 Particle Size: Average 9 µm Composition: ZnO (37.7-38.7%), B_2O_3 (47.5-48.9%), H_2O (12.4-14.8%)

Cloisite® 30B, organoclay, was purchased from Southern Clay Products Inc. It was organically modified with methyl, tallow, bis-2-hydroxyethyl, quaternary ammonium by the supplier. The chemical structure of the organic modifier is given in Figure 3.1.

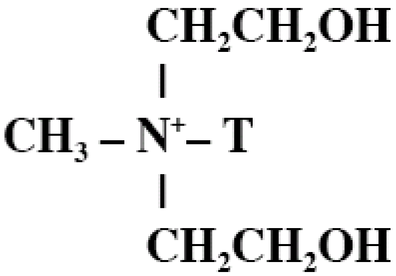

$$\mathrm{CH_3}-\overset{\overset{\displaystyle\mathrm{CH_2CH_2OH}}{|}}{\underset{\underset{\displaystyle\mathrm{CH_2CH_2OH}}{|}}{\mathrm{N^+}}}-\mathrm{T}$$

Figure 3.1 The chemical structure of the organic modifier of Cloisite 30B (T is tallow: 65% C18, 30% C16, 5% C14)

3.1.1.1 Preparation of BPO_4

BPO_4 powder sample was prepared by microwave method. 1:1 mol ratio of H_3BO_3 and $NH_4H_2PO_4$ were weighed and ground to mix in an agate mortar. Then, 40 % of total weight solid urea was added to this mixture and ground gently in an agate mortar. 40 percent was chosen, because below this percentage activation did not start and above this percentage the mixture burned very fast. The white solid mixture was then put into microwave oven and exposed to microwave radiation at 850 W for 10 minutes. The color of mixture changed into black showing that urea was activated. Then, this mixture was heated in muffle furnace at 600°C for 4 hours [160].

The characterization of BPO_4 particles was made through X-ray Diffraction (XRD), TGA and SEM. XRD pattern for BPO_4 sample is given in Figure 3.2 [28]. According to Figure 3.2, the patterns are good in agreement with standard data of BPO_4 (JCPDS No. 34-0132).

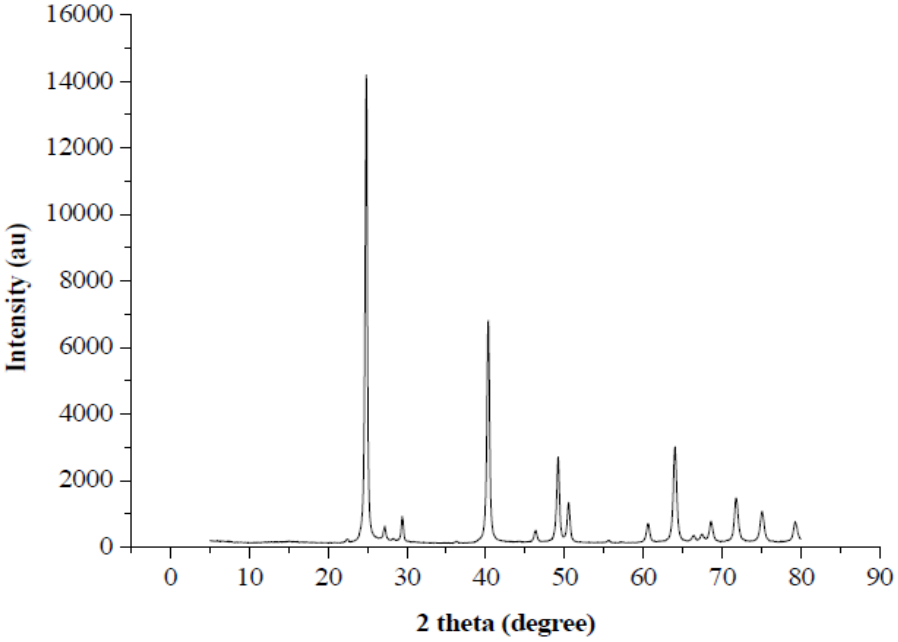

Figure 3.2 XRD pattern for BPO_4 sample [28].

SEM images of BPO_4 and BSi particles are given in Figure 3.3. The image shows that BPO_4 particles have spherical shape and the grains have diameters around 200 nm. The TGA curves of boron containing substances are shown in Figure 3.4. According to Figure 3.4, BPO_4 compound has 1.5% weight loss up to 600 °C. It has a melting point of 1000°C and is very stable when exposed to methane flame [28, 160].

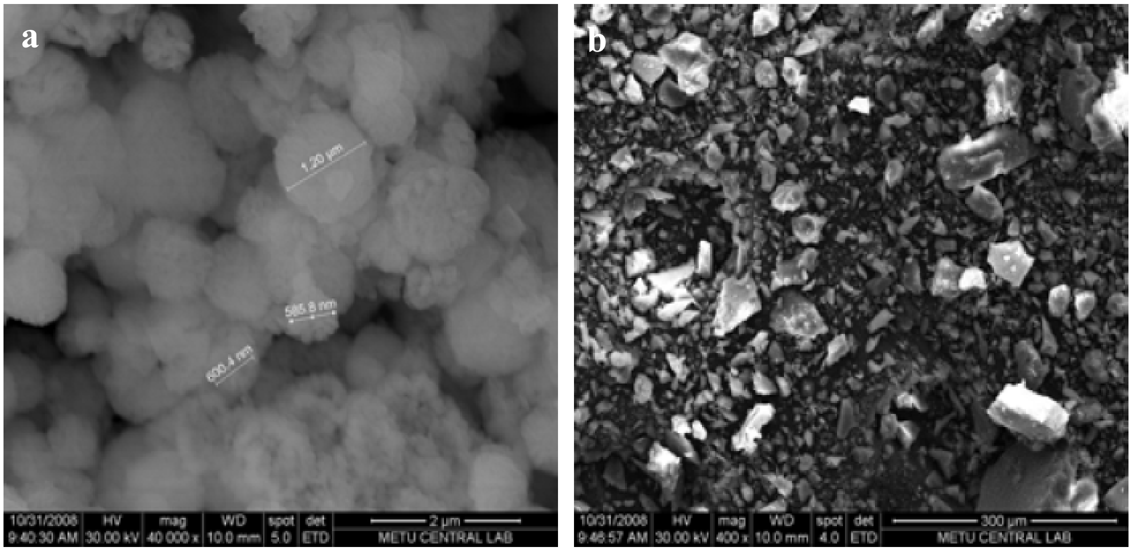

Figure 3.3 SEM images of BPO_4 and BSi particles: (a) BPO_4 (b) BSi [28].

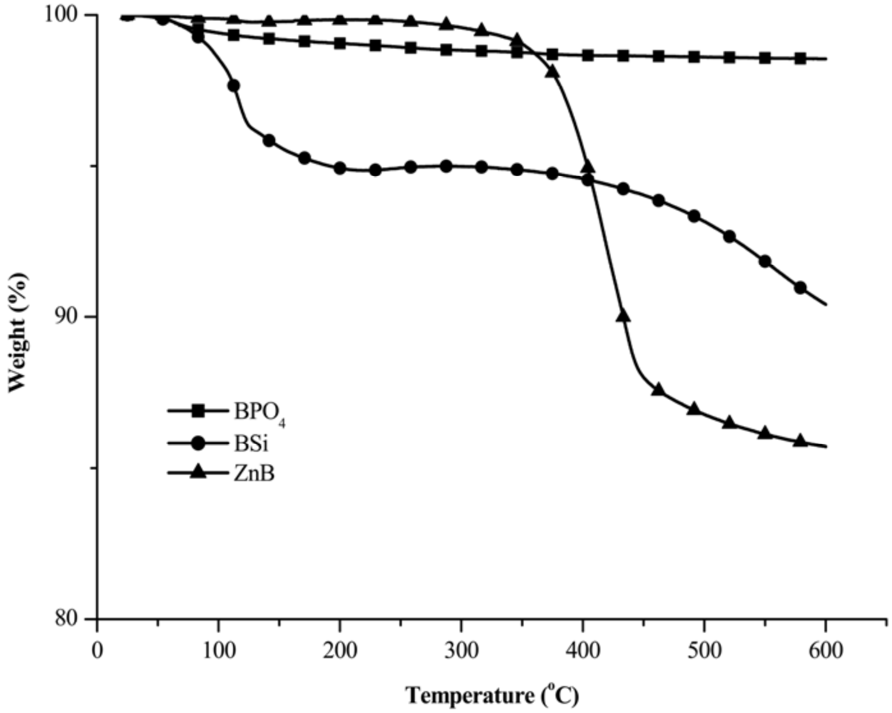

Figure 3.4 The TGA curves of boron containing compounds [28].

3.1.1.2 Preparation of BSi

The synthesis of BSi was made through the condensation of boric acid with vinyltriethoxysilane at a relatively low temperature (150 –160 °C). 0.3 mol vinyltriethoxysilane, 0.15 mol boric acid, 50 ml diglyme and 1 ml concentrated HCl were taken in a three necked flask and the reaction mixture was stirred for 3 hours under nitrogen atmosphere. The product obtained was dried under vacuum for 8 hours. The oligomer was obtained in 75% yield [28, 161]. The molecular structure of BSi is shown in Figure 3.5 [23].

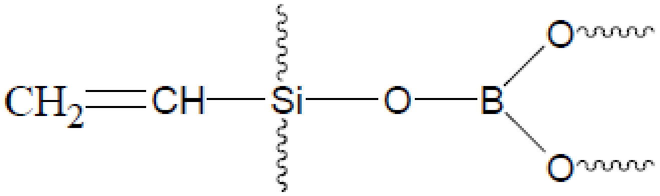

Figure 3.5 The molecular structure of BSi [23].

The characterization of oligomer was made through Gel Permeation Chromatography (GPC), SEM, TGA and FTIR, According to GPC result, the oligomer exhibits with monomodal molecular weight distribution and have M_w of 693. According to the SEM micrograph of BSi (Fig. 3.3), BSi particles have irregular shape and the particle size is larger than that of the BPO_4. According to TGA curve of BSi (Fig. 3.4), it loses 10 % weight up to the 600 °C, and first weight loss may arise from the loss of organic solvent which remains after synthesis. At elevated temperatures, BSi compound forms a passive borosilicate glassy layer. No melting transition is observed due to the formation of a crosslinked structure [23, 28, 161]. The FTIR spectrum of BSi is shown in Figure 3.6 [28]. The characteristic absorption peaks seen at 690 and 890 $cm^{-1}$are due to the Si-O-B linkage. The peaks seen at 1200-1100 cm^{-1} are due to the Si-O-Si linkage [161].

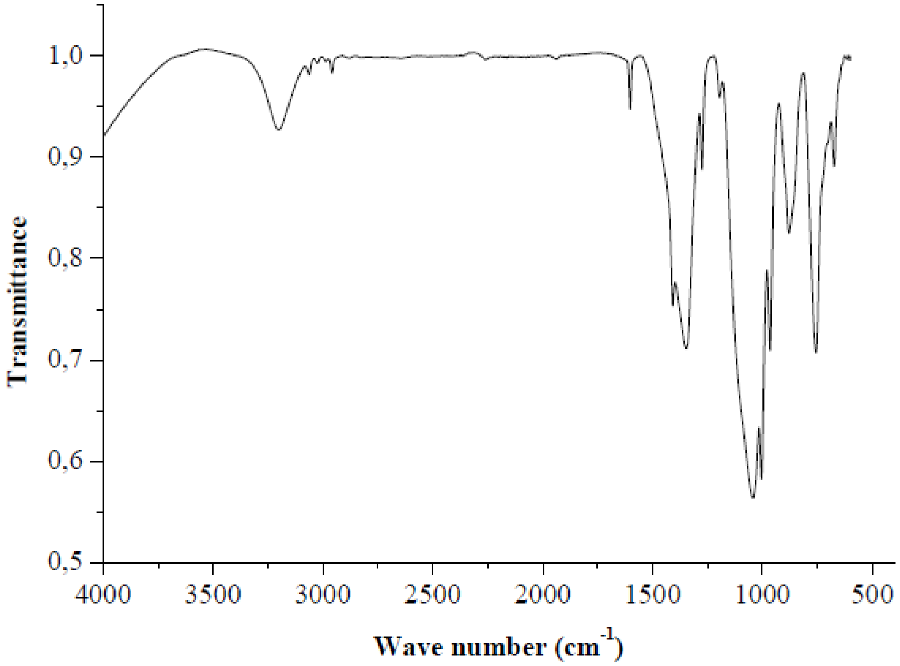

Figure 3.6 The FTIR spectrum of BSi [28].

3.1.2 Preparation of PA-6 Composites

Before PA-6 and the flame retardants were mixed in a corotating twin screw extruder (see Figure 3.7) (Thermoprism TSE 16 TC, L/D=24) at 100 rpm at 230 ºC, PA-6 pellets were dried at 80 ºC for 24 hours. The extrudate was water cooled and chopped into small pellets. The composites for flammability and thermal characterization testing were prepared by compression molding at 230 ºC. A laboratory scale hot-press machine (Rucker PHI) was used (see Figure 3.8).

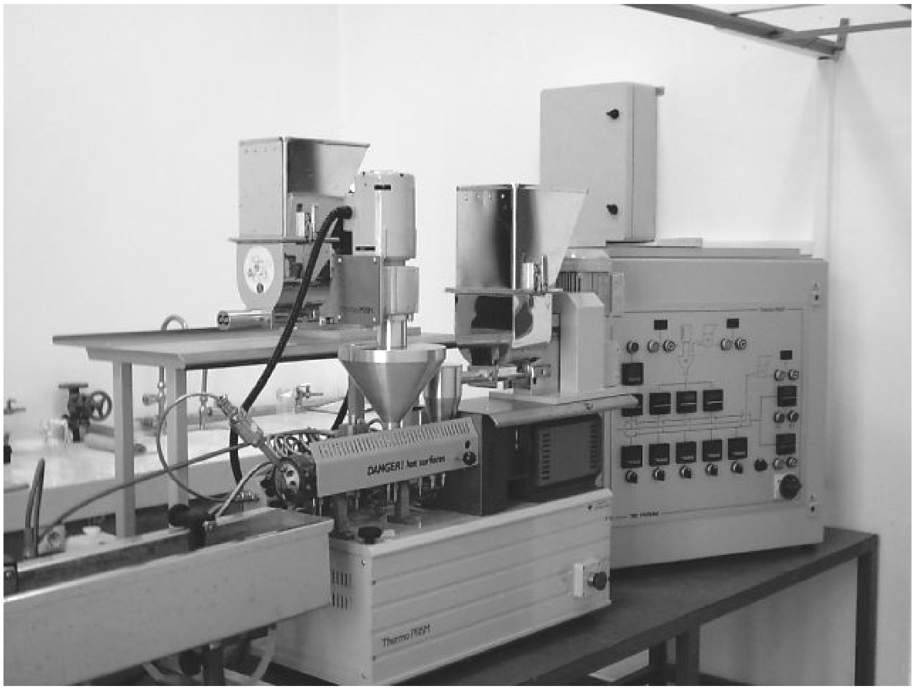

Figure 3.7 The photograph of the twin screw extruder used for composite production in this study [162].

Figure 3.8 The photograph of the hot-press used in this work [163].

3.1.3 Characterization Methods

3.1.3.1 LOI

LOI value was measured by using Dynisco Limiting Oxygen Index Analyzer instrument on test bars of size 130 ×6.5 × 3.25 mm^3, according to the standard oxygen index test ASTM D2863.

3.1.3.2 UL- 94

UL-94 rating was obtained according to ASTM D3801 where V0 indicates the best flame retardancy and V2 is the worst. Bar specimens of 130 × 13 × 3.25 mm^3 were tested.

3.1.3.3 TGA-FTIR

TGA-FTIR was carried out on Perkin Elmer Pyris 1 TGA & Spectrum 1 FTIR Spectrometer at a heating rate of 10 ºC/min up to 600 ºC under nitrogen flow of 50 ml/min.

3.1.3.4 TGA

TGA was conducted on a thermal analyzer (Perkin Elmer Diamond TG/DTA) from RT to 800 °C at 10 ºC/min ramp rate under flowing nitrogen.

3.1.3.5 DSC

DSC was carried out on Mettler Toledo DSC 1 Star System at a heating rate of 10 ºC/min up to 400°C under nitrogen flow of 50ml/min.

3.1.3.6 Cone Calorimeter

The cone calorimeter test was carried out without replication following the procedures in ISO 13927 using Mass Loss Cone with thermopile attachment (Fire testing Technology, U.K). Square specimens (100 × 100 × 4 mm^3) were irradiated at a heat flux of 35 kW/m^2, corresponding to a mild fire scenario.

3.1.3.7 SEM

Microstructure of BSi, BPO_4 and residual chars were observed by using QUANTA 400F Field Emission scanning electron microscope.

3.1.3.8 XRD

Wide angle X-ray scattering (WAXS) scan was performed by Rigaku DMAX 2200 diffractometer in the reflection mode using an incident X-ray wavelength of 1.542 A° at a scan rate of 1°/min over the range of $2\theta = 1°-10°$. X-ray analyses were performed at room temperature to injection molded specimens.

3.2 Production of Flame Retardant PP Composites

For the production of flame retardant PP composites, two different commercial intumescent flame retardants, ammonium polyphosphate (APP) / pentaerythritol (PER) combination and surface modified APP (m-APP) were used with different boron containing compounds and organoclay (Cloisite 15A). ZnB, BPO_4, metal oxide doped BPO_4, BSi, lanthanum borate (LaB), and Cloisite 15A were used with APP/PER combination for their synergistic effect. Cloisite 15A containing composites also contain maleic anhydride grafted polypropylene (PP-g-MA) to increase the dispersion of clay. For the composites containing m-APP, ZnB, BPO_4, BSi and LaB were used.

The combustion and the thermal degradation characteristics of composites were investigated by LOI, UL-94 standard, TGA, cone calorimeter and XRD.

3.2.1 Materials

PP (Petoplen EH-251) with a melt flow index (MFI, 2.16 kg, 230 °C) of 20-28 g/10min, was obtained from PETKIM A.Ş in Turkey. PP-g-MA (Exxelor PO 1015) with a melt flow index (1.2 kg, 190 °C) of 22 g/10 min, was obtained from Exxonmobil. The properties of commercially available flame retardants used in these studies are specified in Table 3.2.

Table 3.2 The properties of commercially available flame retardants

Material	Trade Name and Supplier	Specifications
APP	Exolit AP 423, Clariant	Appearance: White Powder Density: 1.9 g/cm^3 Bulk density: 0.7 g/cm^3 Particle size: D_{50} app. 8 μm P content: 31-32 %(w/w) N content: 14-15 %(w/w) Decomp. Temp.: >275
PER	Pentaerythritol, Merck	Appearance: White Powder Molecular weight: 136.15 g/mol Density: 1. 396 g/cm^3 Melting point: 255-258 ^{o}C
APP 765	Exolit AP 765, Clariant	Appearance: White Powder Density: 1.7 g/cm^3 Bulk density: 0.6 g/cm^3 P content: 23-25 %(w/w) N content: 18-20 %(w/w) Decomp. Temp.: >275

Cloisite® 15A, organoclay, was purchased from Southern Clay Products Inc. It was organically modified with dimethyl, dehydrogenated tallow, quaternary ammonium by the supplier. The chemical structure of the organic modifier is given in Figure 3.9.

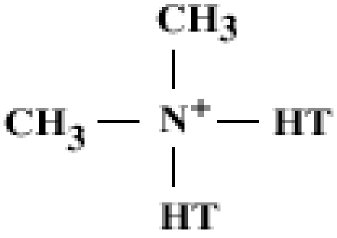

Figure 3.9 The chemical structure of the organic modifier of Cloisite 15A (HT is Hydrogenated Tallow: 65% C18; ~30% C16; ~5% C14)

3.2.1.1 Preparation of LaB

LaB was synthesized by using urea by microwave irradiation method at 1000 W starting with La_2O_3 and H_3BO_3 (molar ratio 1:2) at ambient conditions and two hours of heating was further applied at 950 °C. The characterization of LaB was made through, XRD, TGA and SEM. XRD pattern and SEM images of LaB are given in Figure 3.10 and Figure 3.11, respectively [164]. According to XRD results, LaB has orthorhombic structure Pnma space group (ICSD card no: 01-02-0762) with the unit cell parameters of a= 5.87 Aº, b= 5.26 Aº, c=5.11 Aº. SEM images show that LaB particles have irregular shapes and the grains are in submicron size. The TGA curves of boron containing substances are shown in Figure 3.12 [164]. LaB is stable at 600 ºC and its melting point is over 1000 °C [80, 164].

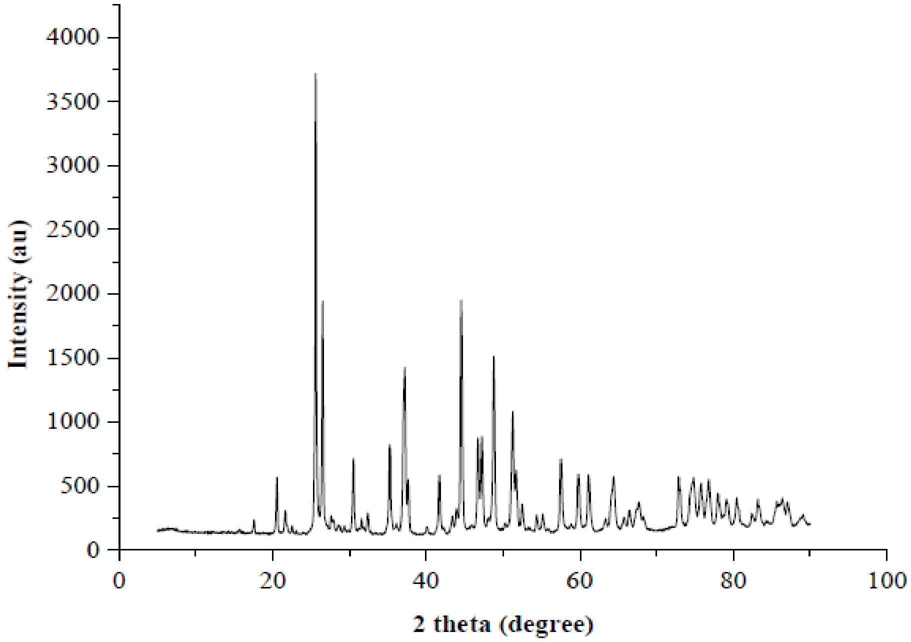

Figure 3.10 XRD pattern for LaB [164].

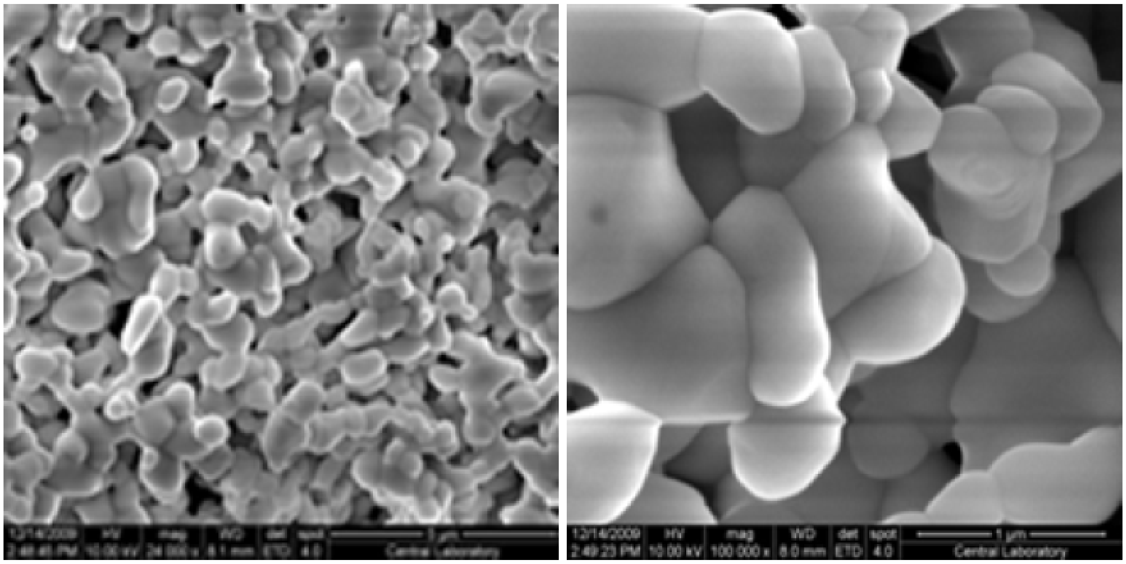

Figure 3.11 SEM images of LaB at two different magnifications [164]

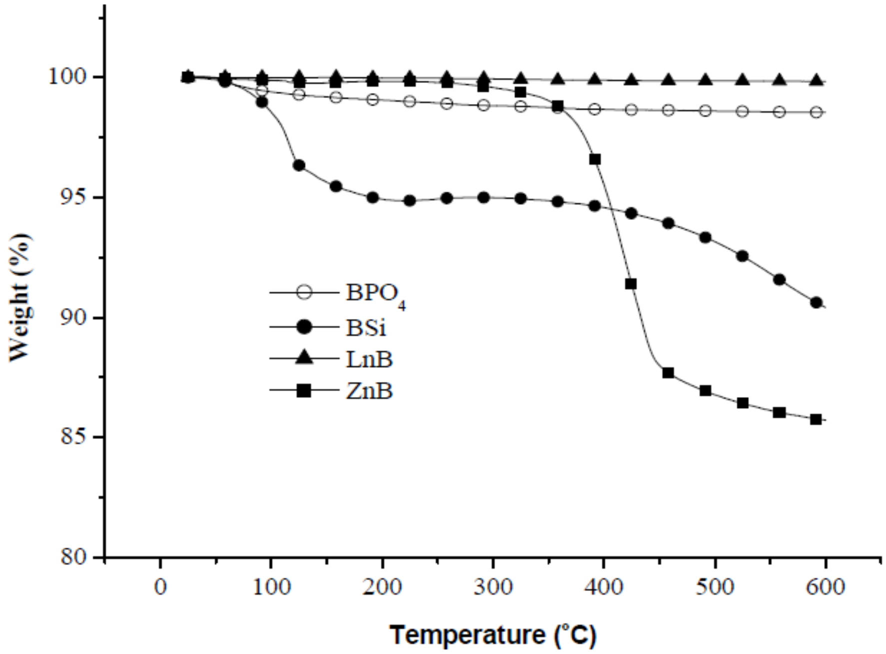

Figure 3.12 TGA curves of boron compounds [164].

3.2.1.2 Preparation of Metal Oxide Doped BPO$_4$s

1.16:1 mole ratio of $NH_4H_2PO_4$:H_3BO_3 were mixed and ground in an agar mortar. Urea (40% moles of mixture) was added to the mixture as a catalyst. Metal oxides (MnO and ZnO) were added as dopants at two different percentages of the mixture (3 and 40%). The solid mixture was placed into crucibles and then they were placed into the microwave which was adjusted to 850W (max). The mixture in each crucible started swelling because of the activation of urea. After 10 minutes of treatment, the crucibles were placed into the furnace (ramp rate: 350 ^{o}C/min). The mixture was heated at 600 ^{o}C for 2-3 hours. At the end, white solids, BPO_4: Mn^{+2} and Zn^{+2} were obtained. The characterization of Mn^{+2} and Zn^{+2} doped BPO_4 were made through XRD and SEM analysis. The XRD graphs and SEM images of Mn^{+2} and Zn^{+2} doped BPO_4s are shown in Figure 3.13 and 3. 14, respectively.

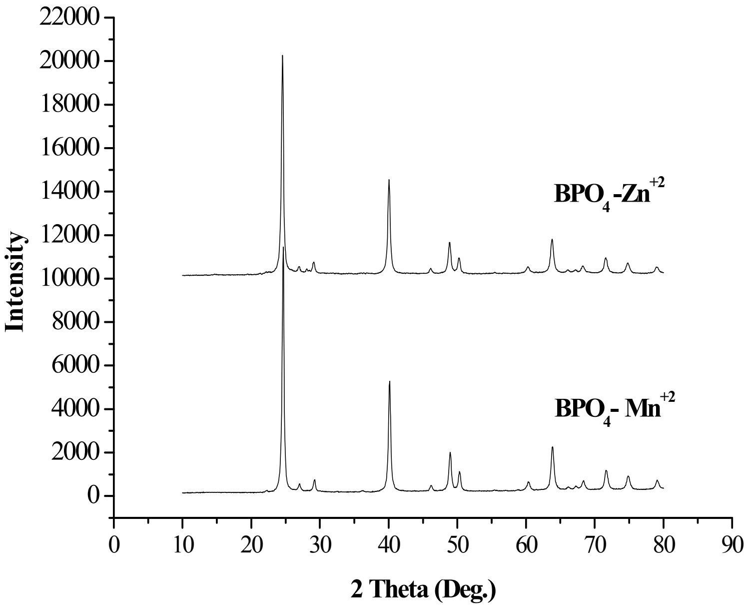

Figure 3.13 The XRD graphs of Mn+2 and Zn+2 doped BPO$_4$s

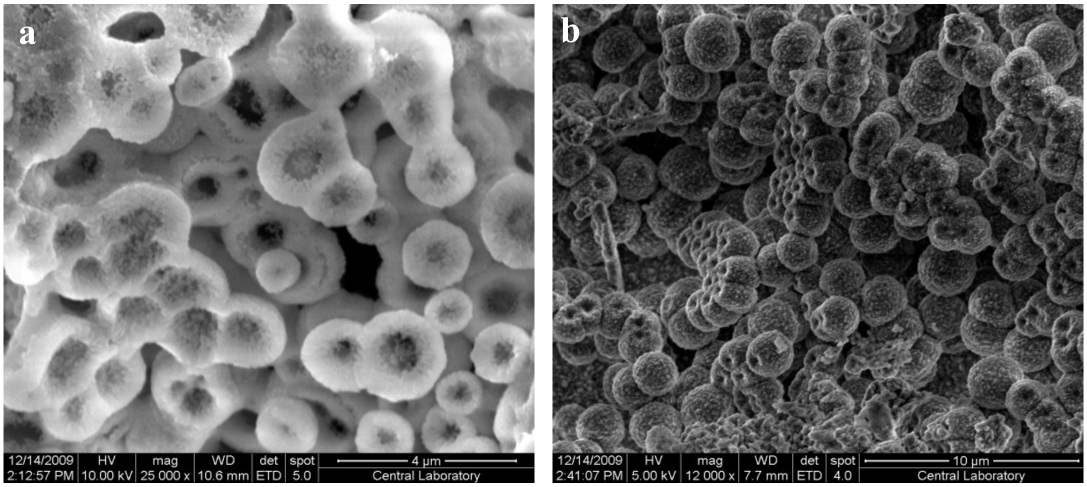

Figure 3.14 SEM images of Mn^{+2} and Zn^{+2} doped BPO$_4$s (a) Mn^{+2} BPO$_4$ (b) Zn^{+2} BPO$_4$

3.2.2 Preparation of PP Composites

Before mixing in twin screw extruder (see Figure 3.7) (Thermoprism TSE 16 TC, L/D=24) at 100 rpm and at 190 ºC, PP pellets and Cloisite 15A were dried at 80 ºC for 8 hours. The extrudate was water cooled and chopped into small pellets. The composites for flammability and thermal characterization testing were prepared by compression molding at 190 ºC. A laboratory scale hot-press machine (Rucker PHI) was used (see Figure 3.8).

3.2.3 Characterization Methods

The characterization methods used were mentioned previously in Section 3.1.3.

3.3 Production of Flame Retardant Monofilament PA-6 Fibers

Two different flame retardant PA-6 fibers were produced. The first type of flame retardant PA-6 fiber contained only BPO_4 in different amounts. For the production of second type of flame retardant PA-6 fiber, zinc bis-diethylphosphinate (ZnPi) based commercial flame retardant were used with ZnB and organoclay (Cloisite 30B) for their synergistic effect. For the first type of fiber, TGA, MFI, DSC, MCC and tensile testing were done for the characterization of samples. For the second type of fiber, TGA, MFI, MCC and tensile testing were done.

3.3.1 Materials

Fiber grade PA-6 with was kindly obtained from KORDSA GLOBAL. The properties of PA-6 and ZnPi used in this study are specified in Table 3.3. The specifications of BPO_4 were given in the previous section (see section 3.1.1.1).

Table 3.3 The properties of PA-6 and ZnPi

Material	Trade Name and Supplier	Specifications
PA-6	Kordsa Global	Density: 1.12-1.15 g/cm^3 Viscosity: 2.3- 2.8 cm^3/g T_m: 221 ^{o}C
ZnPi	Exolit OP 950, Clariant	Appearance: White Powder Density: 1.3 g/cm^3 Decomp. Temp.: >300

3.3.2 Preparation of PA-6 Fibers

PA-6 pellets were dried at 80 ºC for 24 hour before fiber spinning process. PA-6 and the flame retardants were mixed in a twin screw microextruder (15 ml microcompounder®, DSM Xplore) coupled with winding unit (DSM Xplore) at 100 rpm, 240 ^{o}C under nitrogen atmosphere. The photograph of the twin screw extruder and drawing unit is given in Figure 3.15. After mixing was complete, the twin screw extruder was brought to force controlled mode (300 N) which ensures a uniform polymer melt flow. The force was adjusted for every composition to ensure that the melt flow rate was between 0.35 g/min and 0.55 g/min. The diameter of the die was 0.25 mm. The spinning speed was 200 m/min. After the spinning process, as-spun monofilaments were obtained with varying diameters of 46-63 μm. No additional cooling was applied to the extrudate except for the ambient conditions (at about 25 ^{o}C). The as spun fibers were further drawn at 130 ^{o}C with varying draw ratios in order to avoid filament breakage.

Figure 3.15 The photograph of twin screw extruder and drawing unit used for fiber production.

3.3.3 Characterization Methods

3.3.3.1 TGA

TGA was conducted on a thermal analyzer (Perkin Elmer Diamond TG/DTA) from room temperature to 800 °C at 10 ºC/min ramp rate under flowing nitrogen.

3.3.3.2 DSC

DSC was carried out on Mettler Toledo DSC 1 Star System at a heating rate of 10 ºC/min up to 300°C under nitrogen flow of 50ml/min.

3.3.3.3 Micro Combustion Calorimeter

Fiber samples were tested with the MCC (Govmark Organization Inc., Farmingdale, NY), at 1 °C/sec heating rate under nitrogen from 200 to 600 °C, using method of ASTM D7309 (pyrolysis under nitrogen). Each sample was run in triplicate to evaluate the reproducibility of the flammability measurements. No additional conditioning of the samples was attempted prior to testing.

3.3.3.4 MFI

Melt flow index (MFI) test was performed according to ASTM D1238-79 using a Coesfield Material Test, Meltfixer LT. The measurements were done at 240 ^{o}C which corresponds to spinning temperature with a load of 2.16 kg. The weight of sample passing through the die in 10 min, defined as the melt index, was determined for all the compositions. The results were recorded as grams/10 min. The photograph of MFI machine used in this study is shown in Figure 3.16.

Figure 3.16 The photograph of melt flow index machine

3.3.3.5 Tensile Testing

The measurement of the tensile properties of monofilaments was carried out following the standard ASTM D 3822 on a tensile testing machine of Lloyd LR 5K with a load cell of 10 N. All the tests were done at about 25 ^{o}C. The length of the samples was 20 mm and the deformation rate was 20 mm/min. All the results represent an average value of twenty tests with standard deviations. For the calculation of stress values, the diameter of fiber samples was measured with a digital microscope (Veho VMS-004) using imaging software. The diameters of monofilaments were measured at 20 different places on the fiber sample and an average value was reported with standard deviations.

3.4 Production of Flame Retardant Monofilament PP Fibers

Two different types of flame retardant PP fiber were produced. The first type of flame retardant PP fiber contained only BPO_4 at different amounts. For the production of second type of flame retardant PP fiber, m-APP was used with ZnB, BPO_4 and Cloisite 15A for their synergistic effect. For the first type of fiber, TGA, MFI, DSC, MCC and tensile testing were done for the characterization of samples. For the second type of fiber, MCC. MFI. tensile testing were done.

3.4.1 Materials

All materials used for fiber production was given in Section 3.2.1

3.4.2 Preparation of Monofilament PP Fibers

PP pellets were dried at 80 ºC for 8 hours before fiber spinning process. PP and the additives were mixed in a twin screw microextruder (15 ml microcompounder®, DSM Xplore) coupled with winding unit (DSM Xplore) at 100 rpm at 230 ^{o}C for BPO_4 containing fibers and 200 ^{o}C for m-APP containing ones. After mixing was complete, the twin screw extruder was brought to force controlled mode which ensured a uniform polymer melt flow. The force was adjusted for every composition to ensure that the melt flow rate was between 0.3 g/min and 0.35 g/min. The diameter of the die was 0.25 mm. The spinning speed was 200 m/min. After spinning process, as-spun monofilaments were obtained with varying diameters of 55-70 μm. No additional cooling was applied to the extrudate except for the ambient conditions (25 ^{o}C). The as spun fibers were further drawn at 130 ^{o}C with varying draw ratios in order to avoid filament breakage.

3.4.3 Characterization Methods

The same characterization methods which were mentioned previously in section 3.1.3 were used.

CHAPTER 4

RESULTS AND DISCUSSION

In results and discussion part, the flammability characteristics of different flame retardant containing composites are discussed in separate sections with their own conclusions which are given in the conclusions part. After the combustion characteristics of composites are given, brief information is given about the flame retardants and synergistic substances that were chosen to produce flame retardant fiber. The flame retardant characteristics of fibers are again discussed in separate sections with their own conclusion.

4.1 Effect of Boron Containing Materials on Flammability and Thermal Degradation of Polyamide-6 Composites Containing Melamine Cyanurate

The total amount of flame retardants, melamine cyanurate (MC) and the boron compounds, mixed with polyamide-6 (PA-6) were maintained at 15 wt%. 1%, 3% and 5% boron compound addition correspond to 7%, 20% and 33% reduction in the amount of MC respectively. The composition of formulations and UL-94 ratings are shown in Table 4.1.

Table 4.1 The composition of formulations and UL-94 ratings

SAMPLE	PA-6	MC	ZnB	BPO_4	BSi	UL-94	t_1 (s)	t_2 (s)
N0	100	-	-	-	-	V2	7±2	15±3.5
N1	85	15	-	-	-	V0	0	0
N2	85	14	1	-	-	V0	7±1.8	11±2
N3	85	12	3	-	-	V2	9±3	8±2.5
N4	85	10	5	-	-	V2	10±1.6	11±3.2
N5	85	14	-	1	-	V0	2±0.5	2±1
N6	85	12	-	3	-	V0	1±0.4	2±0.8
N7	85	10	-	5	-	V0	3±1	5±1.3
N8	85	14	-	-	1	V0	0	0
N9	85	12	-	-	3	V2	5±2.2	2±0.8
N10	85	10	-	-	5	V2	5±2	5±1.3

4.1.1 LOI and UL- 94 Rating

LOI and UL-94 tests were made to investigate the flame retardancy behavior of PA-6 composites. t_1 and t_2 are the afterflame time after first and second ignitions, respectively. As seen from Figure 4.1, LOI value sharply increases from 22.5 % to 31.8 % when 15 wt % MC is added to PA-6. Similar results can be found in literature [28, 114, 165]. The inclusion of boron compounds causes the reduction of the LOI values of PA-6 composites. In the absence of any synergy, the LOI values will decrease when the amount of the effective FR agent (MC) is reduced. This is the general trend observed in Figure 4.1. Another reason why a large reduction of LOI values is obtained for both BSi and ZnB is due to the ability of glassy surface formation during combustion. This glassy structure formed over the liquid combustion phase slows down the sublimation of melamine which is one of the flame retarding mechanisms. The only discrepancy is for BPO_4 where for 1% BPO_4 addition there is the expected reduction and for 3% and 5% BPO_4 addition the trend is reversed with slight increase in the LOI. BPO_4 increases the dripping rate, hence removing the flame source from location of fire, giving rise to V0 rating and high LOI values. Why the drip rate increases is most probably due to increase in the drop density (heavier) with the inclusion of BPO_4 (stable up to 1200

°C). The other boron compounds (BSi and ZnB) decompose much earlier (from TGA data) and are not as effective as BPO_4 in increasing the density of the drop. The dripping rate is also a function of the surface tension of the pendant drop hanging from the sample tip. BPO_4 being stable in solid form will not change low surface tension of PA-6 and MC where decomposing BSi and ZnB can increase the drop surface tension giving rise the reduced dripping rates.

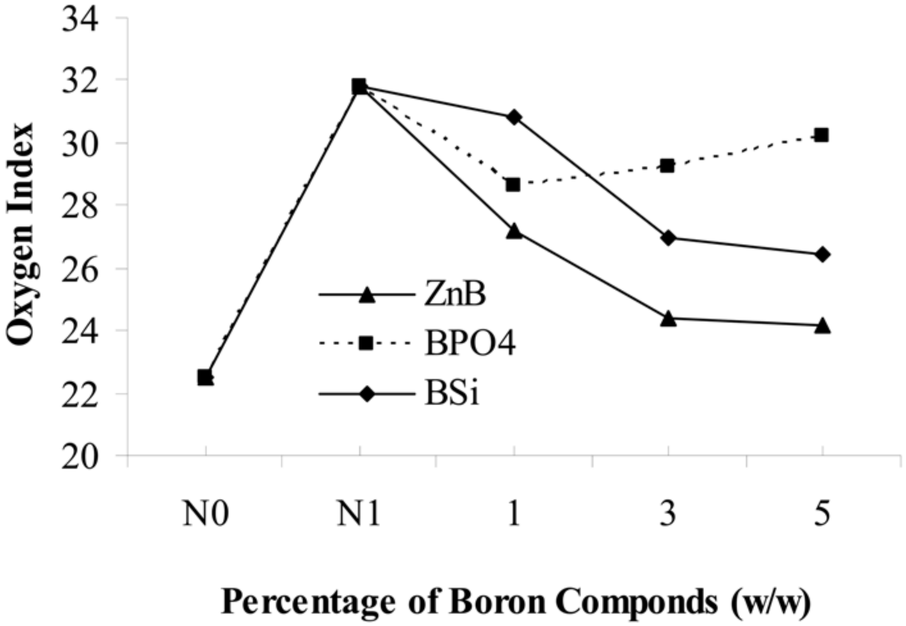

Figure 4.1 The LOI values of composites

According to UL-94 test, total burning time (t_1+t_2) of all samples, except N0, is less than 30 seconds (Table 4.1) and extinguishes after first dripping. t_1 and t_2 are the after-flame time after first and second ignitions, respectively. 1 wt % ZnB and BSi containing composites are V0 and 3 and 5 wt % containing ones are V2. All BPO_4 containing composites were V0 due to increased dripping rate.

4.1.2 Thermogravimetric Analysis (TGA)

TGA can serve as a useful indicator of polymer flammability. TGA curves of selected compositions are shown in Figure 4.2. TGA data of composites are listed in Table 4. 2.

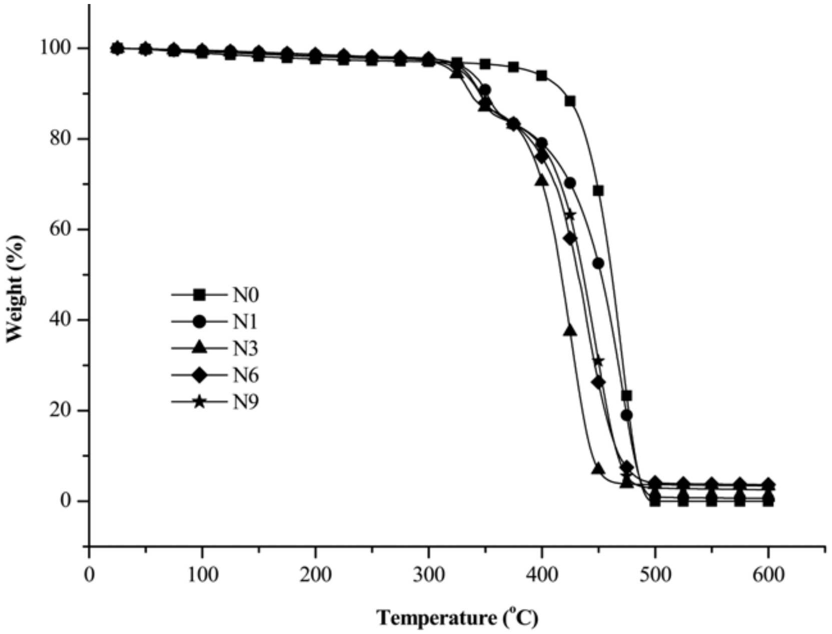

Figure 4.2 TGA curves of selected compositions

According to Figure 4.2 and Table 4.2, the weight loss of pure PA-6 takes place in a single step, with maximum weight loss rate at 471 °C without any char residue at 600 °C. The inclusion of MC slightly increases the char yield from 0 to 0.6 %. It may arise from thermally stable condensates (melam, melem and melon) of melamine [9]. Two weight loss steps are seen in the TGA curves in PA-6 containing MC. The first step can be attributed to the decomposition of MC and the second step arises from the decomposition of PA-6 [14, 28, 114, 165]. Boron compounds slightly increase the decomposition rate of MC around 350 °C. Around 450 °C, there is a larger difference in the amount of decomposition of PA-6 and MC with boron compounds compared to N1 Sample. The largest effect is observed for ZnB which also gives the largest reductions in LOI values. The decomposition of PA-6 and MC is least affected by BSi which also at 1wt% loading gives higher LOI than BPO_4. There may be a relationship between LOI and TGA data in the sense that premature evolution of the decomposition products later reduces the amount of MC available as fire retarding agent close to the flame temperature. The inclusion of boron compounds increases the char yield. The char formation has a negative effect on dripping and causes a reduction of LOI.

Table 4.2 TGA data of all composites

SAMPLE	$T_{5\%}$ (°C)	$T_{50\%}$ (°C)	T_{max} (°C) Stage 1	 Stage 2	Char Yield (%)
N0	335	461	-	471	0
N1	335	452	350	469	0.6
N2	337	442	352	461	1.53
N3	320	417	335	426	3.34
N4	320	415	335	423	4.16
N5	331	432	342	436	2.39
N6	328	428	344	436	3.63
N7	331	431	343	441	6
N8	330	443	340	454	1.1
N9	328	436	344	445	2.49
N10	334	444	336	446	6.26

$T_{5\%}$:5% decomposition temperature; **$T_{50\%}$:** 50% decomposition temperature;
T_{max}: Maximum decomposition temperature.

4.1.3 SEM Analysis

SEM micrographs of char residues after heating of the composites around 500 ºC for 30 minutes are given in Figure 4.3. The surface structure of residual char changes quiet a lot by the addition of MC. The residual char structure of N1 is more compact than pure N0. This can be a proof of condensed phase mechanism of MC. BSi and BPO_4 particles can be easily seen on SEM images of N6 and N9. This can also be a proof of the char yield increase. BPO_4 particles are smaller than that of BSi. On the other hand, the solid decomposition products of ZnB seem to be integrated into the char structure [28].

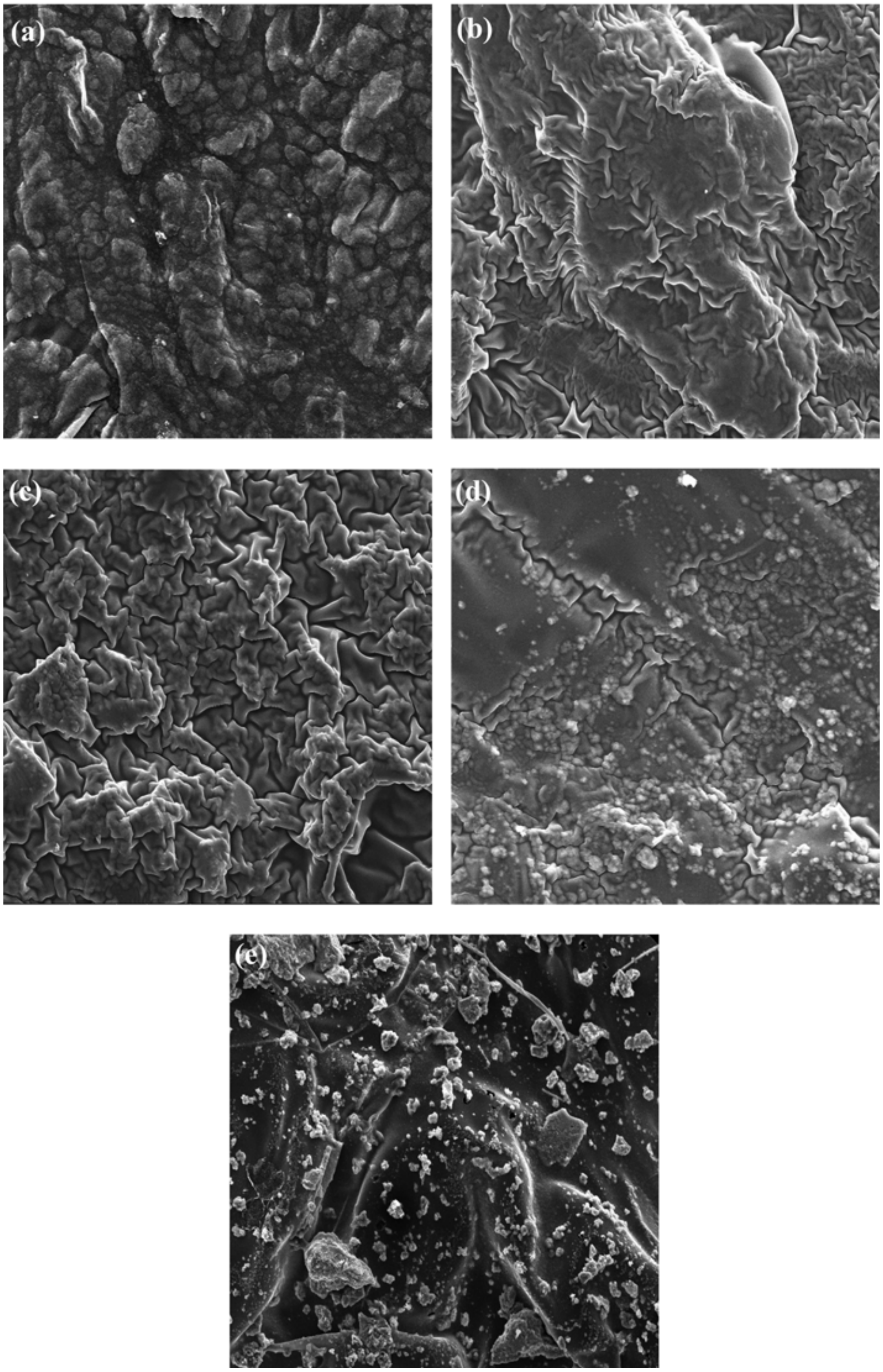

Figure 4.3 SEM micrographs of char residues of a) N0 b) N1 c) N3 d) N6 e) N9

4.1.4 Differential Scanning Calorimeter (DSC)

DSC curves and data of selected compositions are shown in Figure 4.4 and Table 4.3. Two endothermic peaks are seen in DSC curves. First endothermic peak is attributed to melting of PA-6 crystals and the second peak results from the decomposition of MC. According to DSC data, T_m (melting temperature) shifts to lower values with respect to PA-6 (N0). This may result from the formation of thinner and less perfect crystals. The inclusion of MC did not change ΔH_m (enthalpy of melting) whereas the inclusion of boron compounds increases the ΔH_m. This may result from the heterogeneous nucleation role of boron compounds. Addition of boron compounds except BSi reduces T_d (decomposition temperature) onset of the MC. ΔH_d (enthalpy of decomposition) of the ZnB containing sample is higher than that of BSi and BPO_4 ones because ZnB decomposes endothermically like MC at about same temperature. Although the ZnB containing sample shows the highest ΔH_d, it is interesting that it shows lower LOI values than that of BSi and BPO_4 containing ones [28].

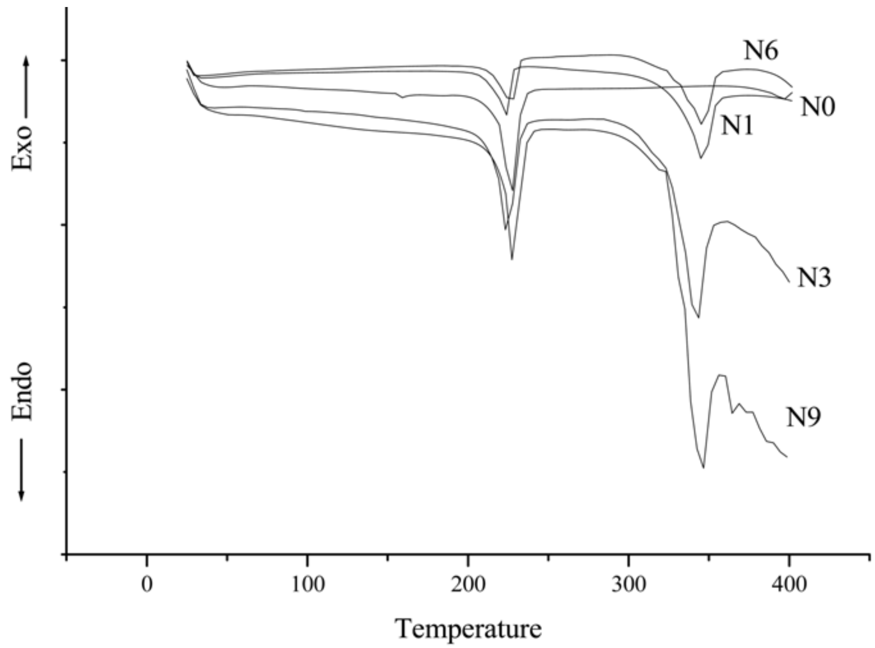

Figure 4.4 DSC curves of selected compositions

Table 4.3 DSC data of selected compositions

SAMPLE	$T_{m\ onset}$ (°C)	ΔH_m (J/g)	T_{sub} (°C)	ΔH_d (J/g)
N0	221	54.0	-	-
N1	216	45.0	337	111.5
N3	219	49.5	330	100.0
N6	214	48.5	328	87.0
N9	220	50.0	339	83.0

ΔH_m: Enthalpy of melting; **ΔH_{sub}:** Enthalpy of sublimation;
T_m: Melting temperature; **T_{sub}:** sublimation temperature.

4.1.5 Thermal Degradation

Thermal degradation of composites was investigated using TGA-FTIR spectroscopy to examine the changes by the addition of MC and boron compounds. FTIR spectra of selected composites at 350 °C and 450 °C are given in Figures 4.5 and 4.6, respectively. According to Figure 4.5, weak absorption peaks seen at 2939 cm^{-1} (CH_2), 1714 cm^{-1} (lactam) and 930 and 965 cm^{-1} (NH_3) show that PA-6 starts to decompose at 350 ºC [166]. The peaks seen at 2251 and 2285 cm^{-1} are due to CN stretching mode of cyanic acid. The characteristic peak of cyanuric acid must be seen at 1787 cm^{-1} which is absent. This result shows that almost all cyanuric acid is converted to the cyanic acid [167, 168]. The characteristic peak of melamine is seen at 1601 cm^{-1} (NH_2 scissoring and ring stretching) and 1440 cm^{-1} (ring and side chain CN stretching), 816 cm^{-1} (ring deformation), 3577 cm^{-1} (asymmetric N-H stretching vibrations), 3453 cm^{-1}(symmetric N-H stretching vibrations). These results show the sublimation of melamine taking place [167-170].

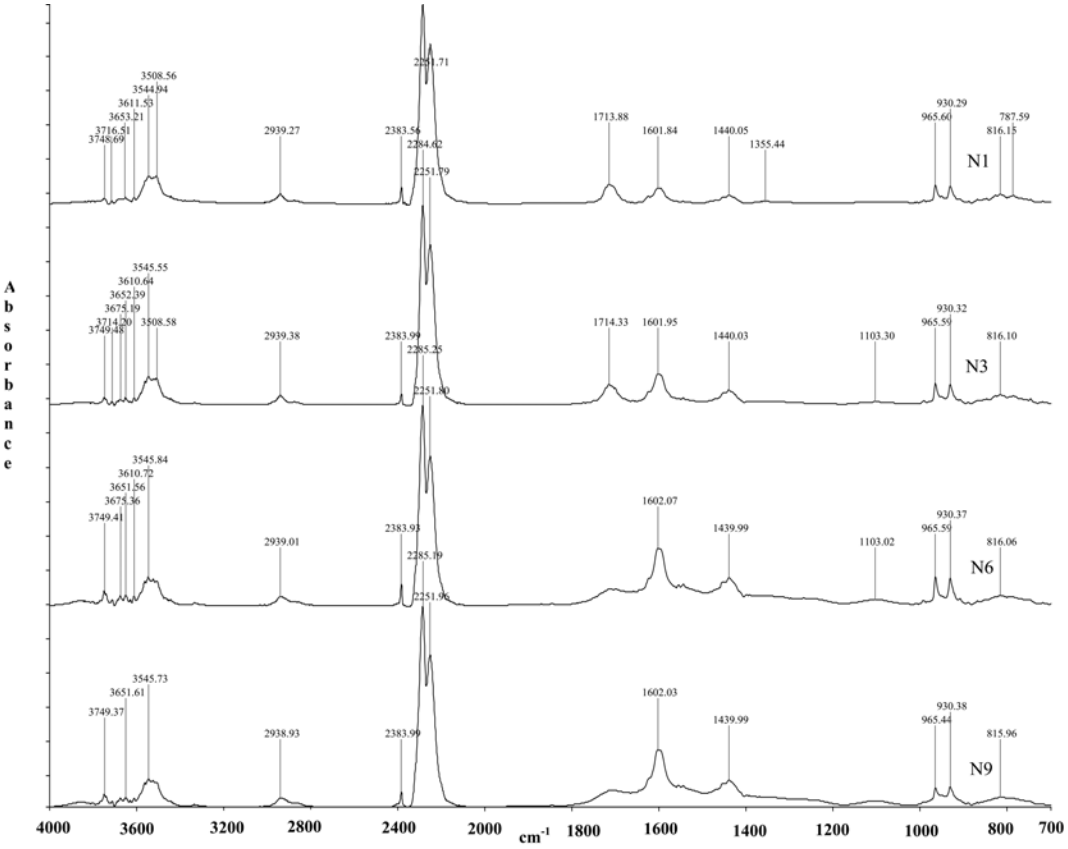

Figure 4.5 FTIR spectra of evolved gases from selected composites at 350 °C

According to Figure 4.6, CH_2 groups (2939 cm^{-1}, 2871 cm-1) and lactam absorption (1714 cm^{-1}) show that PA-6 decomposes by ϵ-caprolactam formation [166]. Vaporization of cyanic acid is completed since the peaks seen at 2284 and 2251 cm^{-1} almost disappeared. The inclusion of MC into PA-6 has no influence on the degradation product distribution. Characteristic peaks of melamine (1601 and 1440 cm^{-1}) show that the sublimation of melamine still continues at 450 ºC. A lot of small peaks, which may result from the compounds containing CN and NH_2 end groups, are observed between 1350 and 1120 cm^{-1} [166,170]. From the TGA-FTIR results, it is concluded that boron compounds used in this study do not change gaseous product distribution formed during both the decomposition of MC and PA-6. The products formed in the condensed phase may be different.

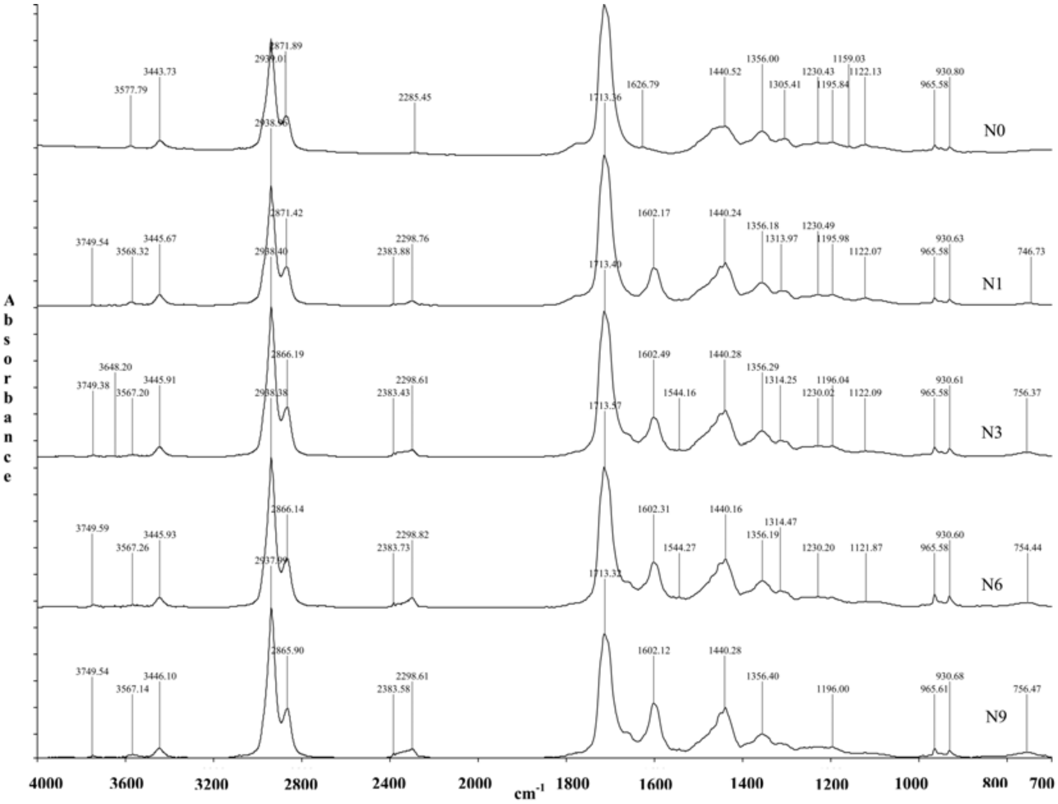

Figure 4.6 FTIR spectra of evolved gases from selected composites at 450 °C

4.2 Effect of Boron Containing Materials on Flammability and Thermal Degradation of Polyamide-6 Composites Containing Melamine

The total amount of flame retardants, melamine and boron compounds, mixed with PA-6 were maintained at 20 wt%. 1, 3 and 5 wt% boron compound addition correspond to 5, 15 and 25 % reduction in the amount of melamine, respectively. The composition of formulations and their UL-94 ratings are shown in Table 4.4.

Table 4.4 The composition of formulations and their UL-94 ratings

SAMPLE	PA-6	Melamine	ZnB	BPO_4	BSi	UL-94
NM0	100	--	--	--	--	V2
NM1	80	20	--	--	--	V0
NM2	80	19	1	--	--	V2
NM3	80	17	3	--	--	V2
NM4	80	15	5	--	--	V2
NM5	80	19	--	1	--	V0
NM6	80	17	--	3	--	V0
NM7	80	15	--	5	--	V0
NM8	80	19	--	--	1	V0
NM9	80	17	--	--	3	V0
NM10	80	15	--	--	5	V2

4.2.1 LOI and UL-94 Rating

LOI and UL-94 tests were made to investigate the flame retardancy behavior of PA-6 composites. As seen from Figure 4.7, LOI value sharply increases from 22.5% to 31% when 20 wt% melamine is added to PA-6. Similar results can be found in the literature [31, 165, 171]. Except for 1 wt% BSi containing composite, addition of boron compounds reduces the LOI value with respect to NM1. Addition of 1 wt % BSi slightly increases the LOI value from 31% to 31.4 %. In the absence of any synergy, the LOI values will decrease when the amount of the effective flame retardant agent (melamine) is reduced. This is the general trend observed in Figure 4.7. Another reason why a large reduction of LOI values is obtained for both BSi and ZnB is due to the ability of glassy surface formation during combustion. This glassy structure formed over the liquid combustion phase slows down the sublimation of melamine. The reduction in the rate of sublimation of melamine has two effects during combustion. First heat sink action of melamine is reduced, and secondly dilution of combustible gases is reduced. Interestingly, it is observed that BPO_4 containing composites reach minimum LOI value (28.8 %) when the composite contained 1 wt % BPO_4 and then LOI value increases to 29.8 % when the amount of BPO_4 reaches to 5 wt %. BPO_4 has spherical shape with high melting point (1000 °C) and thermal stability (up to 1200°C).

BPO_4 particles are stable and increase the dripping rate. The increase of dripping rate of PA-6 which removes the fuel source from the combustion zone gives rise to V0 rating and high LOI values. The dripping rate is also a function of the surface tension of the pendant drop hanging from the sample tip. BPO_4 being stable in solid form will not change the low surface tension of PA-6 and melamine where decomposing BSi and ZnB can increase the drop surface tension giving rise to the reduced dripping rates. To understand the increase of LOI trend at higher BPO_4 loadings, 10 wt % BPO_4 containing composite was prepared and 22 % LOI value and V2 rating was obtained. The trend, therefore, is reversed because of the inadequate amount of melamine.

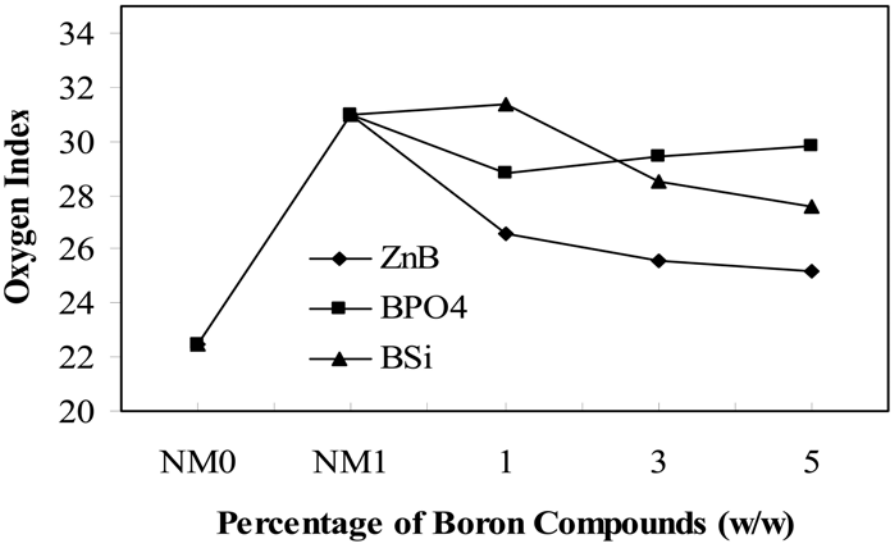

Figure 4.7 The LOI value of composites

According to UL-94 test, total burning time (t_1+t_2) of all samples, except NM0, is less than 20 seconds. t_1 and t_2 are the afterflame time after first and second ignitions, respectively. All BPO_4 and ZnB containing samples show V0 and V2 rating respectively at all concentrations tested. On the other hand, ZnB has the ability of forming glassy surface. This glassy layer slows down the flame retarding mechanism of melamine as mentioned above.

4.2.2 Thermogravimetric Analysis (TGA)

TGA can serve as a useful indicator of polymer flammability. TGA curves of selected compositions are shown in Figure 4.8. TGA data of all composites are listed in Table 4.5.

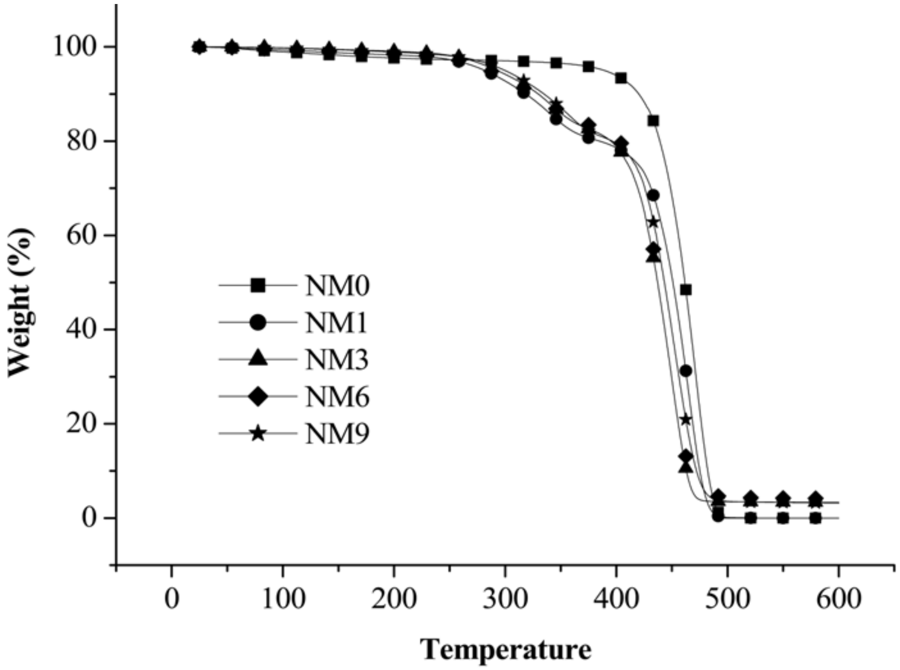

Figure 4.8 TGA curves of selected compositions

Table 4.5 TGA data of all composites

SAMPLE	$T_{5\%}$	$T_{50\%}$	T_{max} (^oC) Stage 1	Stage 2	Char Yield (%)
NM0	335	461	-	471	0.00
NM1	281	450	334	462	0.00
NM2	279	436	319	440	2.79
NM3	292	437	338	445	3.29
NM4	285	435	329	444	4.49
NM5	284	432	337	443	2.15
NM6	285	438	334	442	4.09
NM7	276	439	328	450	6.06
NM8	272	436	325	453	1.73
NM9	299	443	356	446	3.18
NM10	280	430	328	436	5.23

$T_{5\%}$:5% decomposition temperature; **$T_{50\%}$:** 50% decomposition temperature; **T_{max}:** Maximum decomposition temperature.

According to Figure 4.8 and Table 4.5, the weight loss of pure PA-6 takes place in a single step, with a maximum of weight loss rate at 471 °C without any char residue at 600 °C. Two weight loss steps are seen in the TGA curves of PA-6 containing melamine. The first step can be attributed to the sublimation of melamine and the second step is arising from the decomposition of PA-6 [31, 165, 171]. The composite containing only melamine has no char residue at 600 °C. From the previous work with MC, addition of MC increases the char yield from 0 % to 0.6 % [28]. The inclusion of boron compounds increases the char yield. The char yield of BPO_4 and BSi containing composites is higher than the ZnB containing ones, because BPO_4 and BSi were almost thermally stable up to 600 °C. From the $T_{5\%}$ values, it is seen that the melamine destabilizes the PA-6. Although the mechanism of destabilization of PA-6 is not clear, it may be interference of the hydrogen bonding or a basic catalytic effect, aminolysis or ammonolysis by evolved ammonia. [12]. The inclusion of boron compounds reduces $T_{\%50}$ and the decomposition temperature (T_{max}) of PA-6 as shown in Table 4.5.

4.2.3 Differential Scanning Calorimeter (DSC)

DSC curves and data of selected compositions are shown in Figure 4.9 and Table 4.6. Two endothermic peaks are observed in DSC curves except that of NM0 (PA-6). First endothermic peak is attributed to melting of PA-6 crystals and the second peak results from the sublimation of melamine. The inclusion of melamine reduces ΔH_m by nearly 3 J/g taking into account the lower PA-6 content, whereas the inclusion of boron compounds increases the ΔH_m. This may result from the heterogeneous nucleation role of boron compounds. The sublimation enthalpy of ZnB added sample is almost equal to that of melamine due to its endothermic decomposition. The other two boron compounds do not decompose significantly at these temperatures, so, there is a drop in ΔH_{sub} with decrease of melamine percentage. It may be concluded that the addition of boron compounds do not affect the sublimation temperature of melamine.

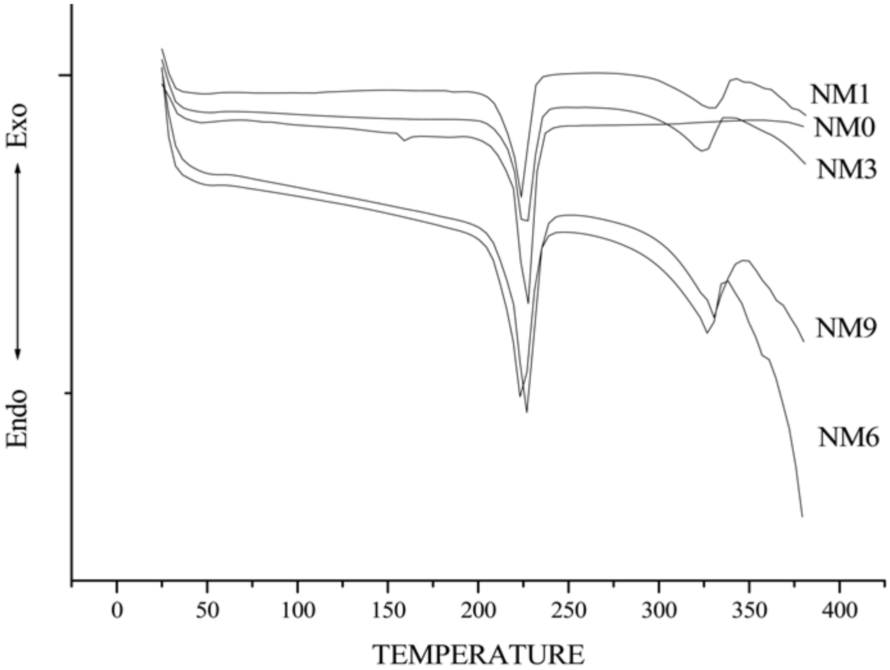

Figure 4.9 DSC curves of selected compositons

Table 4.6 DSC data of selected compositions

SAMPLE	T_m	ΔH_m (J/g)	T_{sub}	ΔH_{sub} (J/g)
NM0	227.5	54.0	-	-
NM1	226.0	40.0	330	21.3
NM3	226.0	42.0	330	21.5
NM6	224.5	44.3	329	20.5
NM9	228.0	44.5	331	20.2

ΔH_m: Enthalpy of melting; **ΔH_{sub}:** Enthalpy of sublimation;
T_m: Melting temperature; **T_{sub}:** sublimation temperature.

4.2.4 Thermal Degradation

Thermal degradation of composites in N_2 atmosphere was investigated using TGA-FTIR spectroscopy to examine the variations when melamine and boron compounds were added. FTIR spectra of decomposition gases of selected composites at 350 °C and 450 °C are given in Figures 4.10 and 4.11, respectively.

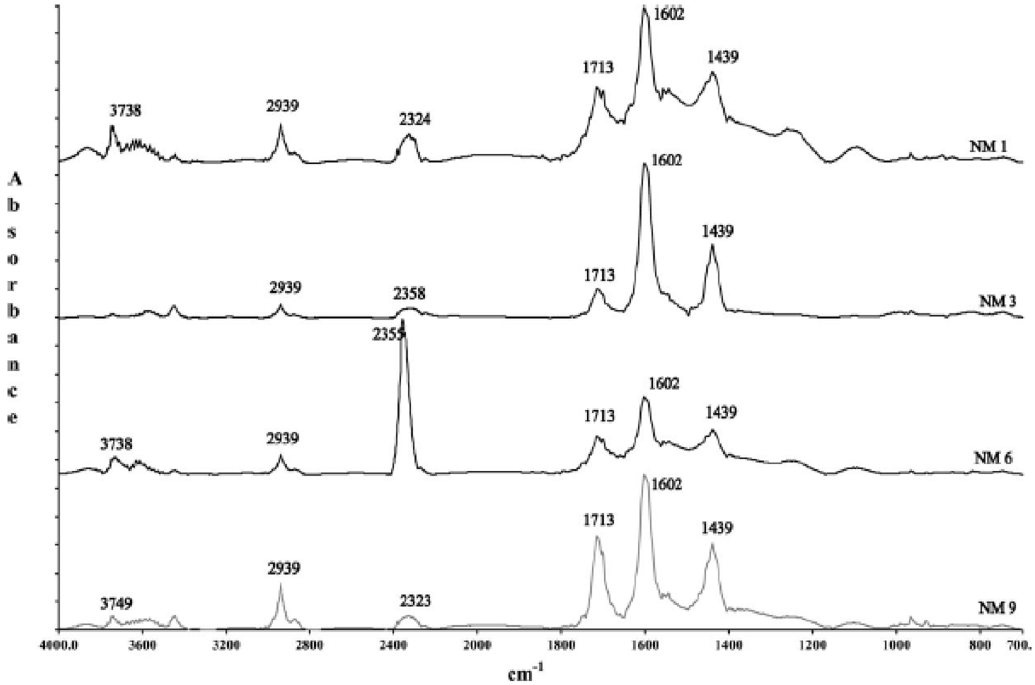

Figure 4.10 FTIR spectra of decomposition gases of selected composites at 350 °C

According to Figure 4.10, CH_2 groups (2939 cm^{-1}) and lactam absorption (1713 cm^{-1}) shows that PA-6 starts to decompose at 350 °C [31, 171]. The characteristic peak of melamine is seen at 1601 cm^{-1} (NH_2 scissoring and ring stretching) and 1440 cm^{-1} (ring and side chain CN stretching). These peaks show that melamine starts to sublime. The peak observed at 2350 cm^{-1} results from the formation of CO_2. Herrara et al. studied the TGA-FTIR of PA-6 under nitrogen atmosphere and in air. CO_2 formation in air is much higher than in nitrogen atmosphere [172]. The formation of CO_2 increases under nitrogen atmosphere when BPO_4 is added into sample composition. Kılınç et al. studied the decomposition product distribution BPO_4 using mass spectroscopy and showed that the decomposition products were BPO_4, BPO_3, $BPO^{\cdot}$, PO_4, O_2 [83]. It may be speculated that the small amount of O_2 formation during the decomposition of BPO_4 (NM6) gives rise to the formation of CO_2 observed at around 2350 cm^{-1}. According to these results, BPO_4 can be a source of oxygen and favors the CO_2 formation under nitrogen atmosphere at given temperature.

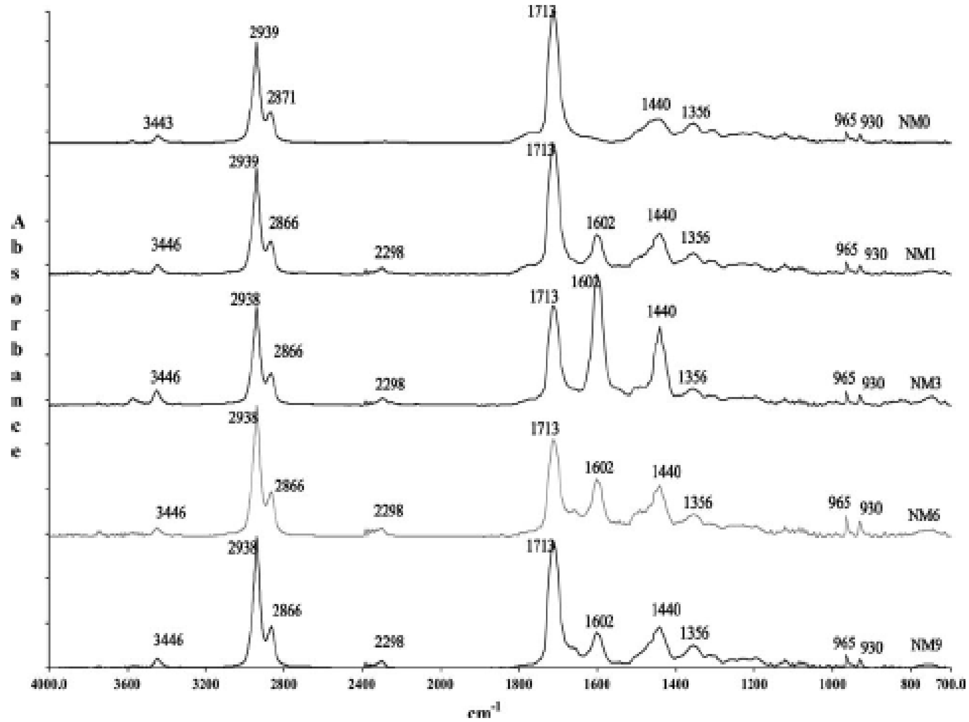

Figure 4.11 FTIR spectra of decomposition gases of selected composites at 450 °C

According to Figure 4.11, the peaks at 2939 cm^{-1} (CH_2 group), 1713 cm^{-1} (lactam absorption) and 930 and 965 cm^{-1}(NH_3) show that PA-6 decomposes by ϵ-caprolactam formation. Characteristic peaks of melamine (1601 and 1440 cm^{-1}) show that the sublimation of melamine still continues at 450 ºC. There are a lot of small peaks, which may result from the compounds containing CN and NH_2 end groups that are observed between 1120 and 1350 cm^{-1} [166-170]. From the TGA-FTIR results, it is observed that boron compounds used in this study do not change gaseous products formed during both the decomposition of melamine and PA-6. The products formed in the condensed phase may be different.

4.3 Effect of Boron Containing Materials on Flammability and Thermal Degradation of Polyamide-6 Composites Containing Red Phosphorus

The total amount of flame retardants, red phosphorus (P-red) and boron compounds, mixed with PA-6 were maintained at 10 wt%. The composition of formulations and their UL-94 ratings are shown in Table 4.7.

Table 4.7 The composition of formulations their UL-94 ratings and LOI values

SAMPLE	PA-6	RP	ZnB	BPO_4	UL-94	LOI
NRP0	100	-	-	-	V2	22.5
NRP1	90	10	-	-	V2	23.0
NRP2	90	9	1	-	V2	24.0
NRP3	90	7	3	-	V2	26.0
NRP4	90	5	5	-	V2	24.5
NRP5	90	9	-	1	V2	25.0
NRP6	90	7	-	3	V2	26.0
NRP7	90	5	-	5	V2	24.0

4.3.1 LOI and UL-94 Rating

LOI and UL-94 tests were done to investigate the flame retardancy behavior of PA-6 composites. As seen from Table 4.7, LOI value of PA-6 slightly increases from 22.5 % to 23 % because of the condensed phase action of P-red by the formation of phosphoric acid ester on burning polymer surface and gas phase action by radical scavenging with the addition of 10 wt % P-red [12, 32, 36, 37, 173]. UL-94 rating does not change both with the addition of P-red and boron compounds because the composites released flaming drips during burning. The LOI value increases with the addition of boron compounds with respect to NRP1. The highest LOI values are obtained when the boron compounds are used at 3 wt % which corresponds to 30 % reduction of the effective flame retardant agent (P-red). Although the addition of boron compounds does not alter the UL-94 rating, the increase at LOI values is the indication of synergy between P-red and boron compounds.

4.3.2 Thermogravimetric Analysis (TGA)

TGA curves of selected compositions are shown in Figure 4.12. TGA data of all composites are listed in Table 4.8. According to Figure 4.12 and Table 4.8, the weight loss of pure PA-6 takes place in a single step, with maximum weight loss rate at 471 °C without any char residue at 800 °C. According to $T_{5\%}$ value which gives information about the initial thermal stability of composites, the inclusion of P-red increases thermal stability at low temperatures. The thermal instability of P-red at higher temperatures due to the formation of toxic phosphine gas formation causes the reduction at $T_{50\%}$ and T_{max} by about 55 ^{o}C with respect to PA-6 [29, 36]. The addition of P-red increases the char yield from 0 to 2% due to formation of phosphoric acid ester [36, 37, 173]. The addition of boron compounds increases the char yield as the amount of boron compound increases. The addition of ZnB increases the thermal stability of P-red by retarding the phosphine gas formation [12, 36].

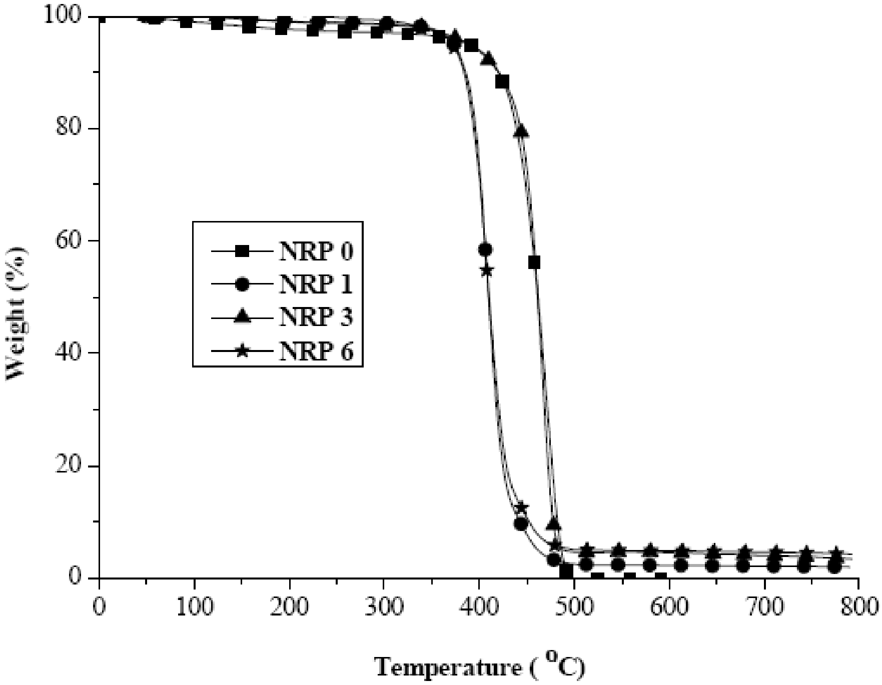

Figure 4.12 TGA curves of selected compositions

Table 4.8 TGA data of all composites

SAMPLE	$T_{5\%}$ (°C)^{a}	$T_{50\%}$ (°C)^{b}	T_{max} (°C)^{c}	Char Yield (%)^{d}
NRP0	335	461	471	0
NRP1	372	409	415	2.0
NRP2	372	413	468	2.5
NRP3	389	461	470	3.4
NRP4	377	416	472	11.0
NRP5	374	410	412	3.6
NRP6	371	410	410	4.3
NRP7	373	410	407	5.4

a: Temperature at 5% weight loss **b**: Temperature at 50% weight loss
c: The maximum rate degradation temperature **d**: Char Yield at 800 °C

4.3.3 Cone Calorimeter

Table 4.9 and Figure 4.13 show the cone calorimeter data of selected compositions and their HRR curves obtained from the cone calorimeter test at a heat flux of 35 kWm^{-2}, respectively. According to Figure 4.13, PA-6 burns very fast after ignition and one sharp HRR peak appears with a heat release peak of 975 kWm^{-2}. The addition of P-red with and without boron compounds changes the shape of HRR curve and they resemble each other. The characteristics of these peaks are a broad shoulder seen at the beginning of the HRR curve and get broadened due to the increasing the total burning time with lower PHRR. The addition of P-red reduces both the maximum HRR and THR from 975 to 700 kWm^{-2} and from 155 to 129 MJ.m^{-2} because of the formation of phosphoric acid ester species on the burning surface. Although the addition of BPO_4 and ZnB causes a further reduction of maximum and average HRR values, only the ZnB causes a further reduction at THR value due to the formation of high amount of phosphoric acid ester species which is the precursor of the char by retarding the phosphine gas formation.

Table 4.9 Cone calorimeter data of selected composites

Sample	TTI (s)	PHRR (Kw.m^{-2})	Average HRR (Kw.m^{-2})	THR (MJ. m^{-2})
NRP0	123	975	475	155
NRP1	51	700	452	129
NRP3	57	560	347	114
NRP6	62	655	380	150

TTI: Time to ignition, **HRR:** Heat Release Rate **THR:** Total Heat Release Rate

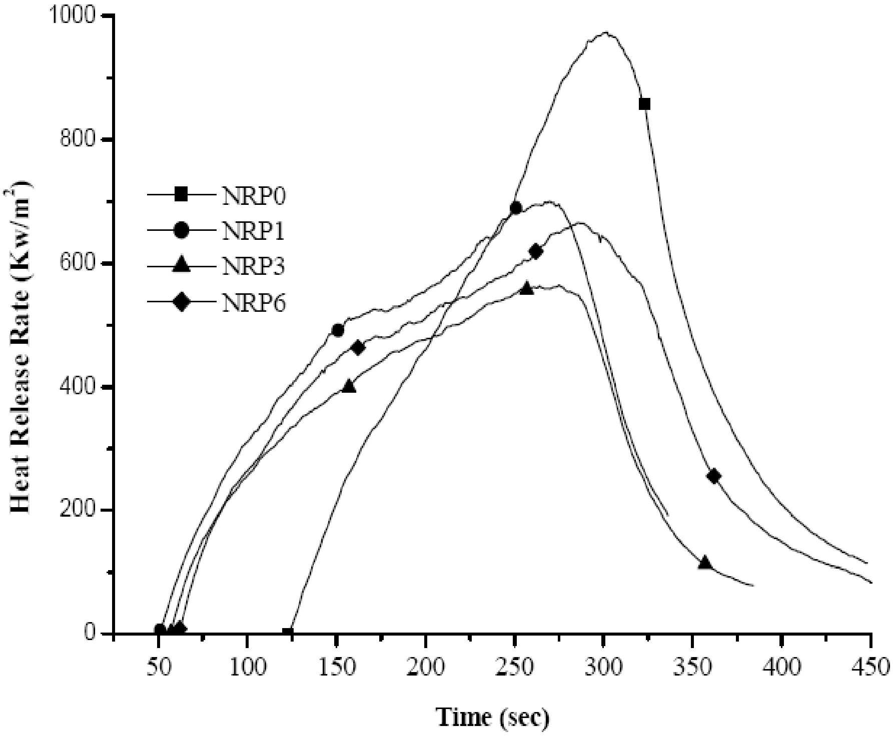

Figure 4.13 HRR curves of selected composites

4.4 The Flame Retardant Effect of Aluminum Phosphinate in combination with Zinc borate, Borophosphate and Nanoclay in PA-6

The total amount of flame retardants mixed with PA-6 were maintained at 15 wt %. The composition of formulations, LOI values and UL-94 ratings are given in Table 4.10.

Table 4.10 The composition of formulations, LOI values and UL-94 ratings

SAMPLE	PA-6	AlPi	ZnB	BPO_4	Closite 30 B	UL-94	LOI
OP1	100	-	-	-	-	V2	22.5
OP2	85	15	-	-	-	V0	29.5
OP3	85	14	1	-	-	V0	29.5
OP4	85	12	3	-	-	V0	30.0
OP5	85	14	-	1	-	V0	29.0
OP6	85	12	-	3	-	V0	29.0
OP7	85	14	-	-	1	V0	29.5
OP8	85	13	1	-	1	V0	31.0
OP9	85	13	-	1	1	V0	29.5

4.4.1 Morphology Characterization by WAXS

Figure 4.14 shows the XRD patterns for Closite 30B and OP7. Closite 30B shows a peak at $2\theta = 4.9^o$ corresponding to basal spacing of 17.9 A°. XRD pattern for OP7 does not show a characteristic basal reflection, which is an indication of completely exfoliated structure [174].

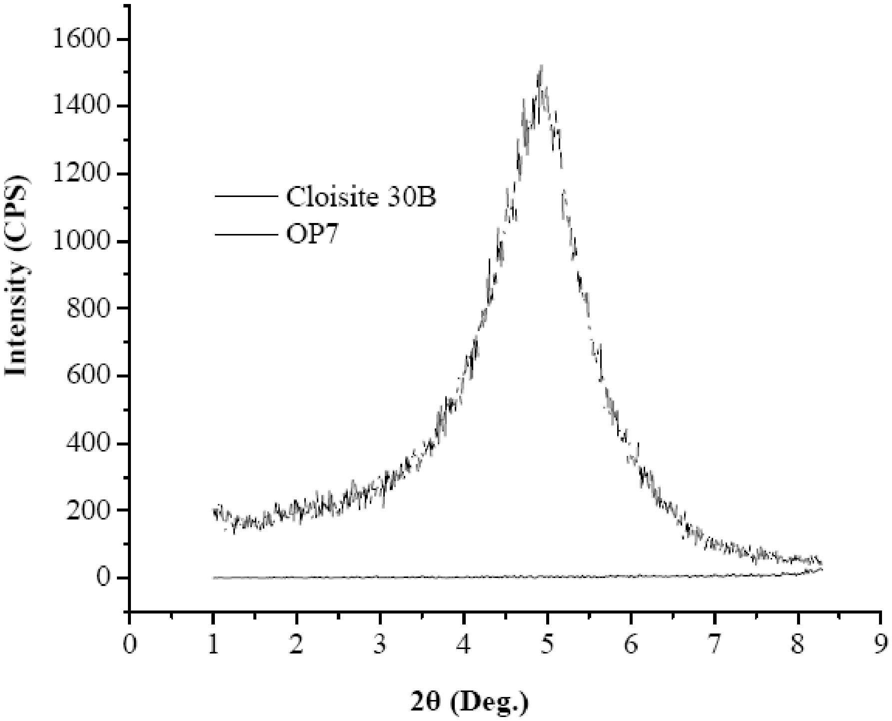

Figure 4.14 XRD Pattern for Cloisite 30B and OP-7

4.4.2 Thermal Decomposition

Thermal decomposition behavior of the composites is characterized by TGA and FTIR analysis of char residues. TGA curves of selected compositions and TGA data of all composites are given in Figure 4.15 and Table 4.11, respectively. According to Figure 4.15, all composites decompose in one main decomposition step. PA-6 (OP1) decomposes with maximum weight loss rate at 463 °C without any char residue at 800 °C. The addition of AlPi into PA-6 (OP2) decreases $T_{5\%}$, $T_{50\%}$ and T_{max} value by 7°C, 15°C, 28 °C, respectively and increases the char yield from 0 to 1%. According to FTIR results of OP2, a broad peak seen at 1030 cm^{-1} is caused by aluminum phosphinate that is the main component of char [175].

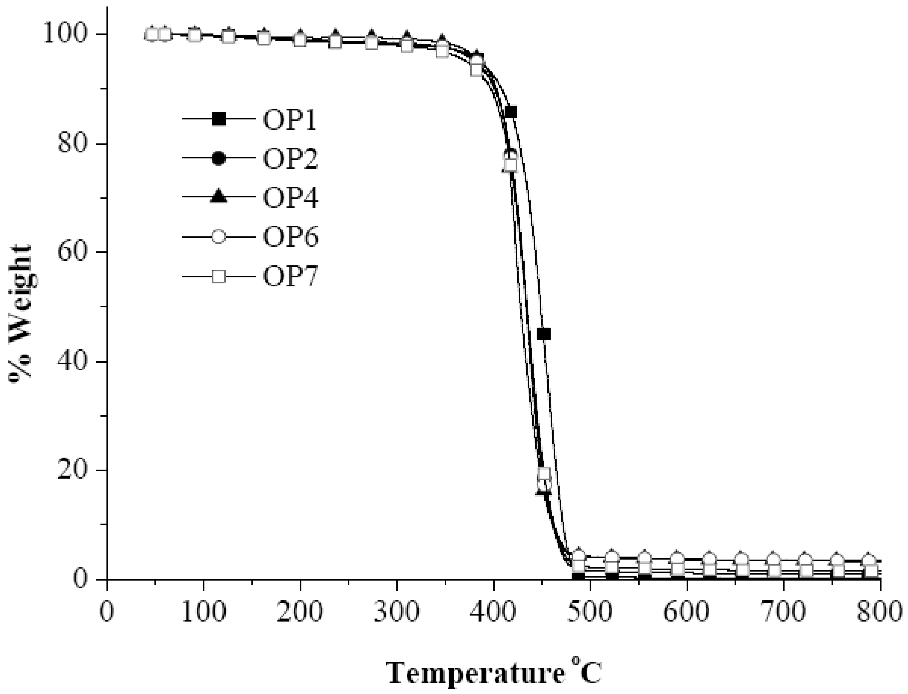

Figure 4.15 TGA curves of selected compositions

Table 4.11 TGA data of all composites

SAMPLE	$T_{5\%}$ (^{o}C)^{a}	$T_{50\%}$ (^{o}C) ^{b}	T_{max} (^{o}C) ^{c}	Char Yield (%) ^{d}
OP1	386	449	463	0.0
OP2	379	434	435	1.0
OP3	385	433	430	2.8
OP4	386	428	423	3.4
OP5	367	433	436	1.5
OP6	382	434	434	3.3
OP7	372	434	442	1.5
OP8	383	433	432	4.3
OP9	382	436	436	2.6

a: Temperature at 5% weight loss **b**: Temperature at 50% weight loss
c: The maximum rate degradation temperature **d**: Char Yield at 800 °C

Addition of organo clay (OP 7) further reduces the $T_{5\%}$ value from 379 ^{o}C to 372 ^{o}C and increases the char yield from 1% to 1.5%. The reduction at $T_{5\%}$ is the catalytic effect of clay on the degradation of PA-6 due to the presence of Bronsted and Lewis acid sites present on the clay lattice and acidic sites which are formed after the decomposition of organic content of Cloisite 30B [92, 100, 101]. According to FTIR spectra of Cloisite 30B and OP7 (Figure 4.16), no additional peak was observed except for the peaks of aluminum phosphates and Cloisite 30 B which mask each other. It follows from the FTIR data that organoclay does not change the main features of the condensed phase mechanism and the increase at char yield arises from the undecomposed part of clay.

The addition of BPO_4 increases the char yield progressively due to the stability of BPO_4 particles up to 800 ^{o}C. The characteristic peaks of BPO_4 seen in Figure 4.16 are also seen in FTIR spectrum of OP6 and there are no additional peaks except for the aluminum phosphates. It is concluded from FTIR data that there is no chemical interaction occurred between BPO_4 and AlPi. The addition of ZnB increases the char formation, progressively. In the case of ZnB, the peak at 1030 cm^{-1} is shifted to 1110 cm^{-1} and additional peaks at 1450 cm^{-1} and 3200 cm^{-1} are observed. The peak at 1100 cm^{-1} can be attributed to the formation boron aluminum phosphate layer which has better barrier properties than aluminum phosphates [43]. The peaks at 1450 cm^{-1} and 3200 cm^{-1} arise from the decomposition products PA-6 which are not totally combusted under the mass calorimeter test due to the higher barrier effect of boron aluminum phosphate layer. Mass loss calorimeter results also support this conclusion.

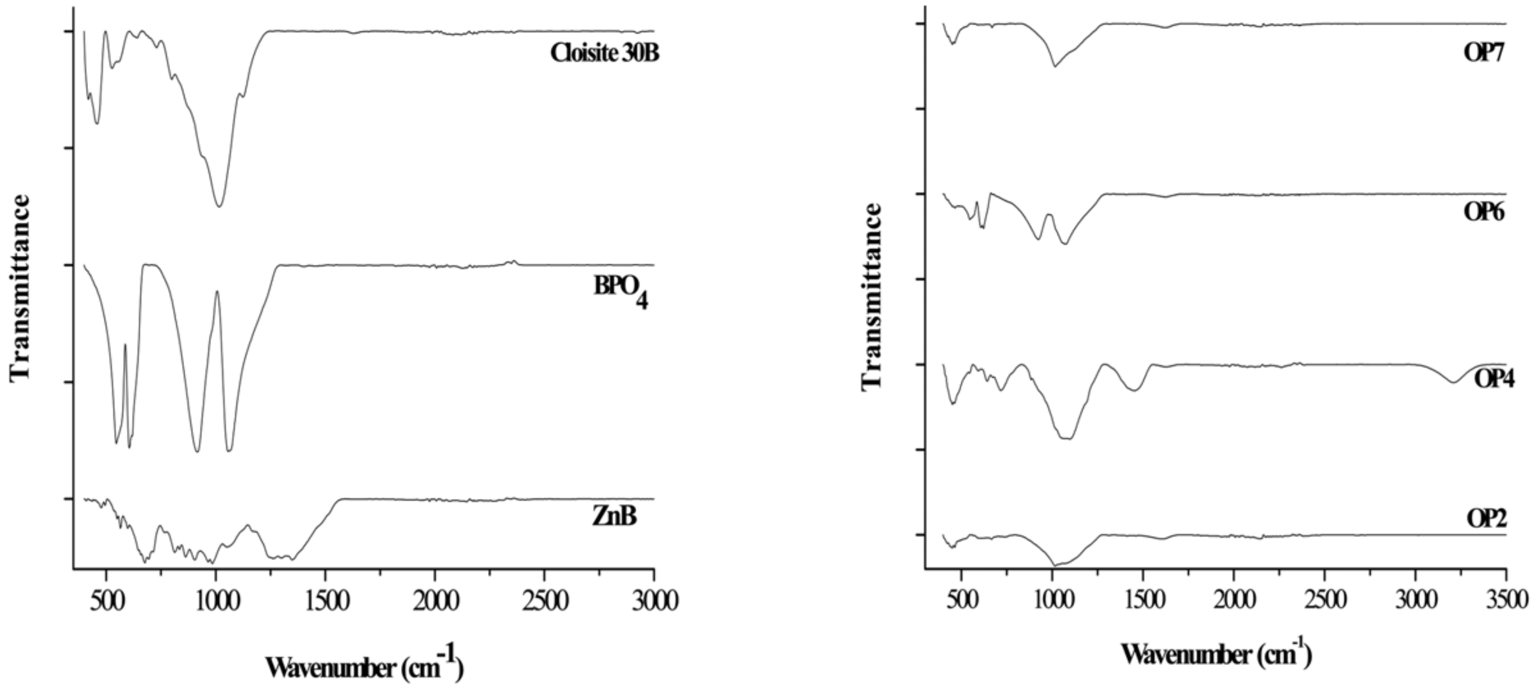

Figure 4.16 FTIR Spectra of synergy agents and char residues remained after cone calorimeter test

4.4.3 Flammability

The flammability characteristics of composites were determined by LOI and UL-94 rating. As seen from Table 4.10, the LOI value of PA-6 (OP1) is 22.5 % and it is increased to 29.5 % by the addition of 15 wt% AlPi (OP2) due to flame inhibition arising from gas phase mechanism of AlPi. Under moderate degradation conditions like LOI and UL-94 tests, the volatilization of AlPi and phosphinic acid formation is more dominant than the formation of aluminum phosphate char [42]. The addition of 1 wt% organoclay (OP 7) does not change the LOI value of composite. Although the addition of 1 and 3 wt % BPO_4 (OP 5 and OP 6) reduces the LOI value slightly, the addition of 3 wt % ZnB (OP 4) slightly increases the LOI value. Highest LOI value, 31 %, is obtained when ZnB and organoclay are used together (OP8). In UL-94 test, all composites except OP1 show V0 rating. According to UL-94 and LOI results, the addition of ZnB, BPO_4 and Cloisite 30 B does not change V0 rating and LOI values to an appreciable extent. One can conclude that these compounds do not alter the rate of volatilization of AlPi and phosphinic acid formation much in such moderate degradation conditions.

4.4.4 Cone Calorimeter Studies

Cone calorimeter is used to monitor heat release rate (HRR) during combustion. Low values of peak heat release rate (PHRR) and total heat release (THR) normally indicate improved flame retardancy. Figure 4.17 and Table 4.12 show the HRR curves of selected compositions and the cone calorimeter data of all composites at a heat flux of 35 kWm^{-2}, respectively.

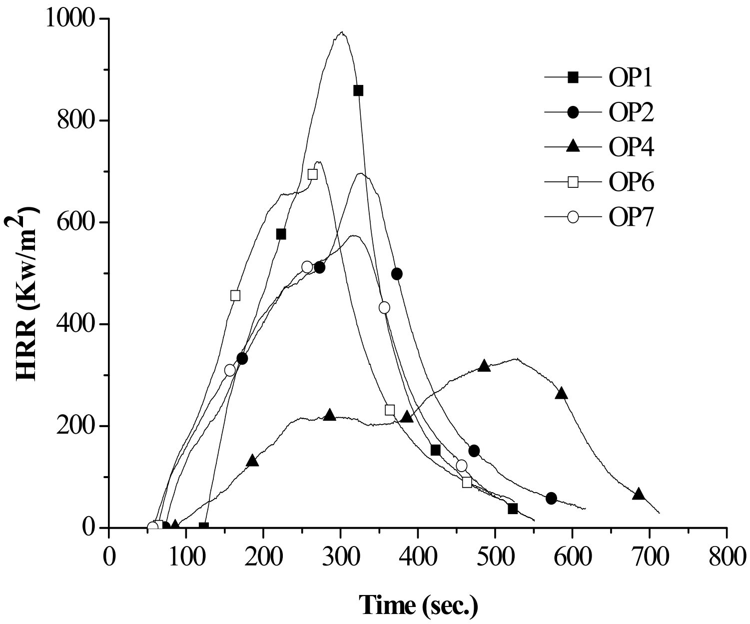

Figure 4.17 HRR curves of selected compositions

Table 4.12 Cone calorimeter data of composites

Sample	**PHRR** (Kw.m^{-2})	**Average HRR** (Kw.m^{-2})	**THR** (MJ. m^{-2})	**THR/TML** (MJ. m^{-2})	**Char Yield** (%)
OP1	975	375	163	4.2	0.2
OP2	695	300	158	3.2	4.3
OP3	480	235	136	3.6	9.8
OP4	335	190	122	3.9	11.4
OP5	755	345	160	3.2	5.4
OP6	720	325	149	3.3	8.2
OP7	575	315	143	3.4	6.3
OP8	380	186	135	3.8	9.4
OP9	535	288	141	3.4	7.2

According to Figure 4.17, PA-6 combusts very fast after ignition and one sharp HRR peak appears with a heat release peak of 975 kWm^{-2}. When AlPi is added to PA-6 (OP2), the PHRR decreases by about 280 kWm^{-2} with extended burning time. The char yield increases to 4.3 wt % due to the formation of aluminum phosphates. The char yield of all composites in mass loss calorimeter studies is much higher than those of

TGA. This result shows that AlPi tends to degrade and it forms aluminum phosphate under the high heat external flux. The THR/TML value decreases by about 1 MJ $m^{-2}g^{-1}$ with the addition of 15 wt % AlPi due to the phosphinic acid formation and vaporized AlPi [43]. With the reduction at THR/TML value and the increase in the char yield, AlPi shows its flame retardant effect both in the condensed phase and predominantly in the gas phase.

The addition of BPO_4 and organoclay (OP6 and OP7) does not change the shape of HRR curve of OP2. The characteristics of these peaks are a small shoulder observed at the beginning of the HRR curve and they get broadened due to the increase in the total burning time with lower PHRR. It is concluded from THR/TML data of BPO_4 containing composites (OP5 and OP6), the addition of BPO_4 in two concentrations does not reduce gas phase action of AlPi. The addition of organo clay (OP7) reduces both PHRR and THR by about 120 $Kw.m^{-2}$ and 15 $MJ.m^{-2}$ with respect to solely AlPi containing composite (OP2) due to the plate like shape of layered silicates which improves barrier properties of intumescent char [44].

The addition of 1% and 3% ZnB causes a higher reduction of PHRRs with respect to OP2 by about 30 % and 50%, respectively. The high reduction is caused by the formation of high amount of boron aluminum phosphate based char arising from the Lewis base character of boron which shows better barrier properties than aluminum phosphates [42]. The addition of 3 wt% ZnB (OP4) changes the shape of HRR curve of totally. It shows the HRR curve of typical insulative protective layer which stays relatively constant during combustion with very low PHRR. From THR/TML results, it is seen that the gas action of AlPi decreases as the amount of ZnB increases. It follows from the low PHRR and THR values, high amount of char and the increased THR/TML value that the predominant mechanism under mass loss calorimeter studies are thought to be condensed phase in the case of ZnB containing composites.

4.5 Synergistic Effect of Boron Containing Substances on Flame Retardancy and Thermal Stability of Clay Containing Intumescent Polypropylene Nanoclay Composites

All composites contain 2 wt% clay and 5 wt% PP-g-MA to increase the dispersion of clay [176-178]. Only one sample is prepared without clay (B2-NC) in order to see the effect of clay on burning behavior of PP containing IFR. The total loading of flame retardants, APP+PER and boron compounds, mixed with PP was maintained at 20 wt%. The ratio of APP/PER mixture was adjusted to 3 which gives the maximum flame retardancy performance for APP+PER combinations [70]. The composition of the formulations and the UL-94 ratings are shown in Table 4.13.

Table 4.13 Formulations of composites and UL-94 ratings

Sample	PP	PPgMA	Closite 15A	IFR	BSi	BPO_4	ZnB	UL-94
B1	93	5	2	-	-	-	-	**BC**
B2	73	5	2	20	-	-	-	**BC**
B2-NC	75	5	-	20	-	-	-	**BC**
B3	73	5	2	17	3	-	-	**V2**
B4	73	5	2	15	5	-	-	**V2**
B5	73	5	2	10	10	-	-	**BC**
B6	73	5	2	17	-	3	-	**V2**
B7	73	5	2	15	-	5	-	**V2**
B8	73	5	2	10	-	10	-	**BC**
B9	73	5	2	17	-	-	3	**V0**
B10	73	5	2	15	-	-	5	**BC**
B11	73	5	2	10	-	-	10	**BC**

BC: Burn to clamp, **NC**: No clay

4.5.1 Morphology Characterization by WAXS

According to the Figure 4.18, Closite 15A showed two peaks at 2θ = 3.03° and 7.24°, corresponding to basal spacing of 29.12 and 12.2 A°, respectively. The first peak is due to intercalated clay platelets. The peak at 7.24° corresponds to unintercalated clay platelets. In the composite structure, B2, the peak for intercalated structure almost completely disappeared which may indicate a possible exfoliated structure. Without TEM data, it is not possible to speculate further. One can say that some of the clay platelets may be exfoliated and some portion remains intercalated.

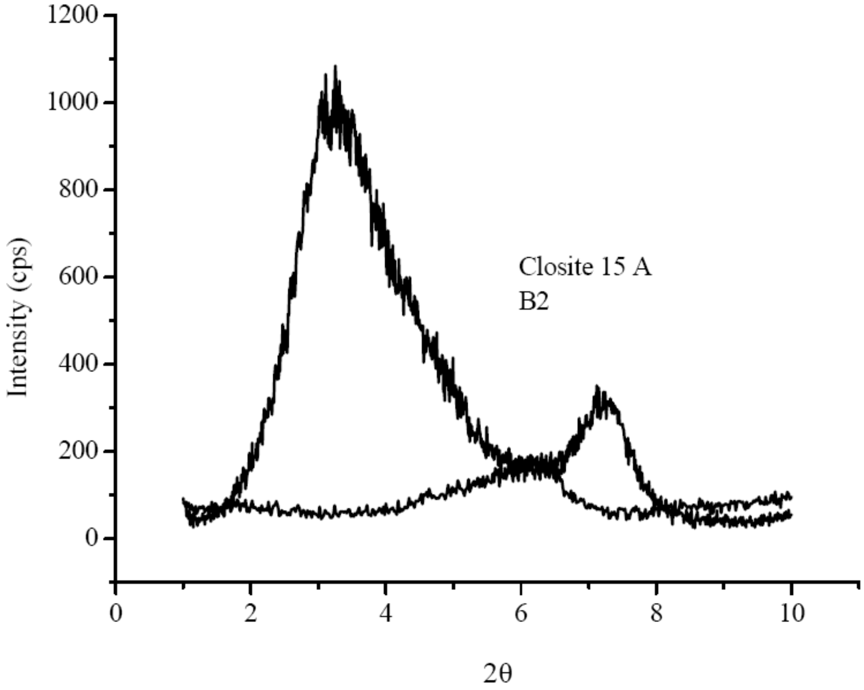

Figure 4.18 XRD graph of Cloisite 15A and B2

4.5.2 LOI and UL-94

LOI and UL-94 tests are widely used to evaluate the flame retardant properties of materials. Table 4.13 and Figure 4.19 show the UL-94 rating and LOI values, respectively. As seen from Figure 4.19, the LOI value of PP- clay composite increases from 18.2 % to 23.5 % when 20 wt% IFR is added to PP but UL-94 rating does not change. The inclusion of clay slightly increases the LOI value from 23 % to 23.5 %, whereas UL-94 rating does not change. The addition of 3 and 5 wt % BSi and BPO_4 into PP-clay composites gives V2, and 3 wt % ZnB containing sample shows the highest rating (V0). The possible reason of V0 rating is the high char yield. High char formation hinders the dripping of burning polymer and gives V0. All composites containing 10 wt % boron compounds burn to clamp, which could be explained by insufficient amount of IFR, not enough to provide flame retardancy. At loadings 3 and 5 wt % BSi, LOI value slightly increased to 24.5 % and 24.2 %, respectively. BPO_4 containing composites at 3 and 5 wt % loading show the best LOI value compared to BSi and ZnB containing composites. The LOI value increased from 23.5 % to 26.5 % at 3 wt % BPO_4 containing sample. As seen from TGA curve of BPO_4, it is thermally stable up to 600 °C. These BPO_4 species are likely to be integrated into phosphorocarbonaceous material formed by decomposition of IFR system. It permits the stabilization of the char and reinforces carbonaceous char and lead to high LOI values. As seen from the LOI value of composites containing ZnB, when the amount of ZnB exceeds 3 wt % LOI value decreases. When the amount of metal compound exceeds a certain value, the catalytic effect of metal compounds is reduced and LOI values decrease. According to UL-94 test and LOI, the optimum concentration of boron compounds in these formulations is 3 wt %.

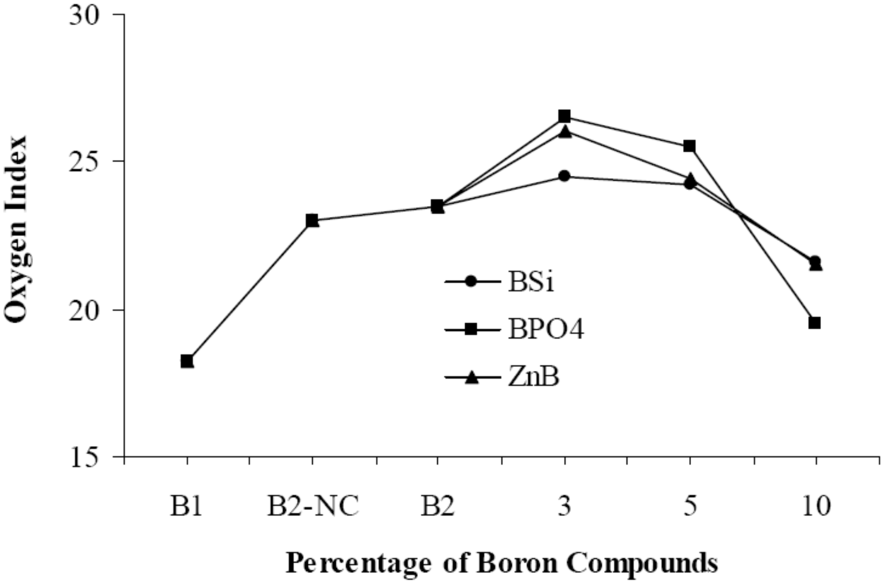

Figure 4.19 LOI values of composites

4.5.3 Thermogravimetric Analysis (TGA)

TGA curves of selected compositions are shown in Figure 4.20. TGA data of all composites are listed in Table 4.14. According to TGA curves of selected composites, the weight loss of PP- clay composite takes place in a single step and it is thermally stable up to 300 °C. Clay containing polypropylene composite (B1) gives 1.4% char residue at 600 °C with a maximum rate of weight loss at 438 °C. The small amount of char results from clay. The inclusion of IFR increased the char yield from 1.4 to 8.8. The reason of the increase in the char yield is the carbonization reactions among PP and IFR system. $T_{5\%}$, $T_{50\%}$ and T_{max} is the temperature at 5% weight loss, 50% weight loss and the maximum degradation rate temperature, respectively. The $T_{5\%}$ gives information about the initial weight loss of composites. The addition of IFR into PP increased $T_{5\%}$ and T_{max} values by 66°C and 43°C, respectively. This indicates a delay in the start of decomposition and in reaching the maximum decomposition rate, which is consistent with the intumescent function of this system. The addition of clay also causes a delay in the start of decomposition, whereas T_{max} does not change significantly. Addition of boron compounds increases the char yield of all composites regardless of the type of boron compound used. The reason for the increase is that the boron compounds retain their weights up to 90 wt%. Interestingly, when 3 wt% ZnB is added the char yield increases from the 8.8 to 17.5 %. There are probably two possible reasons of this high char yield. ZnB acts as a source of B_2O_3 that helps form a glassy layer that prevents further combustion of char that is formed by IFR. Another reason is the interaction between APP and metallic Zn. As in the case of ZnB, zinc may replace ammonia in APP and crosslinking reaction occurs between polyphosphoric acid chains so it reduces the volatility of polyphosphoric acid and more polyphosphoric acid compound will be available for the esterification reaction with PER which is the precursor of the char [21, 66].

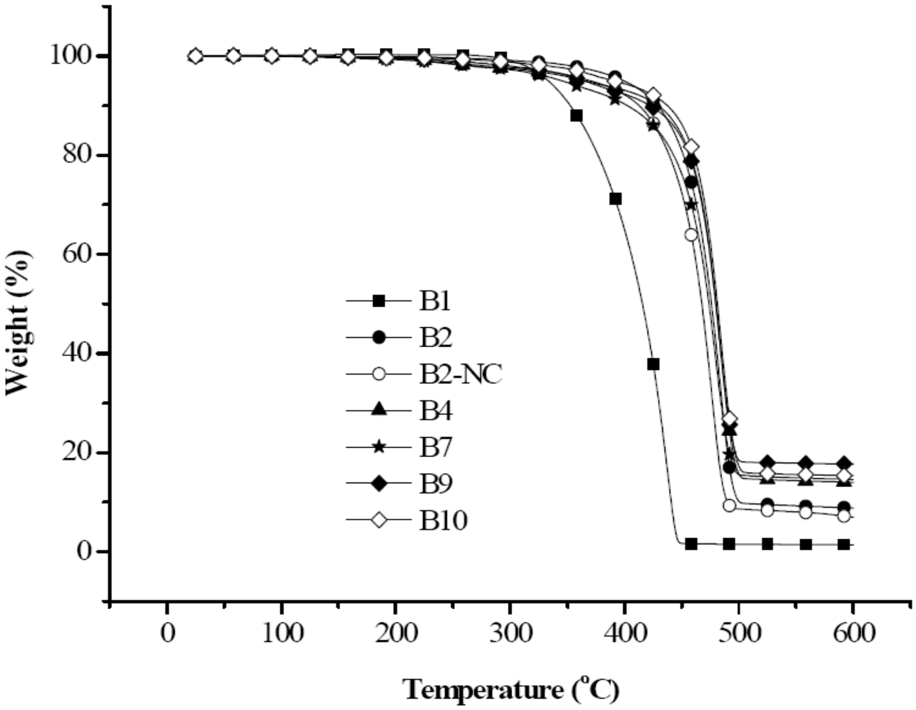

Figure 4.20 TGA curves of selected compositions

Table 4.14 TGA data of all composites

SAMPLE	T $_{5\%}$ (°C)[a]	T $_{50\%}$ (°C) [b]	T$_{max}$ (°C) [c]	Char Yield (%) [d]
B1	333	415	438	1.4
B2	399	475	481	8.8
B2-NC	369	467	478	7.0
B3	366	479	483	12.5
B4	364	479	483	14.0
B5	391	472	475	10.2
B6	344	441	446	13.7
B7	344	473	481	14.6
B8	378	478	484	16.4
B9	364	479	472	17.5
B10	390	481	468	15.3
B11	360	444	454	12.0

a: Temperature at 5% weight loss **b**: Temperature at 50% weight loss
c: The maximum rate degradation temperature **d**: Char Yield at 600 °C

4.5.4 Cone Calorimeter Study

Figure 4.21 and Table 4.15 show the behavior of selected compositions obtained from the cone calorimeter test at a heat flux of 35 kWm^{-2} and Figure 4.22 shows the effect of clay and sample thickness on the cone calorimeter test. According to Figure 4.21, PP-clay containing composite (B1) burns very fast after ignition and one sharp HRR peak appears with a heat release peak of 565 kWm^{-2}. The addition of IFR with and without clay reduced the maximum HRR to 199 and 475 kWm^{-2}, respectively. The HRR curve of typical insulative intumescent layer stays relatively constant and slowly decreases towards the end of combustion. As seen from Figure 4.22, the burning behavior of sample B2-NC with the thickness of 2 mm does not resemble the general shape of IFR systems. These samples are all thermally thin. On the other hand, the HRR curve of B2-NC with thickness of 4 mm shows the characteristic curve of IFR system. This is due to the inadequate sample thickness (2 mm). As seen from Figure 4.22, although the barrier effect of insulative intumescent layer of B2-NC (2mm) is not enough to protect the underlying material, the addition of clay increases the barrier effect of intumescent char. It is concluded that the clay increases the barrier effect of protective char especially in thin samples. Addition of clay also reduces the time to ignition (TTI), maximum HRR and total heat release (THR).

Table 4.15 Cone calorimeter data of selected composites

Sample	TTI	Maximum HRR	Average HRR	THR
B1	42	565	252	61
B2	25	199	85	39
B2-NC	30	475	151	57
B4	20	206	73	44
B7	20	193	84	34
B9	29	220	82	34
B10	43	334	126	48

TTI: Time to ignition, **HRR:** Heat Release Rate **THR:** Total Heat Release Rate

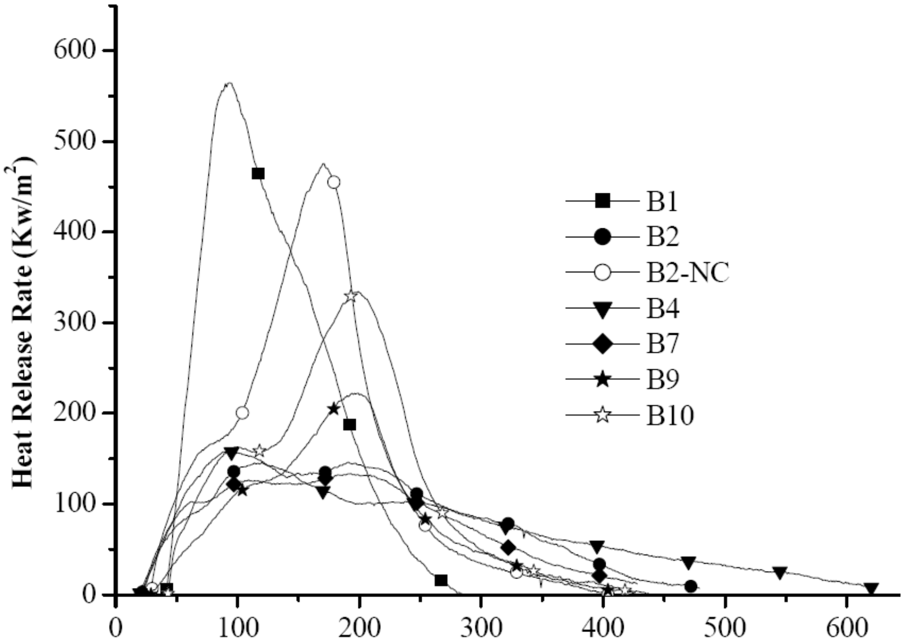

Figure 4.21 HRR curves of selected compositions

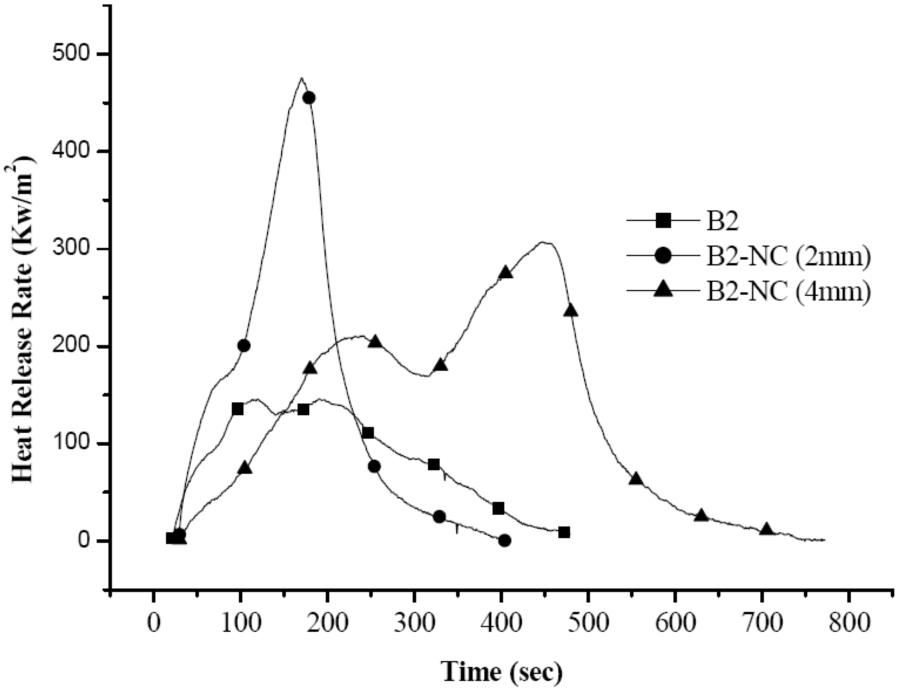

Figure 4.22 The effect of clay and sample thickness on the cone calorimeter test

Total burning time increases with the addition of BSi (B4) but decreases slightly by the addition of ZnB and BPO_4 with respect to B2. HRR of BPO_4 containing sample (B7) becomes constant between the 60 and 83 seconds. This can be an indication of a protective intumescent coating forming immediately after ignition. The maximum HRR decreased from 199 to 193 and THR decreased from 39 to 34. BPO_4 species are likely to be integrated into phosphorocarbonaceous material formed by decomposition of IFR system and BPO_4 species stabilize the phosphate species at high temperatures and keeps the integrity of intumescent structure, giving rise to reduced heat and mass transfer and higher LOI values.

As the amount of ZnB increases in IFR system, TTI increases. As stated before, this result indicates that Zn reacts with APP and increases the evolution of NH_3 and it dilutes combustible gases in the combustion zone, so TTI is increases. As seen from Figure 4.21, the HRR curve of ZnB containing samples become constant after the protective char is formed and then HRR increases sharply. As the amount of ZnB increases in the IFR system, the height of the second peak increases. The second peak indicates the potential or partial destruction of protective char layer. The possible explanation of this behavior is that when the amount of ZnB exceeds a certain value, the quantity of protective char layer decreases.

4.6 Synergistic Effect of Boron Containing Substances on Flame Retardancy and Thermal Stability of Intumescent Polypropylene Composites

The total amount of IFR and boron compounds, mixed with PP was maintained at 20 wt %. The ratio of APP and PER mixture was adjusted to 3 which gave the maximum flame retardancy performance for APP and PER combinations [70]. The composition of formulations and UL-94 ratings are given in Table 4.16.

Table 4.16 Formulations of composites and UL-94 ratings

SAMPLE	PP	IFR	ZnB	BPO_4	BSi	LaB	UL-94
P0	100	-	-	-	-	-	**BC**
P1	80	20	-	-	-	-	**BC**
P2	80	19	1	-	-	-	**V0**
P3	80	17	3	-	-	-	**V2**
P4	80	19	-	1	-	-	**V0**
P5	80	17	-	3	-	-	**V2**
P6	80	19	-	-	1	-	**V0**
P7	80	17	-	-	3	-	**V2**
P8	80	19	-	-	-	1	**V0**
P9	80	17	-	-	-	3	**V2**

BC: Burn to clamp

4.6.1 LOI and UL-94

LOI and UL-94 tests are widely used to evaluate the flame retardant properties of materials. Table 4.16 and Figure 4.23 show the UL-94 rating and LOI values, respectively. As seen from Figure 4.23, the LOI value of PP (P0) increases from 17.5 % to 23 % when 20 wt% IFR is added to PP (P1) but UL-94 rating does not change. The addition of 1 wt % boron compounds into IFR containing PP composites gives V0 and the addition of 3 wt % boron compounds into PP composites gives V2. The addition of 1 and 3 wt % BSi increases the LOI value from 23 % to 25.5 % and 25 %, respectively. 1 wt % BPO_4 containing composite shows the highest LOI value (30 %) when compared to that of other boron containing composites. The LOI value decreased from 30 % to 27 % when the amount of. BPO_4 is increased to 3 wt %. BPO_4 species are likely to be integrated into phosphorocarbonaceous material formed by decomposition of IFR system. It permits the stabilization of the char, reinforces carbonaceous char and leads to high LOI values. The LOI values of 1 and 3 wt% ZnB containing composites are 29.5 % and 25.5 %, respectively. When the amount of metal bearing compound exceeds a certain value, the catalytic effect of metal compounds is reduced and LOI value decreases. The LOI values of composites containing 1 and 3 wt % LaB are 27 %

and 24 %, respectively. For the same reason with ZnB, the LOI value of LaB containing composites decreases as the amount of LaB increases. According to UL-94 and LOI tests, the optimum concentration of boron compounds in these formulations is 1 wt %.

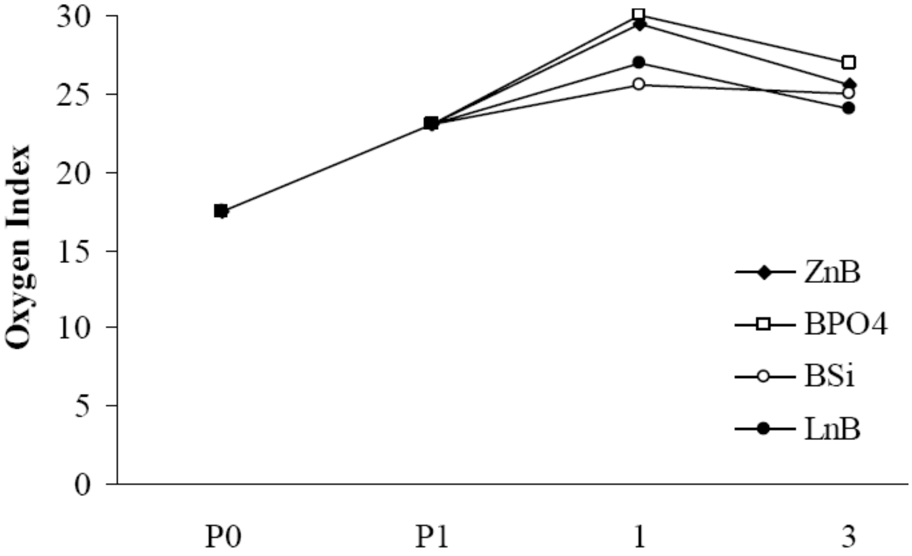

Figure 4.23 LOI values of the composites

4.6.2 Thermogravimetric Analysis (TGA)

TGA curves of selected compositions are shown in Figure 4.24. TGA data of all composites are listed in Table 4.17. According to TGA curves of selected composites, the weight loss of PP takes place at a single step with a maximum rate of weight loss at 430 °C with no char residue. The inclusion of IFR increased the char yield from 0 to 7%. The reason for the increase at char yield is the carbonization reactions between APP and PER. $T_{5\%}$, $T_{50\%}$ and T_{max} is the temperature at 5% weight loss, 50% weight loss and the maximum degradation rate temperature, respectively. The $T_{5\%}$ gives information about the initial weight loss of composites. The addition of IFR into PP increased $T_{5\%}$ and T_{max} value by 50 °C. This indicates a delay in the start of decomposition and maximum decomposition rate, which is consistent with intumescent function of this system. Addition of boron compounds slightly reduces the T_{max} of PP-IFR composite regardless of its type.

The char yield of all composites increases with the addition of boron compounds regardless of the type. The reason for the increase is that the boron compounds retain their weight up to 90 wt%. The char yield is high when ZnB or LaB is added into PP-IFR composites. A possible reason for this is the interaction between APP and metallic Zn and La. As in the case of ZnB and LaB, metal atoms may replace ammonia in APP and crosslinking reaction occurs between polyphosphoric acid chains and metal atoms resulting in the reduction of the volatility of polyphosphoric acid. Thus, more polyphosphoric acid will be available for the esterification reaction with PER which is the precursor of the char [21, 67, 69, 70]. Although 3 wt % boron compound containing composites give char yield higher than 1 wt % containing ones, the flame retardancy of 1 wt% boron compounds are better than that of 3 wt% containing composites. Among the boron compounds BPO_4 is the most effective flame retardant material which is likely to increase the integrity of the char and it increases the barrier effect.

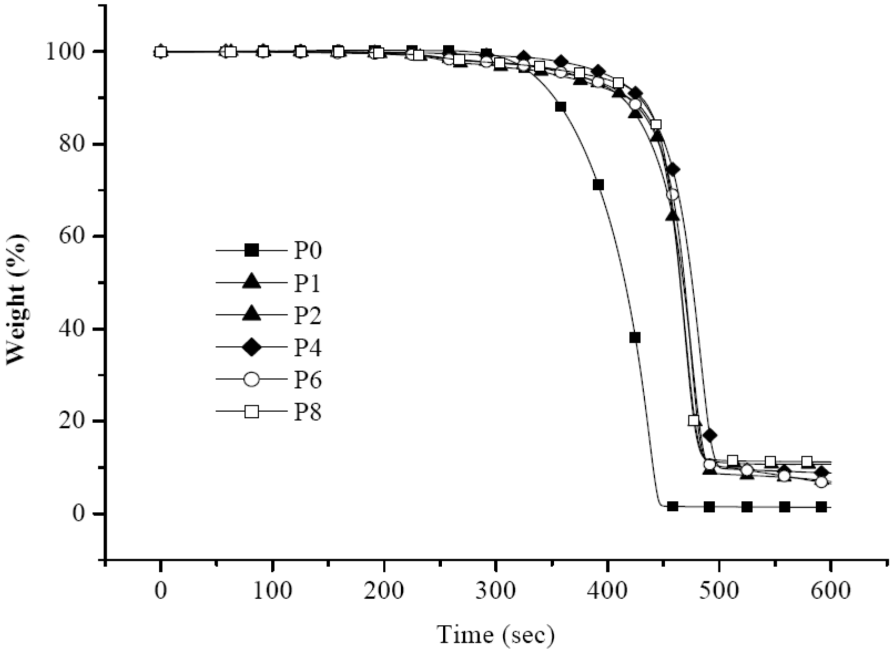

Figure 4.24 TGA graphs of selected compositions

Table 4.17 TGA data of all composites

SAMPLE	**$T_{5\%}$ (°C)^{a}**	**$T_{50\%}$ (°C)^{b}**	**T_{max} (°C)^{c}**	**CharYield (%)**
P0	320	405	430	0.0
P1	370	465	480	7.0
P2	352	465	476	10.7
P3	362	450	460	12.0
P4	350	460	472	8.8
P5	353	446	465	9.5
P6	367	469	463	7.2
P7	352	458	460	11.0
P8	380	464	475	11.0
P9	382	470	470	12.5

a: Temperature at 5% weight loss **b**: Temperature at 50% weight loss
c: The maximum rate degradation temperature **d**: Char Yield at 600 °C

4.6.3 Cone Calorimeter Study

Figure 4.25 and Table 4.18 show the behavior of selected compositions obtained from the cone calorimeter test at a heat flux of 35 kWm^{-2}. According to Figure 4.25, PP burns very fast after ignition and one sharp HRR peak appears with a heat release peak of 920 kWm^{-2}. The IFR containing PP composites show the HRR curve of typical insulative intumescent layer which stays relatively constant and slowly decreases towards the end of combustion. The addition of IFR reduces both the maximum HRR from 920 to 305 kWm^{-2} and reduces the time to ignition (TTI) from 65 to 32 seconds. Except for ZnB containing composite, the addition of boron compounds gives rise to lower maximum and average HRR values. The addition of ZnB and LaB increases TTI from 32 to 37 and 43, respectively. As stated before, this result indicates that Zn and La react with APP and increase the evolution of NH_3 which dilutes combustible gases at the combustion zone, so TTI increases. The high char yield in TGA is also proof of the synergistic effect of these metal compounds. The lowest maximum HRR and THR values are obtained from BPO_4 containing composite (P4). The maximum HRR decreases from 305 to 226 and THR decreases from 93 to 53. BPO_4 species are likely to be more integrated into phosphorocarbonaceous material formed by the decomposition of IFR system, so BPO_4 stabilizes the phosphate species at high temperatures and strengthens the integrity of intumescent structure that gives rise to reduced heat and mass transfer and high LOI values.

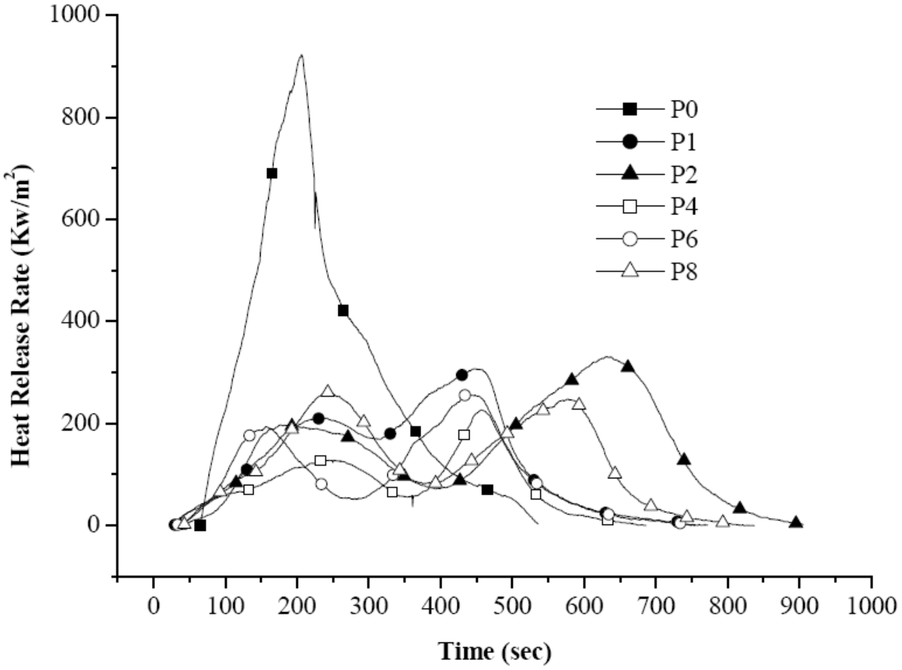

Figure 4.25 HRR curves of selected copositions

Table 4.18 Cone calorimeter data of selected composites

Sample	TTI	Maximum HRR	Average HRR	THR
P0	65	920	335	145
P1	32	305	125	93
P2	37	330	145	125
P4	33	226	80	53
P6	34	255	98	70
P8	43	260	122	97

TTI: Time to ignition, **HRR:** Heat Release Rate **THR:** Total Heat Release Rate

4.7 The effect of metal oxide doped boron phosphates on flame retardancy and thermal stability of intumescent polypropylene composites

According to the previous studies, metal oxides show synergistic effect with IFR systems. The previous studies made by us showed that BPO_4 has a good synergistic effect with IFR system. From this point of view, it is predicted that the combination of BPO_4 and metal oxide shows much more synergistic effect than either of them used alone.

The total amount of IFR and metal oxides doped boron phosphates mixed with PP was maintained at 20 wt %. The ratio of APP and PER mixture was adjusted to 3 which gave the maximum flame retardancy performance for APP and PER combinations [70]. The composition of formulations, LOI values and UL-94 ratings are given in Table 4.19.

Table 4.19 The composition of formulations, LOI values and UL-94 ratings

SAMPLE	PP	IFR	MnO(%3)	MnO (%40)	ZnO (%3)	ZnO (%40)	UL-94	LOI
PB0	100	-	-	-	-	-	BC	17.5
PB1	80	20	-	-	-	-	BC	23.0
PB2	80	19	1	-	-	-	V2	26.0
PB3	80	17	3	-	-	-	V2	24.5
PB4	80	19	-	1	-	-	V2	25.0
PB5	80	17	-	3	-	-	V2	25.5
PB6	80	19	-	-	1	-	V2	26.5
PB7	80	17	-	-	3	-	BC	25.5
PB8	80	19	-	-	-	1	V2	26.5
PB9	80	17	-	-	-	3	BC	25.0

B.C: Burn to clamp

4.7.1 LOI and UL-94

According to LOI and UL-94 tests, the LOI value of PP (PB0) increases from 17.5 % to 23 % when 20 wt% IFR is added to PP (PB1) but UL-94 rating does not change. The addition of metal oxide doped BPO_4 causes an increase in LOI values. Except for the ZnO doped BPO_4's loaded at 3 wt %, UL-94 rating changes from B.C. to V2. Although the addition of metal oxide doped BPO_4 into IFR system shows synergistic effect, BPO_4 shows higher synergistic effect. For this reason, further detailed study could not be made.

4.8 The Effect of Boron Compounds on the Fire Retardant Properties of Intumescent Polypropylene Composites Containing Surface Modified APP

The surface modified APP (m-APP) based IFR is coated with a component containing nitrogenous and carbonaceous species. In these systems, when exposed to flame, carbonization reaction occurs between APP and the surface coating material [60, 61, 179]. Bourbigot et al. showed that m-APP systems have a performance better than APP/PER system because they show their effectiveness through phosphorus and nitrogen synergism [21]. The m-APP used in this study is coated with an ester of tris (2-hydroxyethyl) isocyanurate (THEIC) acting as carbonizing and blowing agent during combustion. As a result of carbonization reaction between APP and THEIC, a foamed charred layer which acts as physical barrier between condensed phase and gas phase is formed. The total loading of flame retardants, m-APP and boron compounds, mixed with PP was maintained at 20 wt%. The boron compounds were used at two different loading levels which are 1 and 3 wt %. The composition of formulations, UL-94 ratings and LOI values are shown in Table 4.20.

Table 4.20 Formulations of compositions, UL-94 ratings and LOI values

Sample	PP	AP765	BSi	BPO_4	ZnB	LnB	UL-94	LOI
AP0	100	-	-	-	-	-	BC	17.5
AP1	80	20	-	-	-	-	V0	31.0
AP2	80	19	1	-	-	-	V0	31.5
AP3	80	17	3	-	-	-	V0	31.5
AP4	80	19	-	1	-	-	V0	32.0
AP5	80	17	-	3	-	-	V0	32.0
AP6	80	19	-	-	1	-	V0	32.0
AP7	80	17	-	-	3	-	V0	32.0
AP8	80	19	-	-	-	1	V0	30.5
AP9	80	17	-	-	-	3	V0	32.0

BC: Burn to clamp

4.8.1 LOI and UL-94

As seen from Table 4.20, the LOI value of pure PP (AP0) increases from 17.5 % to 31 % and UL-94 rating changes from burn to clamp (BC) to V0 when 20 wt % m-APP is added to PP (AP1). The addition of boron compounds does not change the UL-94 rating of the compounds and all composites have V0 rating. The LOI value of the composites increases slightly with the addition of boron compounds except the 1 % LaB containing composite (AP8). This slight increase is not so meaningful for claiming synergy. It is thought that the reason of this slight increase in LOI value is the increase of the char yield.

4.8.2 Thermogravimetric Analysis (TGA)

TGA curves of selected compositions are shown in Figure 4.26. TGA data of all composites are listed in Table 4.21. The weight loss of PP takes place in a single step with a maximum rate of weight loss at 430 °C with no char residue. The inclusion of m-APP with and without boron compounds does not change the single step degradation behavior of compounds. The addition of m-APP increased the char yield from 0 to 5 % at 600 ° C due to the carbonization reaction between THEIC and APP. $T_{5\%}$, $T_{50\%}$ and

T_{max} are the temperatures at 5% weight loss, 50% weight loss and the maximum rate degradation temperature, respectively. The $T_{5\%}$ gives information about the initial weight loss of compounds. The addition of AP 765 into PP increased $T_{5\%}$ and T_{max} value by 60 °C and 45 °C, respectively. This indicates a delay in the start of decomposition and maximum decomposition rate arising from the barrier effect of formed char which protects the underlying material from the effect of heat. Addition of boron compounds slightly reduces the T_{max} of AP1 regardless of its type. This result may also suggest that the boron compounds reduce the barrier effect of foamed char.

Addition of boron compounds increases the char yield of all compounds regardless of its type despite a reduction of the barrier effect of the char. The main reason for the increase is that the boron compounds retain their weight up to about 90 wt%. The highest char yields are obtained when of 3% ZnB and LaB are added into PP-IFR composites. The possible reason of high char yield is the interaction between APP and metallic Zn and La. As in the case of ZnB and LaB, metal ions may replace ammonia in APP and crosslinking reaction occurs between polyphosphoric acid chains, so it reduces the volatility of polyphosphoric acid and more polyphosphoric acid compound will be available for the char formation [21, 67, 69, 70].

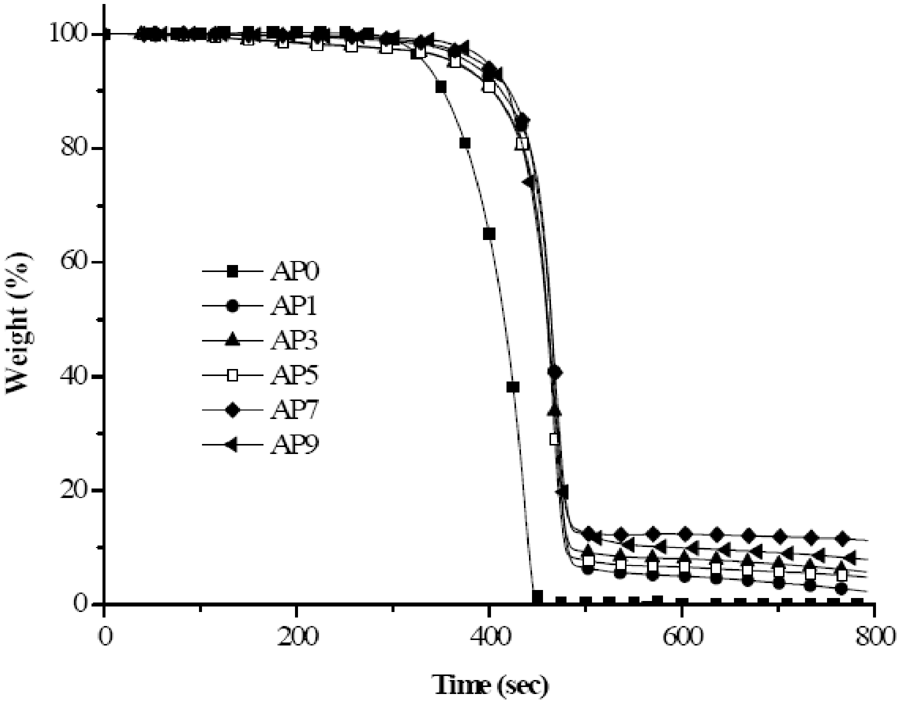

Figure 4.26 TGA curves of selected compositions

Table 4.21 TGA data of compositions

SAMPLE	$T_{5\%}$[a] (°C)	$T_{50\%}$[b] (°C)	T_{max}[c] (°C)	Char Yield (%)[d] 600 °C	800 °C
AP0	320	405	430	0.0	0.0
AP1	380	465	475	5.0	2.4
AP2	392	464	470	7.9	6.1
AP3	365	460	468	8.1	5.8
AP4	342	442	457	5.9	4.2
AP5	366	460	467	6.5	4.8
AP6	395	459	466	7.2	5.7
AP7	391	464	465	12.4	11.3
AP8	403	462	467	6.0	4.0
AP9	397	460	467	10.0	7.9

a: Temperature at 5% weight loss **b**: Temperature at 50% weight loss
c: The maximum rate degradation temperature **d**: Char Yield at 600 °C and 800 °C

4.8.3 Cone Calorimeter Studies

Figure 4.27 and Table 4.22 show the behavior of selected compositions obtained from the cone calorimeter test at a heat flux of 35 kWm^{-2}. According to Figure 4.27, PP (AP0) burns very fast after ignition and one sharp HRR peak appears with a heat release peak of 655 kWm^{-2}. The m-APP containing PP composite (AP1) shows the two peaked HRR curve of typical insulative intumescent layer. First peak results from the ignition and the formation of protective char and the second peak results from the destruction of protective char. After the formation of protective char, the HRR curve of AP1 is very flat up to the destruction of char structure. This result shows that the insulating effect of the protective char is very efficient. Addition of 20 wt% m-APP (AP1) reduces the average HRR and THE values about 70 % and 53 % with respect to the AP0, respectively. The inclusion of boron compounds regardless of their type causes higher average HRR and THE values.

With the addition of boron compounds except for LaB, the Ist peak shifts to the right and gets higher values. It proves that boron compounds delay both the formation of protective char and reduce the barrier effect of the char. When the THE and average HRR values are considered, those of LaB containing one are the highest values. In the case of LaB, necking is observed at the beginning of HRR curve and HRR values steadily increase. This curious result indicates that the formed char does not exhibit effective protective effect. From the locations of second peaks which shift to the right with respect to that of AP1, the addition of boron compounds delays the destruction of protective char due to the higher char yield which increases the thickness of foamed char. Char morphologies also give additional reasoning for cone calorimeter results.

Table 4.22 Cone calorimeter data of selected composites

SAMPLE	TTI	Peak HRR		Average HRR	THR
	(s)	**I. peak**	**II. peak**	(Kw.m^{-2})	(MJ. m^{-2})
AP0	46	-	655	219	68
AP1	23	20	198	65	32
AP3	20	75	150	71	49
AP5	27	30	225	67	37
AP7	36	28	205	68	44
AP9	24	27	186	84	52

TTI: Time to ignition, **HRR:** Heat Release Rate **THR:** Total Heat Release Rate

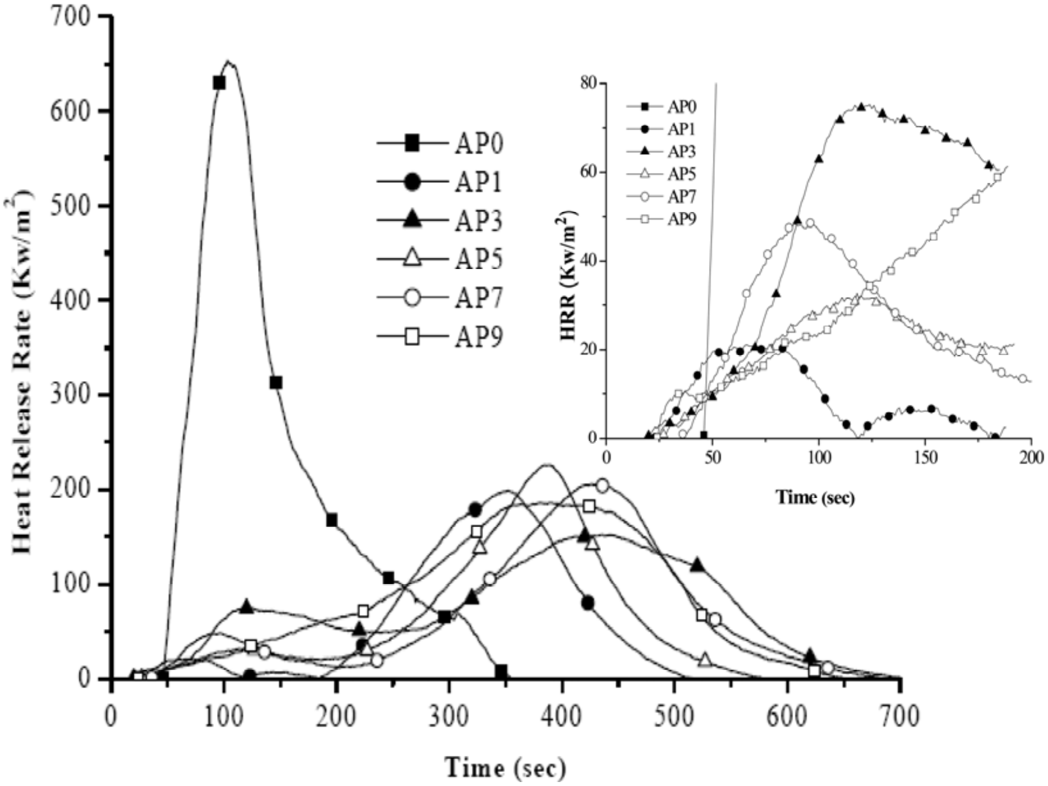

Figure 4.27 HRR curves of selected compositions

4.8.4 Macrostructures of char residues

Figure 4.28 shows the macroscopic char structures of compositions obtained by heating for 10 min at 550 ^{o}C. The 20X magnified microscopic images are located at upper left of the photograph. As seen from Figure 4.28, the char thickness increases with the addition of boron compounds. The char surface of AP1 is smoother than that of the boron containing compounds and intumescence occurs throughout the whole surface. The microscope pictures indicate that the exterior char structure of AP1 is continuous without defects. With the addition of boron compounds the exterior surface of char becomes rough with thick intumescent regions. The microscope image shows that small holes are present at the top of the intumescence points. Cracks are observed at the lower part of the intumescent regions (see Figure 4.28 upper left corner). It is thought that the addition of boron compounds alters the viscoelastic behavior of fluid that expands and forms foamed char giving rise to intumescent regions with small holes and cracks on the exterior char surface. These small holes and cracks permit the diffusion of heat and oxygen between condensed and gas phases. Accordingly, the barrier effect of the char is reduced with the addition of boron compounds.

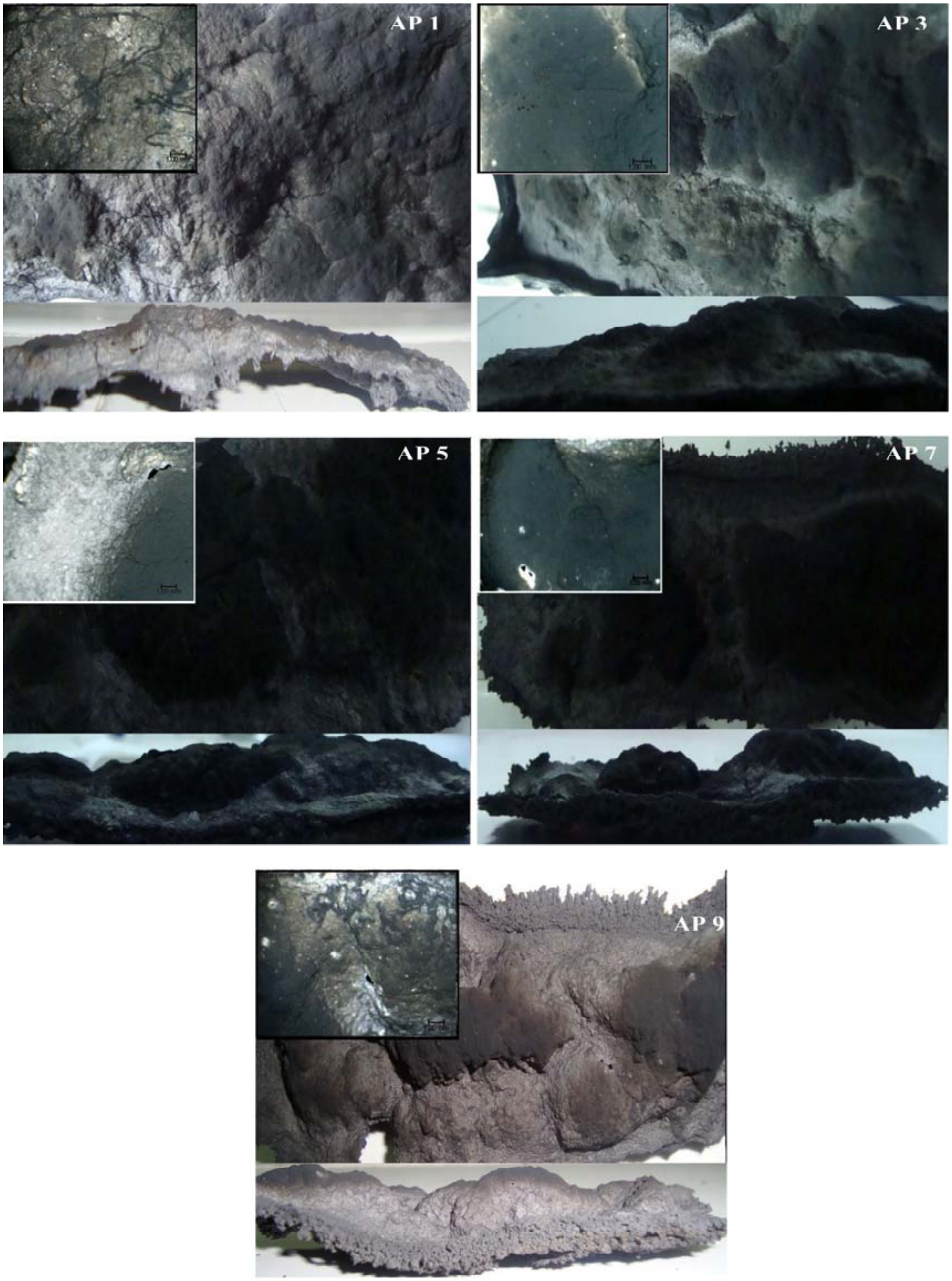

Figure 4.28 Macroscopic char structures of compositions obtained by heating for 10 min at 550 °C.

4.9 Inferences from Flame Retardant Composite Results to Produce Flame Retardant Fiber

In last years, there were quiet a number of studies made on the production of fire retardant fibers by inclusion of nanoparticles into polymers before spinning process [17-23]. The effect of nearly nano-sized BPO_4 with 200 nm average particle size is studied with PP and PA-6 in terms of fiber forming capacity and flame retardancy. Up to 10 wt % BPO_4 containing fibers are produced and their flame retardancy is studied together with mechanical and other properties.

For the production of flame retardant PA-6 composite, nitrogen containing flame retardants (MC and melamine) which give good flame retardant property to PA-6 were chosen and their synergistic effect with boron compounds was investigated. According to the test results, boron compounds did not show any synergistic effect. For this reason, the usage of MC and melamine for fiber production was abandoned. For the second part of the study, the synergistic effect of boron compounds with P-red was investigated. Although synergistic effect was observed, the flame retarding effect of P-red in combination with boron compounds was not at a desired level. For this reason, the usage of P-red for fiber production was also abandoned. The last part of the study, the synergistic effect of AlPi was studied with BPO_4 and ZnB. ZnB showed good synergistic effect with AlPi and the total flame retarding effect was at a desired value. For this reason, AlPi was chosen for the fiber production. But the as spun fiber samples could not be drawn further to increase the mechanical properties. For this reason, ZnPi was used instead of AlPi for the production of flame retardant PA-6 fiber. Although the AlPi is much more effective than the ZnPi for obtaining flame retardant PA-6, ZnPi was chosen due to its low melting point. It melts during spinning process and easily integrates into fiber structure.

Both APP+PER combination and m-APP were used for the production flame retardant PP composites. First fiber production trials were made on the APP+PER combination which shows better synergistic effect with boron compound than the m-APP. Fiber spinning was attempted at 230 ^{o}C which is the preferred fiber spinning temperature for PP fiber. Fiber production cannot be accomplished due to fiber breakage during spinning arising from the decomposition products of APP (NH_3) and reaction products of APP and PER (H_2O). The spinning temperature was reduced to 200 ^{o}C and the fiber spinning was attempted but the breakage still continued. Then the fiber production was again attempted with m-APP which is thermally more stable than the APP+PER combination at 230 ^{o}C but the fiber breakage still continued. The spinning temperature was reduced to 200 ^{o}C and fibers were produced without any breakage both during spinning and drawing processes.

4.10 Effect of Boron Phosphate on the Mechanical, Thermal and Fire Retardant Properties of Polypropylene and Polyamide-6 Fibers

4.10.1 Tensile Properties

The BPO_4 was used at two different concentrations (3 wt% and 10 wt %) with both polymers to obtain flame retardant fiber. Tensile tests on monofilament fiber samples were made to investigate the effects of BPO_4 on the mechanical properties of fibers. Youngs' modulus (E), stress at break values (σ) and elongation at break values (ε) at given draw ratios are listed in Table 4.23**.** Although the drawability of PA-6 in the presence of BPO_4 at two different concentrations does not change, that of PP is slightly reduced from 5 to 4 at 10 wt % loading due to restricted chain mobility. It can be concluded that the BPO_4 particles have little effect on drawability of monofilament yarns at the compositions given. The addition of BPO_4 reduces the E, σ and ε values of the PP and PA-6 fibers with increasing amount of BPO_4. Without using any compatibilizer, the interaction between BPO_4 particles and the matrix is poor and the polymer will not sufficiently wet the BPO_4 particles resulting in debonding process and void formation in the matrix. These reductions can be explained by these two phenomena which occur in the matrix. The σ values are reduced by 35 % and 50 % for

PA-6 and PP fibers containing 10 % BPO_4, respectively. The larger reduction in σ for PP fiber with respect to PA-6 fiber may have arisen from the polar groups on the surface of BPO_4 which may facilitate better dispersion of BPO_4 particles in PA-6 matrix than in PP [180].

Table 4.23 The mechanical properties and MFI values of the BPO_4 containing fibers

SAMPLE	**Draw ratio**	**MFI (g/10 min)**	**Ø (µm)**	**E (GPa)**	**σ (MPa)**	**ε (%)**
PA-6	3	24±1.8	34±1.8	1.8±0.2	297±32	50±20
PA-6+ 3 BPO_4	3	32±2.2	31±1.6	1.4±0.2	234±30	40±18
PA-6+ 10 BPO_4	3	36±2.8	34±1.5	1.3±0.1	192±14	32±5
PP	5	34 ± 4.5	31 ± 0.4	1.49 ± 0.4	195 ± 14	59 ± 15
PP+ 3 BPO_4	5	44 ± 4.5	35 ± 2.9	1.43 ± 0.3	114 ± 21	57 ± 19
PP+ 10 BPO_4	4	36 ± 3.8	37 ± 2.1	1.37 ± 0.4	99 ± 16	50 ± 10

Ø: Diameter of the fiber **E:** Youngs' modulus **σ:** Stress at break values **ε:** Elongation at break values

4.10.2 Melt Flow Index (MFI)

The effect of BPO_4 on flow properties PP and PA-6 was investigated by MFI measurements at spinning temperatures of fibers. The MFI values of the fibers are listed in Table 4.23. In the case of PA-6 fiber, the MFI value increases as the amount of BPO_4 increases. For PP fiber, the addition of 3 wt % BPO_4 increases the MFI value then the MFI value is reduced at 10 wt % BPO_4 loading, but it is still higher than that of pure PP. The chain slippage may increase in the presence BPO_4 particles so the MFI values increases.

4.10.3 Differential Scanning Calorimeter (DSC)

The DSC data of fiber samples are listed in Table 4.24. In order to estimate the percent crystallinity (X) the following equation is used:

$$X= [\Delta H_f / ((1-\Phi_p)^* \Delta H^0_f)]^*100$$

Φ_p is the mass fraction of BPO_4, ΔH_f is the heat of fusion of the sample analysed (J/g) and ΔH^0_f is a reference value that represents the heat of fusion for a %100 crystalline PP which is 209 J/g. The addition of 3 wt % BPO_4 increases the melting point (T_m) and percent crystallinity (X) of PA-6 crystals. This may result from the heterogeneous nucleation role of BPO_4. The previous studies show that the nano particles act as a nucleating agent when they are well dispersed in the polymer matrix [130, 181, 182]. When the amount of BPO_4 increases to 10 wt %, T_m and X value decrease but are still higher than the pure PA-6. As the amount of BPO_4 increases, they tend to form agglomerates. These agglomerates deteriorate the crystallization process and T_m and X values are reduced. In the case of PP, both T_m and X values decreases due to the poor filler dispersion that arises from apolar character of PP.

Table 4.24 DSC data of BPO_4 containing fibers

SAMPLE	Tm (^oC)	X (%)
PA-6	215.8	26.0
PA-6+ 3 wt % BPO_4	218.2	36.5
PA-6+ 10 wt % BPO_4	217.6	29.3
PP	164.9	40.2
PP+ 3 wt % BPO_4	161.5	39.8
PP+ 10 wt % BPO_4	162.5	39.1

Tm: Melting point **X:** Percent crystallinity

4.10.4 Thermal Gravimetric Analysis (TGA)

TGA curves and data of fibers are shown in Figure 4.29 and Table 4.25, respectively. According to Figure 4.29 and Table 4.25, the weight loss of pure PA-6 and PP takes place in a single step, with a maximum weight loss rate at 462 °C and 468 °C, respectively. The inclusion of BPO_4 increases the amount of residue. The residue mainly consists of the undecomposed BPO_4 part. Although the addition of BPO_4 does not change the decomposition temperature (T_{max}) of PP, that of PA-6 is reduced by about 30 ^{o}C. Kılınç M. et.al studied the decomposition product distribution BPO_4 using mass spectroscopy and showed that the decomposition products were BPO_4, BPO_3, $BPO^{\cdot}$, PO_4, O_2 [83]. According to these results BPO_4 can be a source of oxygen and reduces the T_{max} of PA-6 which is more sensitive to thermo oxidative degradation than PP.

Table 4.25 TGA data of BPO_4 containing fibers

SAMPLE	$T_{5\%}$ [a] (°C)	$T_{50\%}$ [b] (°C)	T_{max} [c] (°C)	Char Yield (%)
PA-6	386	449	462	0.1
PA-6+ 3 wt % BPO_4	379	428	430	2.7
PA-6+ 10 wt % BPO_4	381	425	430	7.9
PP	425	460	468	0.0
PP+ 3 wt % BPO_4	412	463	471	2.1
PP+ 10 wt % BPO_4	417	460	465	8.6

a: Temperature at 5% weight loss **b**: Temperature at 50% weight loss
c: The maximum rate degradation temperature

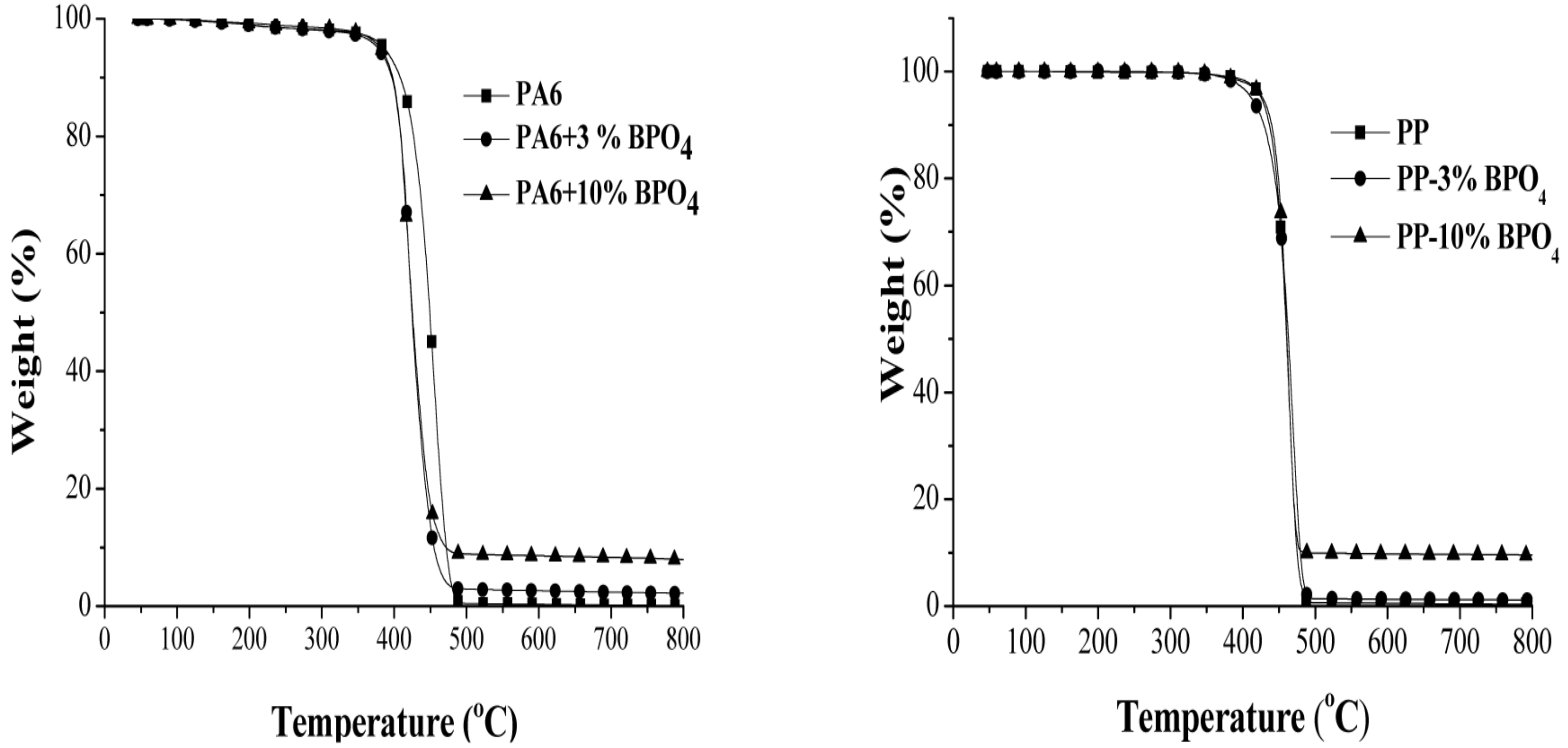

Figure 4.29 TGA graphs of fibers containing BPO_4

4.10.5 Micro Combustion Calorimeter (MCC)

The char yield, HRR Peak, THR and char character obtained from the MCC are listed in Table 4.26. The HRR curves of the fibers and the photograph of char residues are shown in Figure 4.30 and Figure 4.31, respectively. The general shape of HRR curves and derivative of TGA curves are almost the same. Morgan et al. showed that when both peaks are aligned with each other, the main prylosis product of composites is flammable [146]. As a result of MCC test, the amount of residue increases with increasing amount of BPO_4, and the T_{max} of PA-6 is reduced with the addition of BPO_4. These results are in accordance with TGA results.

The addition of BPO_4 reduces the THR value of fibers but the reduction is not meaningful because the percent reduction in THR corresponds to the percent decrease in the amount of matrix material. The reduction in HRR peaks is not so much due to the thermally thin character of fiber samples and the particle shape of BPO_4. The previous studies showed that the particles in a nanometer size with fiber or plate like shape have better barrier formation ability than the spherical ones [14, 84]. When HRR peaks are considered separately, HRR peaks remain almost the same for PP fiber, and HRR peaks are reduced by about 5 % and 12 % with respect to PA-6 with the addition of 3 and 10 % BPO_4. The reason why the BPO_4 causes more reduction in HRR peaks of PA-6 than PP arises from the char forming ability of polymer itself. Without char formation, the BPO_4 particles are not able to form continuous barrier formation which is the general flame retardant mechanism in polymer nanocomposites, so no reduction is observed for PP composites. PA-6 degrades by the formation of thin black film, and BPO_4 particles are integrated into the char and increases the barrier effect of the char, and HRR values are reduced more compared to PP. It can be concluded that the nanoparticles show better flame retarding effect with char forming polymers without using any conventional flame retardant.

Table 4.26 MCC data BPO_4 containing fibers

SAMPLE	Char Yield (wt%)	HRR Peak(s) Value (W/g)	Max Temperature (°C)	Total HR (kJ/g)	Char Observations
PA-6	0.67	563	491	28.2	thin black
	0.57	568	491	28.2	film all over
	0.60	570	491	28.2	pan, no ash
PA-6+3 BPO_4	2.11	531	476	27.5	thick dark
	2.85	559	475	27.5	black film all
	1.46	529	475	27.3	over pan
PA-6 +10 BPO_4	8.74	467	476	25.7	thick darker
	9.1	497	479	25.7	black film
	6.81	543	477	25.7	than %3
PP	0.07	763, 632	477	36.4	No char
	0.08	769, 642	477	36.3	
	0.08	763, 639	478	36.4	
PP+3 BPO_4	3.56	728, 618	484	36.2	Grey ash all
	3.55	752, 644	484	36.7	over pan
	3.56	729, 627	483	36.4	
PP+10 BPO_4	8.78	742, 623	482	33.4	Grey ash all
	8.71	773, 651	487	33.7	over pan
	8.70	747, 624	485	33.5	

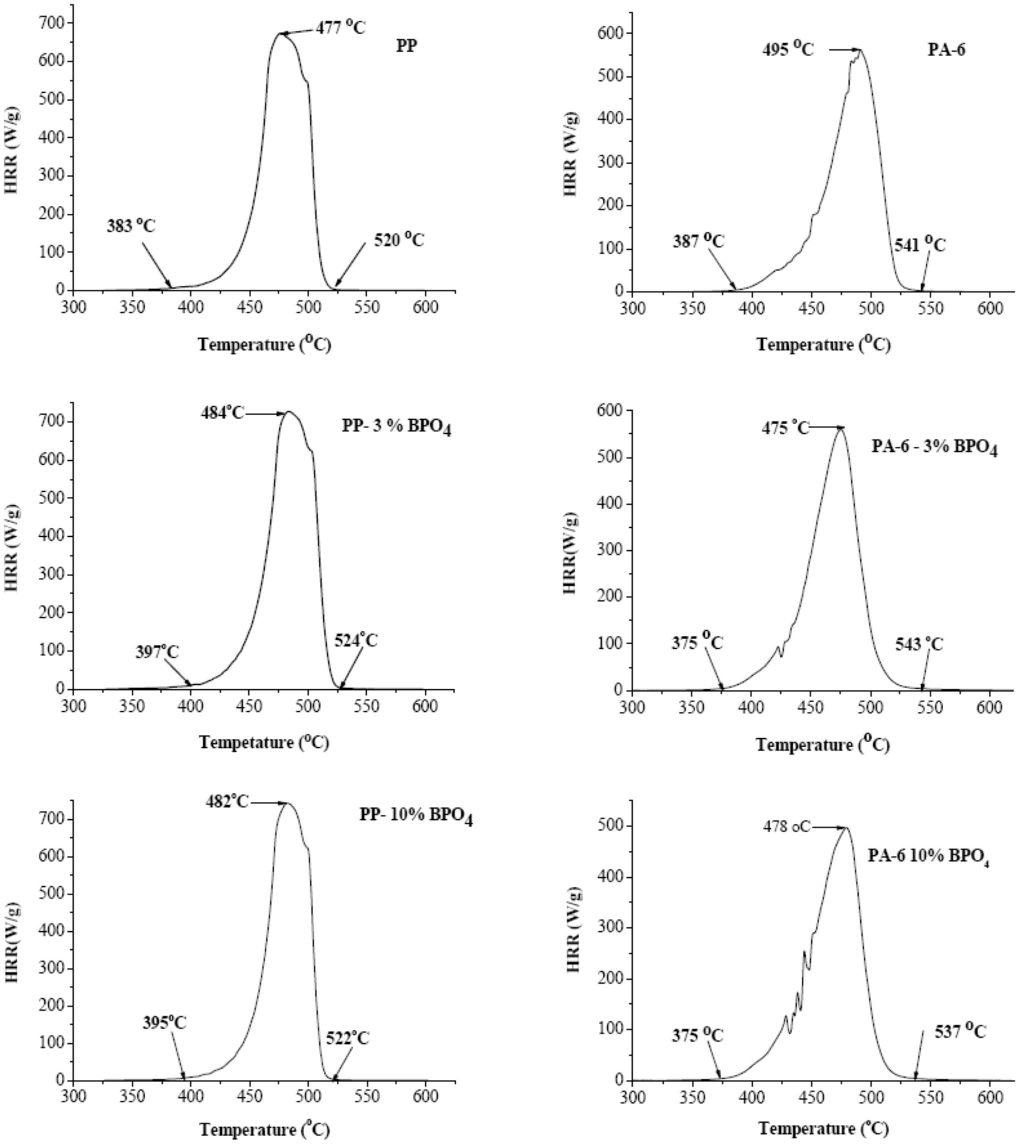

Figure 4.30 HRR curves of BPO_4 containing fibers

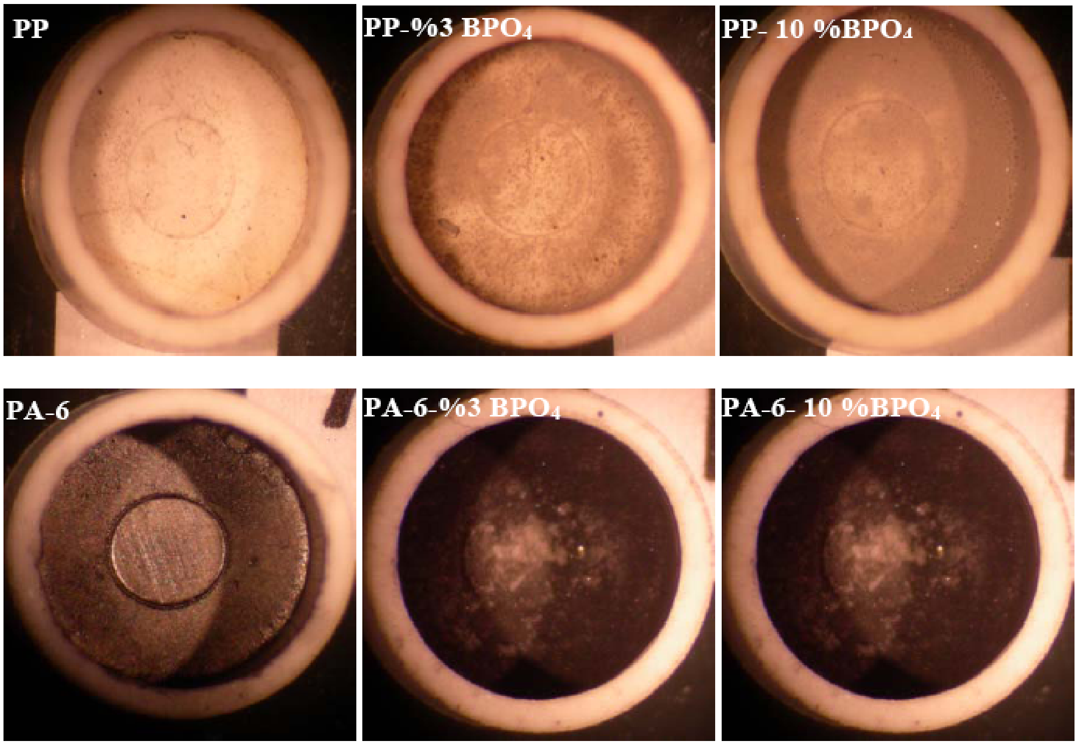

Figure 4. 31 The photographs of char residues

4.11 The Mechanical, Thermal and Fire Retardant Properties of Polyamide-6 Fibers Containing Zinc Phosphinate, Zinc Borate and/ or Clay

ZnPi is a kind of organic phosphinate and melts at about 220 °C and ΔH_m is 24.9 J/g as seen from Figure 4.32. In order to see effect of ZnPi on mechanical properties of fiber samples, 5, 10 and 15 wt% ZnPi loaded fiber samples were prepared and the 10 wt% loading was chosen in order to see the effect of ZnPi and other synergy agents on mechanical, flow, thermal and fire retardant properties of the fibers.

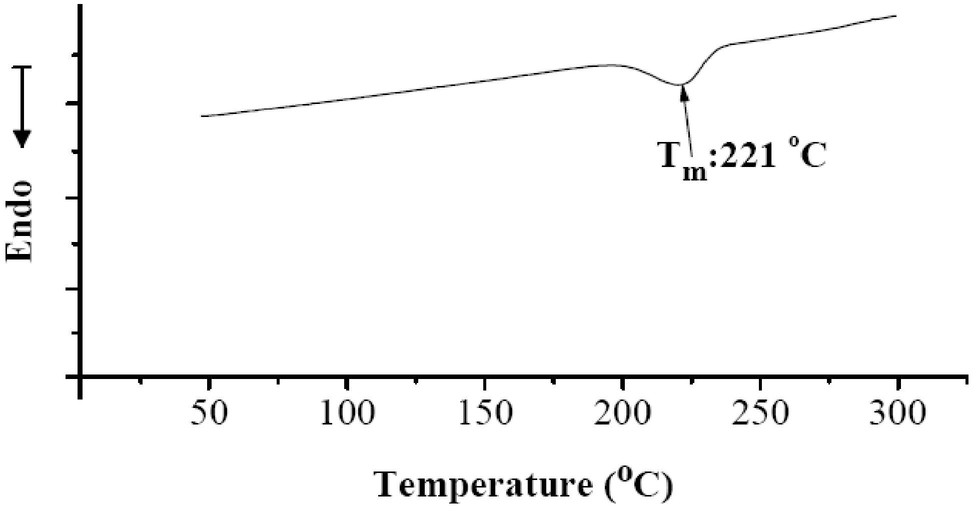

Figure 4.32 DSC curve of ZnPi

4.11.1 Morphology Characterization by WAXS

Figure 4.33 shows the XRD patterns for Closite 30B and Closite 30B containing composite (PA-6+ 8 ZnPi + 2Clay). Closite 30B shows a peak at 2θ = 4.9° corresponding to basal spacing of 17.9 A°. The clay containing compound shows two peaks at 2θ = 2.8° and 5.3° corresponding to basal spacings of 31.5 A° and 16.7 A°, respectively. This result indicates that the amount of shear is insufficient and the residence time is too short to obtain fully exfoliated structure. As a result, mechanical mixing facilitates the intercalation and collapse of clay layers to take place at the same time. Without TEM data, it is not possible to speculate further on exfoliated structure.

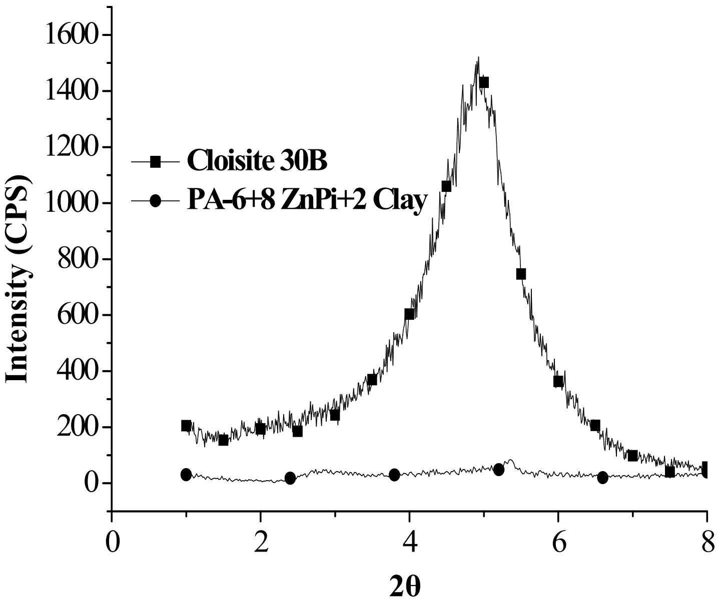

Figure 4.33 XRD graph of Cloisite 30 B and PA-6+8 ZnPi+2 Clay

4.11.2 Tensile Properties

Tensile tests on monofilament fiber samples were made to investigate the effect of additives on the mechanical properties of fibers. Stress at break values (σ) and elongation at break values (ε) at given draw ratios are listed in Table 4.27**.** Although the drawability of PA-6 in the presence of 5 wt% ZnPi does not change, further addition of ZnPi slightly reduces the drawability of the fiber. When 10 wt % flame retardant containing fibers are taken into consideration, the addition of both clay and ZnB does not change the drawability of PA-6 fiber. The addition of 5 % ZnPi does not deteriorate mechanical properties of PA-6 fiber and slightly increases the σ due to the fusible character of ZnPi at mixing temperature. The further addition of ZnPi reduces the σ value due to the lower draw ratio. The ε value of the fibers is reduced as the amount of ZnPi increases. When 10 wt % flame retardant containing fibers are considered, the incorporation of ZnB particle which has large particle size for fiber applications causes a reduction in both σ and ε values, since it is not fusible at process temperature and may form weak points along the fiber axis. The addition of clay reduces the ε due to the reduction in chain slippage arising from the constrained regions formed by the intercalated part of PA-6 chains [117].

Table 4.27 Draw ratios, MFI values and tensile properties of PA-6 fibers

SAMPLE	Draw Ratio	MFI (g/10 min)	Ø (µm)	σ (MPa)	ε (%)
PA-6	3	24±1.8	34±1.8	297±32	50±20
PA-6+ 5 ZnPi	3	23±0.8	33±2.4	312±21	48±20
PA-6+ 10 ZnPi	2.5	23±0.2	39±3.2	247±32	42±15
PA-6 + 15 ZnPi	2.5	22±0.4	37±3.5	203±32	33±16
PA-6+ 8 ZnPi +2 ZnB	2.5	19±0.8	34±4.8	217±35	36±15
PA-6+ 8 ZnPi + 2 Clay	2.5	15±0.1	35±2.5	260±37	48±19
PA-6+ 8 ZnPi+1ZnB+1Clay	2.5	18±0.6	37±1.4	206±20	21±8

Ø: Diameter of the fiber **σ:** Stress at break values **ε:** Elongation at break values

4.11.3 Melt Flow Index (MFI)

The effect of flame retardant additives on flow properties PA-6 was investigated by MFI measurements at spinning temperature of 240 ^{o}C. The MFI values of the fibers are listed in Table 4.27. The MFI value decreases as the amount of ZnPi increases. When 10 wt % flame retardant containing fibers are taken into consideration, the addition of ZnB and clay causes a further reduction of MFI values. The lowest MFI value is obtained when 2 % clay is added due to the intercalated part of the polymer chain, since the polymer chains at the polymer layered silicate interface may act as physical crosslinking points and increase the melt viscosity [183].

4.11.4 Thermal Gravimetric Analysis (TGA)

TGA curves and data of selected fibers are shown in Figure 4.34 and Table 4.28, respectively. According to Figure 4.34 and Table 4.28, the weight loss of pure PA-6 takes place in a single step, with a maximum of weight loss rate at 462 °C by leaving small amount of residue at 600 °C. The inclusion of ZnPi reduces the maximum degradation temperature of PA-6 and increases the amount of residue due to the formation of phosphorus species like phosphonates, phosphates, etc. [46]. The addition of both ZnB and organo clay increases the amount of char residue due to its own degradation products. It can be thought that both organoclay and ZnB do not increase the condensed phase products of ZnPi since the increase in char yield corresponds to the weight of residue that remained after the decomposition of ZnB and organoclay heated at 600 ^{o}C.

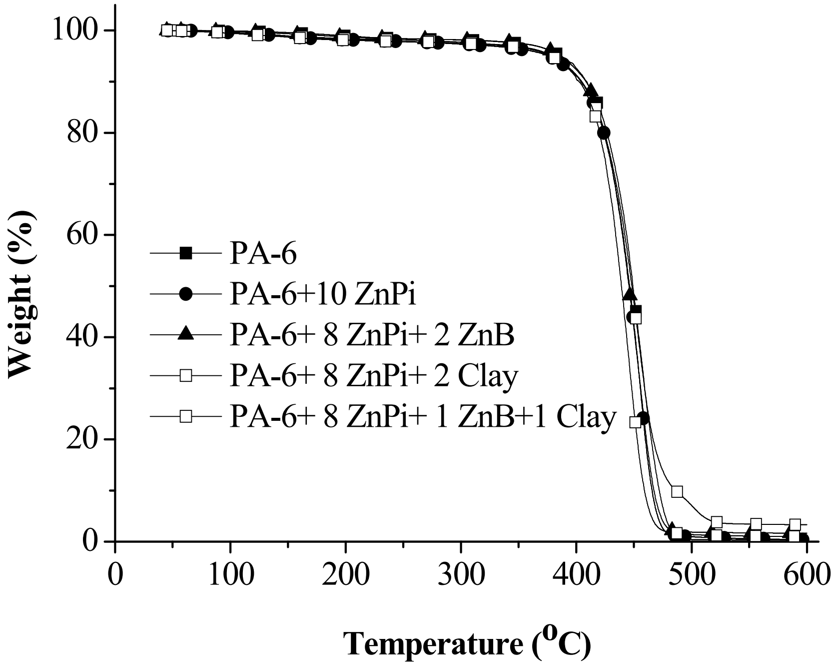

Figure 4.34 TGA curves of selected compositions

Table 4.28 TGA data of selected compositions

SAMPLE	$T_{5\%}$ [a] (°C)	$T_{50\%}$ [b] (°C)	T_{max} [c] (°C)	Char Yield (%)
PA-6	386	449	462	0.1
PA-6+ 10 ZnPi	395	451	454	0.8
PA-6+ 8 ZnPi +2 ZnB	386	445	462	1.9
PA-6+ 8 ZnPi + 2 Clay	378	448	454	3.3
PA-6+ 8 ZnPi+ 1 ZnB+ 1 Clay	377	439	443	2.2

a: Temperature at 5% weight loss **b**: Temperature at 50% weight loss
c: The maximum rate degradation temperature

4.11.5 Micro Combustion Calorimeter (MCC)

The char yield, HRR Peak, THR and char character obtained from the MCC are listed in Table 4.29. The HRR curves of the fibers and the photograph of the char residues are shown in Figure 4.35 and Figure 4.36, respectively.

In parallel with the TGA results, the inclusion of ZnPi, ZnB and organoclay increases the amount of char residue. It is thought that the predominant flame retardant mechanism of ZnPi is the vapor phase mechanism by the formation of diethyl phosphonic acid and the vaporization of intact molecule. Small amount of char formation and no reduction in HHR values of fibers with the inclusion of ZnPi is indicative of vapor phase mechanism. The reduction in HRR value is only observed in the clay containing PA-6 fiber samples due to the formation of multilayered carbonaceous-silicate layer on the burning surface [118-123]. This layer acts as a barrier for mass and heat transport and slows down the escape of the flammable volatiles generated during combustion. By the barrier effect of carbonaceous-silicate layer, the release rate of flammable fuel is reduced. When THR values of fiber samples are considered, the addition ZnB and organoclay further reduces the THR values with respect to the 10 wt% ZnPi containing fiber. The lowest THR value is obtained when the ZnB and organoclay are used together, the reduction in HRR and THR is not however, sufficient to give a flame retarding property to the fibers investigated.

Table 4.29 MCC data of selected fiber samples

SAMPLE	Char Yield (wt%)	HRR Peak(s) Value (W/g)	Max Temp. (°C)	Total HR (kJ/g)	Char Observations
PA-6	0.67	563	491	28.2	thin black film all over pan,
	0.57	568	491	28.2	No ash
	0.60	570	491	28.2	
PA-6+ 10 ZnPi	1.36	604	497	27.2	thin black film over ¾ pan,
	1.44	595	496	27.6	No ash
	1.38	604	496	27.6	
PA-6+ 8 ZnPi +2 ZnB	2.13	582	489	26.1	thin black film over ¾ pan,
	2.14	581	492	26.9	No ash
	2.07	590	491	26.7	
PA-6+ 8 ZnPi+ 2 Clay	3.26	515	491	26.9	thin black film over ¾ pan,
	3.18	524	490	27.1	one chunk of black ash
	3.19	516	490	26.3	
PA-6+ 8 ZnPi+ 1 ZnB+ 1 Clay	2.44	552	484	26.1	thin black film over ¾ pan,
	2.35	546	485	26.3	Speckled black spot all over pan
	2.36	548	485	26.0	

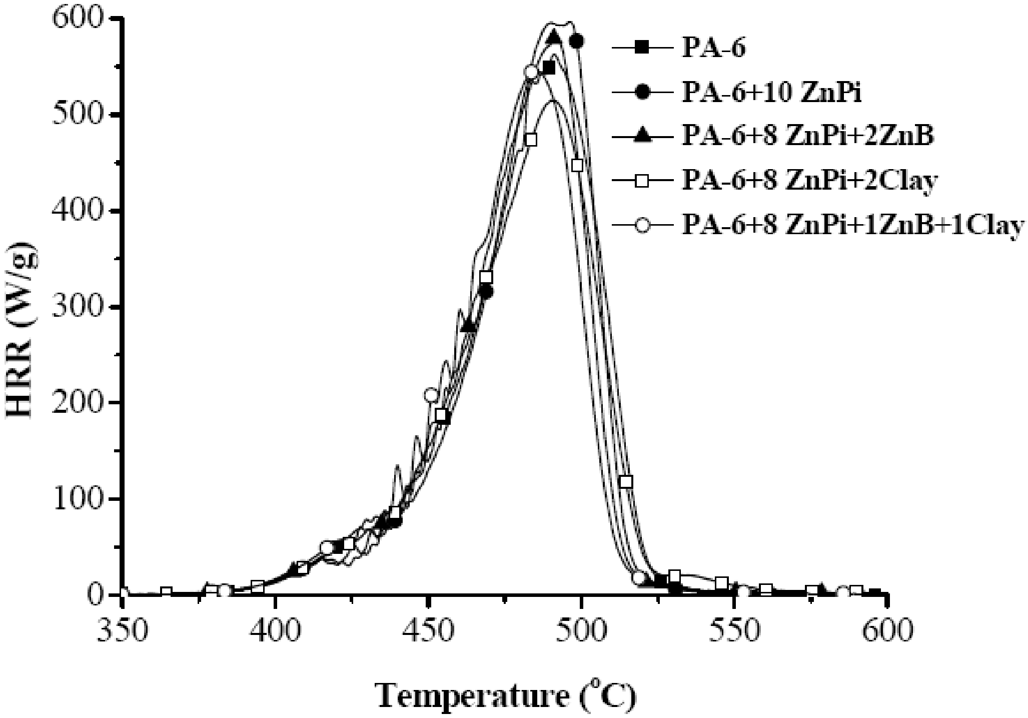

Figure 4.35 HRR curves of the fiber samples

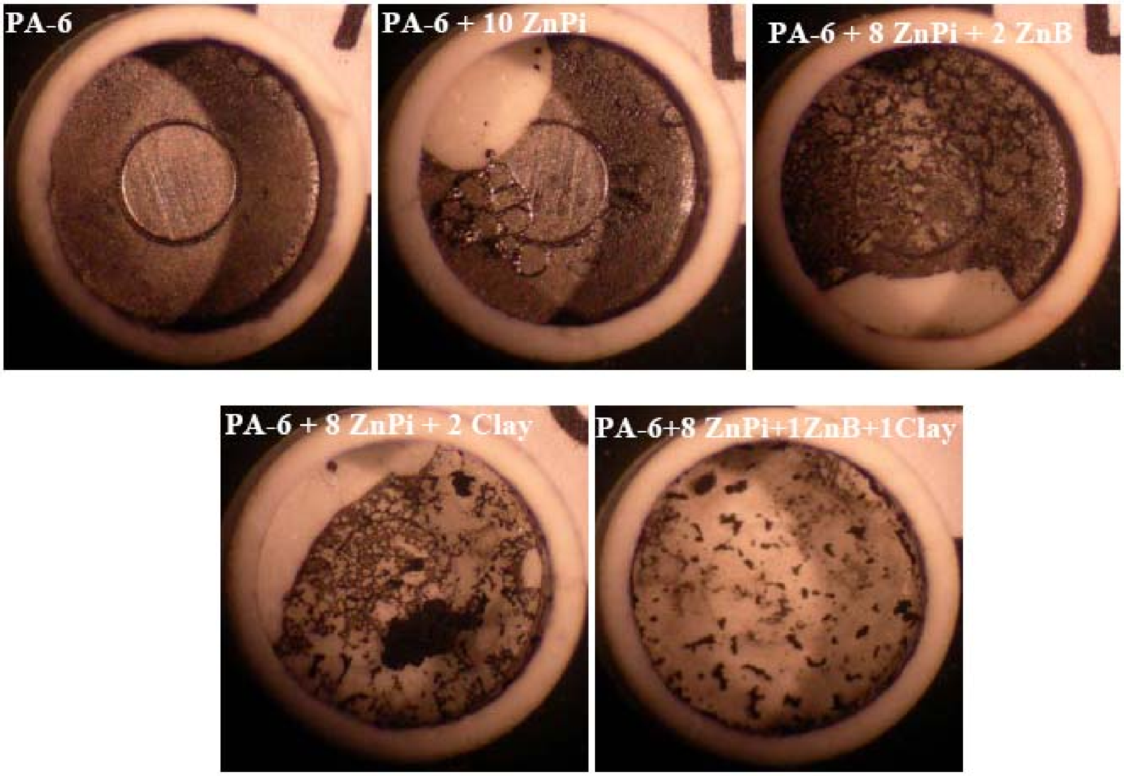

Figure 4.36 Char photos of the fiber samples

4.12 The Production of Flame Retardant Polypropylene Fibers Containing Intumescent Flame Retardant Additive

The flame retardant PP fiber is produced with modified APP (m-APP) which is much more effective than the APP/PER combination through phosphorus and nitrogen synergism [23] In order to see effect of m-APP on mechanical properties of fiber samples, 5, 10 and 15 wt% m-APP loaded fiber samples were prepared and the 10 wt% loading was chosen in order to see the effect of m-APP and other synergy agents (ZnB, BPO_4 and organo clay) on mechanical, flow, thermal and fire retardants properties of the fibers. The composition of the prepared fiber samples are given in Table 4.30

Table 4.30 The composition of the fiber samples

SAMPLE	PP	IFR	Clay	ZnB	BPO_4
F1	100	-	-	-	-
F2	95	5	-	-	-
F3	90	10	-	-	-
F4	85	15	-	-	-
F5	90	9	1	-	-
F6	90	9	-	1	-
F7	90	9	-	-	1
F8	90	8	1	1	-
F9	90	8	1	-	1

4.12.2 Morphology Characterization by WAXS

According to the Figure 4.37, Closite 15A shows two peaks at 2θ = 3.03° and 7.24°, corresponding to basal spacing of 29.12 and 12.2 A°, respectively. The first peak is due to organic modification which facilitates the increase between the silicate layers. The smaller peak at 7.24° corresponds to unintercalated clay platelets during modification. The composite F5 shows a peak at 2θ= 6.3° corresponding to basal spacing of 14 A°. The peak seen at 2θ= 3.03° completely disappeared and the peak seen at 2θ=7.24 shifted to the left. This result indicates that some of the clay platelets may be exfoliated and some portion remains intercalated. Without TEM data it is not possible to speculate further.

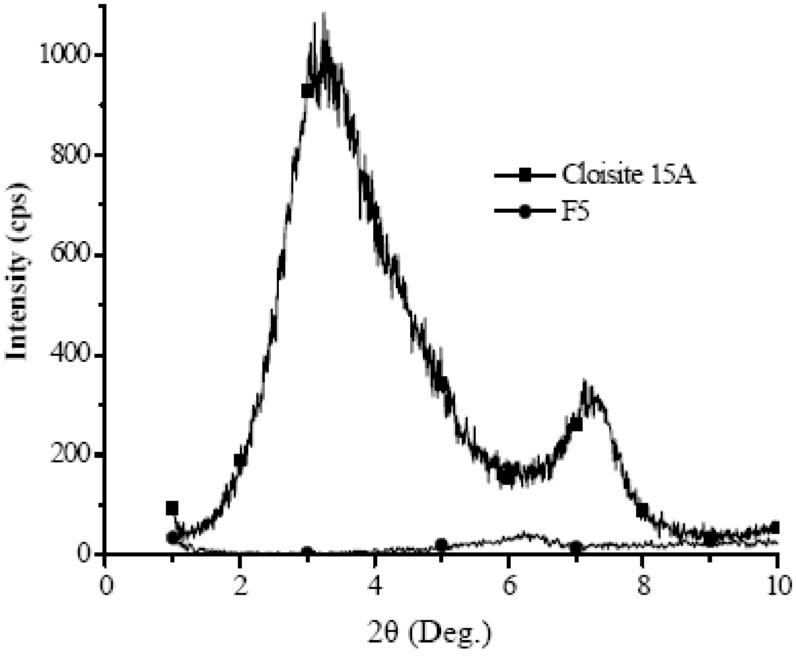

Figure 4.37 XRD Graph of Cloisite 15 A and F5

4.12.2 Flow Characteristics and Mechanical Properties

The MFI values, draw ratios and the mechanical properties of fibers are given in Table 4.31. As seen from Table 4.31, the addition of m-APP up to 10 wt % increased the MFI value of PP. The addition of clay, BPO_4 and ZnB causes the reduction of MFI values. PP fiber is produced at a draw ratio of 5 without any breakage during drawing process. The draw ratio is reduced in order to avoid the filament breakage as the amount of m-APP is increased. Breakage may arise from the large particle size of m-APP which is not fusible at spinning temperatures and its incompatibility with PP matrix. During drawing process, m-APP forms weak points and reduces the drawability of the fiber. The possible reflections of these weak points are seen as imperfections along the fiber containing 15 wt % m-APP given in Figure 4.38. The addition of clay, BPO_4 and ZnB does not alter the drawability of fibers since all the fibers containing 10 wt % flame retardant additive can be drawn at a ratio of 3.

Figure 4.38 The imperfections seen along the fiber axis containing 15 wt % m-APP

The stress value of PP is reduced as the amount of m-APP is increased in the fiber. The reduction in stress value results from the lower draw ratio and the inhomogeneties arising from the incompatibility and large particle size of m-APP. Elongation at break values of fibers are almost the same in spite of the varying draw ratios, since breakage depends on the amount of weak spots or inhomogeneties seen in fiber samples.

Table 4.31 The MFI values, draw ratios and the mechanical properties of fibers

SAMPLE	Draw Ratio	MFI (g/10 min)	Ø (µm)	σ (MPa)	ε (%)
F1	5.0	13.9±0.6	32±1.2	206±14	60±12
F2	4.0	17.0±1.4	30±1.6	180±26	59±13
F3	3.0	16.2±0.9	36±2.1	125±15	46±8
F4	2.5	12.7±0.9	36±2.3	93±13	61±15
F5	3.0	11.4±0.5	39±1.7	114±8	63±22
F6	3.0	11.4±0.7	30±1.9	138±23	63±18
F7	3.0	11.6±0.7	37±2.1	114±21	59±19
F8	3.0	11.4±1.2	32±2.3	152±21	66±25
F9	3.0	11.3±0.8	33±1.6	133±18	66±18

Ø: Diameter of the fiber **σ:** Stress at break values **ε:** Elongation at break values

4.12.3 Flame retardant properties of PP fibers

The char yield, HRR Peak, THR and char character obtained from the MCC are listed in Table 4.32. The HRR curves of the fibers and the photograph of the char residues are shown in Figures 4.39 and 4.40, respectively.

The pure PP degrades without giving any char residue. With the addition of 10 wt% m-APP, a fluffy black char residue is formed at about 3.9 wt %. The reason of the increase in the char yield is the carbonization reaction between the APP and the surface coating material. With the addition of clay, BPO_4 and ZnB, the amount of char residue further increases. The highest char yield is obtained when of 1% ZnB is added in the presence of 9 wt% m-APP. The possible reason of higher char yield is the interaction between APP and metallic Zn. The Zn ion may replace ammonia in APP and crosslinking reaction can occur between polyphosphoric acid chains, so it reduces the volatility of polyphosphoric acid and more polyphosphoric acid compound will be available for the char formation. The maximum degradation temperature (T_{max}) increased by about 5 °C with the addition of m-APP and the addition of synergy agents makes negligible effect on T_{max} value.

The addition of m-APP with and without synergy agents BPO_4 does not change the shape of HRR curve. The shape of HRR curve is not in accordance with the HRR curve of typical insulative intumescent layer which stays relatively constant and slowly decreases towards the end of combustion. Although the shape of HRR curve does not change due to the thermally thin character, the addition of m-APP reduces the HRR and THR values slightly. The addition of boron compounds with or without clay does not provide any further reduction in terms of PHRR and THR. If a fabric is made from these fibers, it may show better flame retardant property due to its thickness which is much higher than that of a monofilament fiber.

Table 4.32 MCC data of selected fiber samples

SAMPLE	Char Yield (wt%)	HRR Peak(s) Value (W/g)	Max Temperature (°C)	Total HR (kJ/g)	Char Observations
F1	0.07	763, 632	477	36.4	No char
	0.08	769, 642	477	36.3	
	0.08	763, 639	478	36.4	
F3	3.93	731, 619	484	34.7	Fluffy black char/residue filling 1/3 of sample crucible
	3.95	730, 625	485	35.0	
	3.72	741, 635	481	35.2	
F5	4.43	741, 615	483	34.1	Fluffy black char/residue filling 2/3 of sample crucible
	4.62	754, 641	485	35.1	
	4.28	732, 619	481	34.8	
F6	6.08	749, 634	484	34.5	Fluffy black char/residue Crucible completely full of Char
	6.23	761, 657	483	35.4	
	5.84	768, 657	484	35.3	
F7	4.92	761, 651	484	34.6	Fluffy black char/residue filling 1/3 of sample crucible
	4.76	755, 650	484	34.7	
	4.64	749, 643	484	34.6	
F8	5.10	783, 658	483	34.9	Fluffy black char/residue Crucible completely full of Char
	5.07	761, 635	482	34.5	
	5.35	775, 650	485	34.8	
F9	5.39	735, 622	483	33.8	Fluffy black char/residue filling 1/2 of sample crucible
	5.25	736, 623	486	34.1	
	5.23	753, 636	479	34.3	

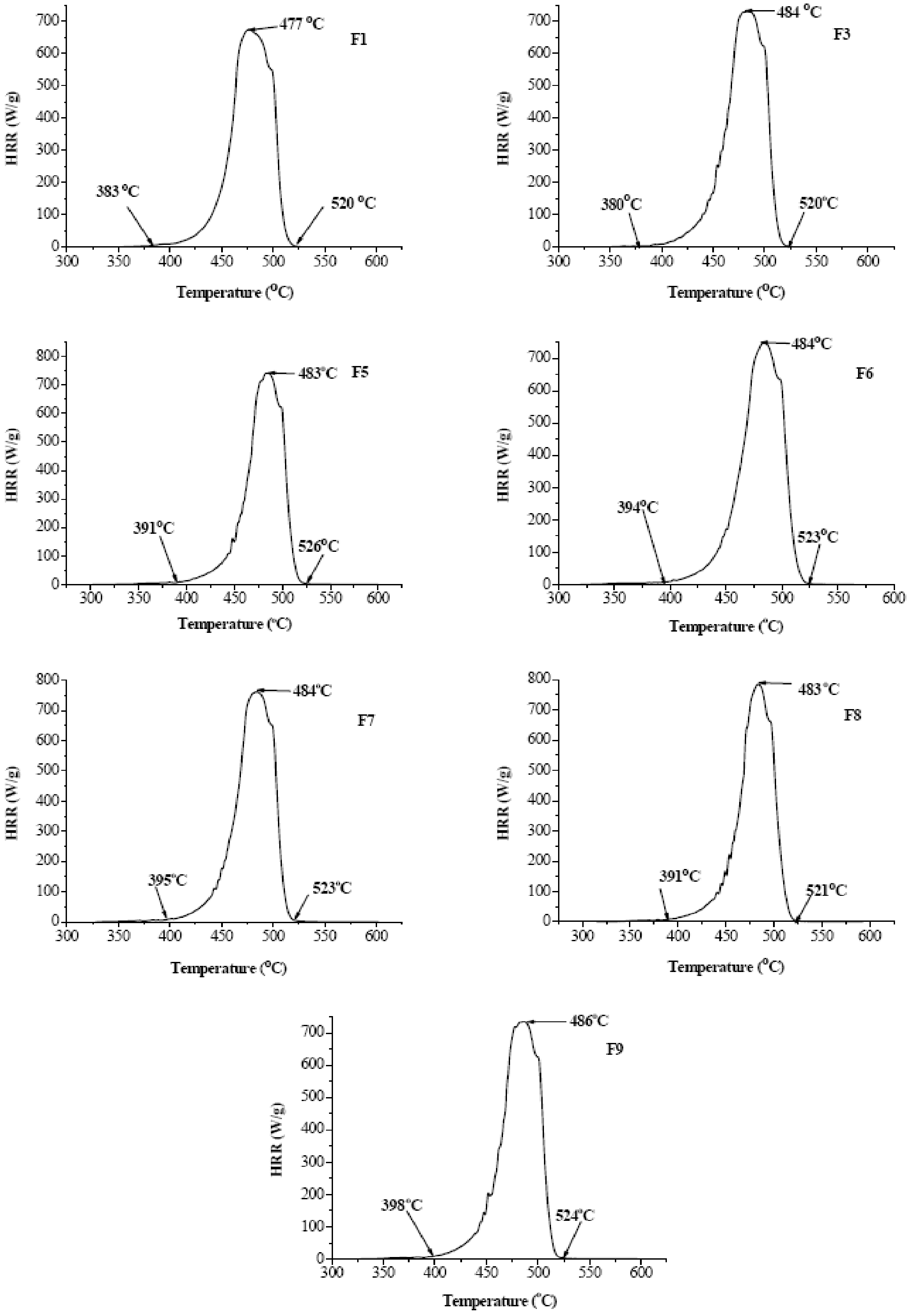

Figure 4.39 HRR curves of selected fiber samples

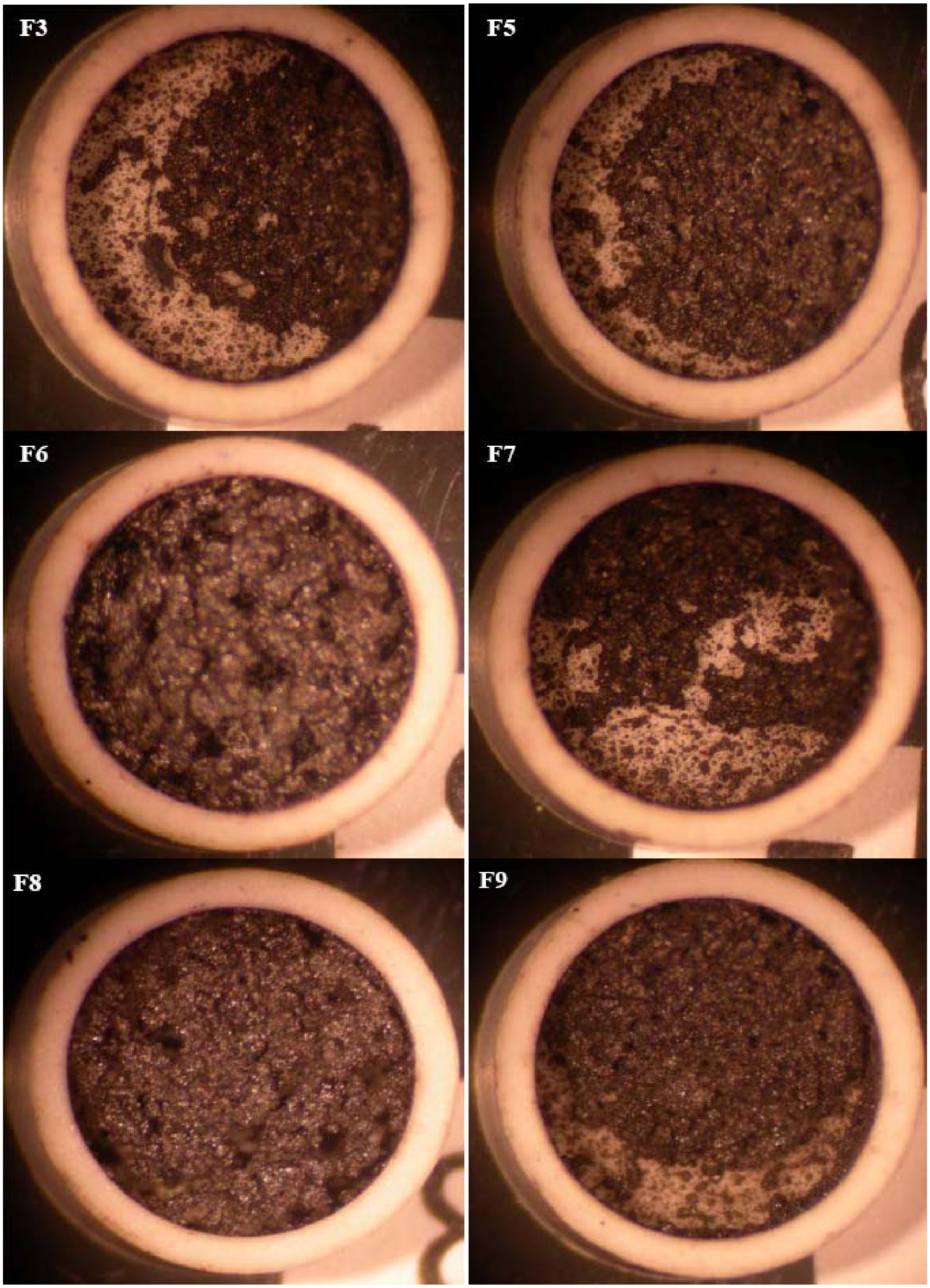

Figure 4.40 Char photos of selected fiber samples

CHAPTER 5

CONCLUSIONS

5.1 Effect of Boron Containing Materials on Flammability and Thermal Degradation of Polyamide-6 Composites Containing Melamine Cyanurate

The effect of the addition of boron compounds on the UL-94 testing and LOI is studied. TGA-FTIR, DSC and SEM investigations are also performed to understand the relevant basic mechanisms. According to the results, the inclusion of 15 % MC is enough for obtaining a V0 PA-6 compound. There is no synergistic effect observed between boron compounds and MC. Only BPO_4 containing samples show an improvement when the amount of BPO_4 reaches 3 and 5 wt % but, still giving lower LOI than only MC containing samples. This improvement is found to be due to an increase in dripping rate which seems to be one of the important flame retarding mechanisms in these systems. The combination of 10 wt % MC and 5 wt % BPO_4 can be an alternative to use 15 wt % MC. According to TGA-FTIR results, boron compounds do not change the degradation path of MC containing composites, but they do increase the char yield and reduce the T_{max} of both MC and PA-6 which can give rise to increased flame retardancy.

5.2 Effect of Boron Containing Materials on Flammability and Thermal Degradation of Polyamide-6 Composites Containing Melamine

The effect of the addition of boron compounds on the UL-94 test and LOI is studied. TGA-FTIR and DSC investigations are also performed for an understanding of the relevant basic mechanisms. According to results, the addition of 20 wt % melamine is enough for obtaining a V0 PA-6 compound. According to LOI test, there is a synergistic effect seen between BSi (1 wt%) and melamine. BPO_4 containing samples show promising results when the amount of BPO_4 reaches 3 and 5 wt %, but still giving lower LOI than only melamine containing sample. This improvement found is due to an increase in dripping rate which seems to be one of the important flame retarding mechanisms in these systems. According to TGA-FTIR results, boron compounds do not change the degradation path of melamine containing composites and reduce the decomposition temperature of PA-6.

5.3 Effect of Boron Containing Materials on Flammability and Thermal Degradation of Polyamide-6 Composites Containing Red Phosphorus

The addition of 10 wt % P-Red to PA-6 improves the flame retardancy mainly by the condensed phase action of P-red by the formation of phosphoric acid ester on burning polymer surface. The LOI value slightly increases from 22.5 % to 23 % but UL-94 rating does not change. According to UL-94 test, boron compounds do not show any synergy and all composites have a rating of V2. According to LOI test, they show maximum flame retardancy effect at 3 wt % loading. According to TGA data, as the boron compound percentage increases in the composite, the char yield increases. According to cone calorimeter studies, the addition of P-red reduces the ignition time, maximum HRR and THR of PA-6 composites. The lowest maximum HRR and THR values are obtained in ZnB containing composites.

5.4 The Flame Retardant Effect of Aluminum Phosphinate in combination with Zinc borate, Borophosphate and Nanoclay in PA-6

The addition of 15 wt % AlPi increases the LOI value from 22.5 % to 29.5 % and V0 rating is obtained from UL-94 test. It is concluded that the AlPi shows its flame retarding action depending on degradation conditions both in the condensed and gas phase. Although the condensed phase action of AlPi increases under the high external fluxes, the predominant action of AlPi is in the gas phase due to the volatilization of AlPi during LOI, UL-94 and cone calorimeter studies. The addition of clay and BPO_4 does not change the predominant gas phase mechanism of AlPi during LOI, UL-94 and cone calorimeter studies. The addition of organoclay increased the condensed phase action of AlPi physically by the formation of thicker char in cone calorimeter studies. The addition of ZnB does not change predominant mechanism of AlPi in LOI and UL-94 tests, but cone calorimeter results indicate that an effective condensed phase mechanism becomes predominant by favoring formation of high amount of boron aluminum phosphate species due to the Lewis base character of boron.

5.5 Synergistic Effect of Boron Containing Substances on Flame Retardancy and Thermal Stability of Clay Containing Intumescent Polypropylene Nanoclay Composites

The addition of 20 wt % IFR to PP and nanoclay formulation improves the flame retardancy by forming about 9 wt% char, and delaying decomposition of the compound to higher temperatures. LOI value increases from 18.2 % to 23.5 %. Here, the basic mechanism is the formation of char that protects the underlying material. The addition of clay slightly increases the LOI value from 23 % to 23.5 %, whereas UL-94 rating does not change. The addition of clay increases the barrier effect of protective char, especially in thin samples and reduces TTI, maximum HRR and THR. According to LOI and UL-94 test, the addition of boron compounds to IFR formulation improves the intumescent function. Boron compounds show their maximum flame retardancy effect at 3 wt% loading. BPO_4 containing sample has highest LOI value (26.5 %) and ZnB containing sample shows highest rating (V0) in UL-94 test. According to cone calorimeter studies, the addition of IFR reduces the ignition time and HRR of PP composites. When the amount of ZnB exceeds a certain value, the protective effect of char decreases and HRR in cone calorimeter shows a second peak.

5.6 Synergistic Effect of Boron Containing Substances on Flame Retardancy and Thermal Stability of Intumescent Polypropylene Composites

The addition of 20 wt % IFR to PP improves the flame retardancy by forming char and delaying the decomposition of the compound. LOI value increases from 17.5 % to 23 %. The basic mechanism is the formation of char that protects the underlying material. According to LOI and UL-94 tests, boron compounds show their maximum flame retardancy effect at 1 wt % loading. 1 wt % boron compound containing composites show the highest UL-94 rating (V0). 1 wt % BPO_4 containing composite has the highest LOI value (30 %). According to TGA data, as the boron compound percentage increases in the composite, the char yield increases. According to cone calorimeter studies, the addition of IFR reduces the ignition time, maximum HRR and THR of PP composites. The lowest maximum HRR and THR values are obtained in BPO_4 containing composites. The main result of this study is that the boron compounds show their synergistic effect by reinforcing and increasing the barrier effect of the char.

5.7 The Effect of Metal Oxide Doped Boron Phosphates on Flame Retardancy and Thermal Stability of Intumescent Polypropylene Composites

According to the LOI and UL-94 test, metal oxide doped BPO_4s does not show better flame retardant properties with respect to BPO_4. For this reason, no further investigation was made.

5.8 The Effect of Boron Compounds on the Fire Retardant Properties of Intumescent Polypropylene Composites Containing m-APP

The results show that the addition of 20 wt % IFR to PP improves the flame retardancy by forming about 5 wt % highly insulative protective char, and delays decomposition of the compound to high temperatures. LOI value of pristine PP increases from 17.5 % to 31 % and UL-94 rating increases from BC to V0. According to UL-94 and LOI tests, boron compounds did not alter UL-94 rating and slight increase was observed in at LOI values except 1 wt% LaB containing one. This slight increase may have arisen from the increased the amount of char formation. According to cone calorimeter results, addition of IFR reduces the ignition time, maximum HRR and THR of PP. The addition of boron compounds extends the total burning time and delays the destruction of protective char. However, the increase in the average and total heat release values of compounds with the addition of boron compounds showed that the boron compounds reduced the barrier effect of foamed char due to the formation of cracks and small holes on char surfaces. The addition of boron compounds also increases the burning time and delays the destruction of protective char.

5.9 Effect of Boron Phosphate on the Mechanical, Thermal and Fire Retardant Properties of Polypropylene and Polyamide-6 Fibers

According to the results, the inclusion of BPO_4 particles has little effect on drawability of monofilament yarns. The mechanical properties of both fibers are reduced as the amount of BPO_4 increases. BPO_4 particles act as a nucleating agent in PA-6, whereas they deteriorate the crystallization process in PP. The addition of BPO_4 does not change the thermal stability of PP fiber and reduces the thermal stability of PA-6 fiber at about 30 ^{o}C. According to MCC results, the addition of BPO_4 does not change the total heat evolution and heat release rate (HRR) peak for PP fibers. Although the inclusion of BPO_4 does not change the total heat evolution of PA-6 fiber, it reduces the HRR peaks due to the increase the barrier effect of formed char. It can be inferred that the nanoparticles show better flame retarding effect with char forming polymers without using any conventional flame retardant

5.10 The Mechanical, Thermal and Fire Retardant Properties of Polyamide-6 Fibers Containing Zinc Phosphinate, Zinc Borate and/or Clay

According to the results, the inclusion of ZnPi particles at 5 wt% does not change the drawability of the fiber sample but the further addition of ZnPi slightly reduces the drawability. The tensile strength of the PA-6 fiber decreases with the addition of 10 wt ZnPi but the reduction is not so much due to the fusible character of ZnPi at spinning temperature. The addition of clay causes an increase in tensile strength, but the addition of ZnB causes a reduction of mechanical propeties due the its large particle size for fiber applications. From the mechanical point of view, the addition of clay moderately tolerates the reduction of tensile strength. According to the TGA and MCC results, the addition of ZnPi, ZnB and organo clay increases the char yield. The lowest HRR values are obtained when the organo clay is added in the presence of ZnPi. The lowest THR values are obtained when ZnB and organo clay is used together with ZnPi. It is evident that if these produced fiber samples get into fabric form, they show more distinctive flame retardant properties.

5.11 The Production of Flame Retardant Polypropylene Fibers Containing Intumescent Flame Retardant Additive

According to the results, the drawability of the fibers are reduced as the amount of m-APP is increased in the fiber structure. The addition of clay, BPO_4 and ZnB does not alter the drawability of the fiber samples. The tensile strength of the fiber is reduced as the amount of m-APP increased in the fiber structure due to the larger particle size and low compatibility with the matrix material. The addition of m-APP increases the char yield and the usage of synergy agents with m-APP causes a further increase in char yield. The inclusion of AP-765 decreases the HRR and THR values slightly. The addition of boron compounds with or without clay does not provide any further reduction in terms of PHRR and THR. If a fabric is made from these fibers, it may show better flame retardant property due to its thickness which is much higher than that of a monofilament fiber.

CHAPTER 6

RECOMMENDATIONS

When the total number of commercially available flame retardants are considered and the numerous boron compounds which are commercially available and those that can be synthesized, many combinations are possible on the flame retarding effect of boron compounds with or without commercially available flame retardants. In the scope of this study, boron compounds show synergistic effect with selected commercially available phosphorus substances and they do not show any synergistic effect with selected nitrogen containing flame retardants. These findings are important for the future studies made by boron compounds. The researchers who want to work on flame retarding effect on boron compounds should focus on the synergistic effect of boron compounds with different phosphorus compounds or same phosphorus compounds with different types of polymers. As a result of composite trials, boron compounds can find new application areas for increasing the flame retarding character of polymeric materials. If the studies are widened to different polymers or different phosphorus compounds, the usage of boron compounds can further be increased.

Although certain companies manufacture flame retardant additives for fiber applications, they do not find wide usage due to adverse effect on textile properties of fibers such as dyeability, appearance, handle etc. In the view of developments in nanotechnology, many fiber specialists started to use them as flame retardants by additive approach and melt spinning technique with acceptable textile properties. For the time being, the layered silicates show best flame retardant property with respect to the other nano size particulates. The nano particles to be synthesized and the developments to be made on increasing the dispersion of layered silicate into polymer matrix may enable the researchers to produce flame retardant fiber by this approach. The studies made on the synergistic effect of different flame retardants with each other may also enable the researchers to produce flame retardant fibers. The investigation of new flame retardants which are fusible and stable at fiber spinning temperatures also enable the researchers to produce flame retardant fibers.

In this thesis study, the amount of fibers produced is not sufficient to weave or knit the fiber samples. If these fibers are produced in a commercial mill, they can show more flame retardant property than the monofilament form. As a continuation of this study,

(1) If the fiber samples are produced in fiber spinning mill in the form of threads (collection of fiber bundles), they can be characterized as fabric both for their flame retardant properties and other textile properties.

(2) Instead of using micron size ZnB, these fibers can be produced with nano ZnB which was not commercially available during this study.

(3) The synergistic effect of boron compounds can be investigated with some commercially available nano size flame retardants. If any synergy is seen, the fibers can be produced from these combinations.

(4) Out of scope of this study, flame retardant PET fiber which shows better flame retardancy effect than PP and PA-6 fiber produced in this study can be produced in our laboratory. These findings are thought to be very important for finding new application areas of boron compounds. The production of PET flame retardant fiber can be widened.

REFERENCES

1. Kar Y., Şen N., Demirbaş A., "Boron Minerals in Turkey, Their Application Areas and Importance for the Country's Economy", Minerals&Energy, vol 20, 2006.

2. Woods G.W., "An Introduction to Boron: History, Sources, Uses and Chemistry", Environmental Health Perspectives, vol 102, 5-11, 1994.

3. Calamari T.A., Harper R.J., "Flame Retardants for Textiles", Kirk-Othmer Encyclopedia of Chemical Technology, 2000.

4. Grand A.F., Wilkie A.C., "Fire Retardancy of Polymeric Materials", Marcel Dekker, Inc., New York, 2000.

5. Lewin M., Atlas S.M., Pearce E.M., "Flame Retardant Polymeric Materials", Plenum Press, New York and London, 1975.

6. Lomakin S.M., Zaikov G.E., "Modern Polymer Flame Retardancy", VSP, Boston, 2003.

7. Pearce M.E., Liepins R., "Flame Retardants", Environmental Health Perspectives, vol 11, pp 59-69, 1975.

8. Kuryla W.C., Papa A.J., "Flame Retardancy of Polymeric Materials", vol. 2, Marcel Dekker, New York, 1973.

9. Morgan A.B., Wilke C.A., “Flame Retardant Polymer Nanocomposites”, John Wiley & Sons, New Jersey, 2007.

10. Zhang S., Horrocks A.R., “A Review of Flame Retardant Polypropylene Fibres”, Progress in Polymer Science, vol. 28, 1517-1538, 2003.

11. Subbulakshmi M.S., Kasturiya N., Bajaj P., Agarwal A.K., “ Production of Flame Retardant Nylon 6 and 6.6”, Macromol. Chem. Phys., vol. 40, 85-104, 2000.

12. Levchik V. S., Weil E.D., “Featured Article Combustion and Fire Retardancy of Aliphatic Nylons”, Polymer International, vol. 49, 1033-1073, 2000.

13. Tsafack M.J., Levalois-Grützmacher J., “Plasma-induced Graft-polymerization of Flame Retardant Monomers onto PAN Fabrics”, Surface &Coating Technology, vol. 200, 3503-3510, 2006.

14. Hull T. R., Kandola B.K., “Fire Retardancy of Polymers New Strategies and Mechanisms”, RSC Publishing, Cambridge, 2009.

15. Horrocks A.R., Kandola B.K., Davies P.J., Zhang S., Padbury S.A., “Developments in Flame Retardant Textiles- A Review”, Polymer Degredation and Stability, vol. 88, 3-12, 2005.

16. Horrocks A.R., “Flame Retardant Challenges for Textiles and Fibres: New Chemistry Versus Innovatory Solutions”, Polymer Degredation and Stability, DOI: 10.1016/j.polymerdegradstab.2010.03.036.

17. Mouritz A.P., Gibson A. G., “Fire Properties of Polymer Composite Materials”, Springer, Dordrecht, 2006.

18. Lu S., Hamerton I., “Recent Developments in the Chemistry of Halogen-free Flame Retardant Polymers”, Progress in polymer Science, vol. 27, 1661-1712, 2002.

19. Xanthos M., “Funtional Fillers for Plastics”, Wiley-VCH, Weinheim, 2005.

20. Li Q., Pingkai J., Wei P., “Thermal Degradation Behavior of Poly(propylene) with a Novel Silicon- Containing Intumescent Flame Retardant”, Macromolecular Materials and Engineering, vol.290, 912-919, 2005.

21. Bourbigot S., Le Bras M., Duquesne S., Rochery M., “Recent Advances for Intumescent Polymers”, Macromolecular Materials and Engineering, vol. 289, 499-511, 2004.

22. Xie F., Wang Y., Yang B., Liu Y., “A Novel Intumescent Flame-Retardant Polyethylene System”, Macromolecular Materials and Engineering, vol. 291, 247-253, 2006.

23. Doğan M., Bayramli E., “Synergistic Effect of Boron Containing Substances on Flame Retardancy and Thermal Stability of Clay Containing Intumescent Polypropylene Nanoclay Composites”, Polymers for Avanced Technologies, DOI: 10.1002/pat.1650.

24. (Melamine based flame retardants mechanism of action), http://www.specialchem 4polymers.com /tc/melami ne-flame-retardants/index.aspx?id=4005, last accessed on 05/05/2011.

25. Isıtman N. A., Gunduz H. O., Kaynak C., “Nanoclay Synergy in Flame retarded/glass Fibre Reinforced Polyamide 6”, Polymer Degradation and Stability, vol. 94, 2241-2250, 2009.

26. Kiliaris P., Papaspyrides C. D., Pfaendner R., "Polyamide 6 Filled with Melamine Cyanurate and Layered Silicates: Evaluation of Flame Retardancy and Physical Properties", Macromolecular Materials and Engineering, vol. 293, 740- 751, 2008.

27. Wikipedia, Melamine cyanurate, http://en.wikipedia.org/wiki/Melamine_cyanurate, last accessed on 05/05/2011.

28. Doğan M., Yılmaz A., Bayramlı E., "Effect of Boron Containing Materials on Flammability and Thermal Degradation of Polyamide-6 Composites Containing Melamine Cyanurate", Polymers for Advanced Technologies, DOI: 10.1002/pat.1545.

29. Weil E. D., Levchik S., "Current Practice and Recent Commercial Developments in Flame Retardancy of Polyamides", Journal of Fire Sciences, vol. 22, 251-264, 2004.

30. Wikipedia, Melamine, http://en.wikipedia.org/wiki/File:Melamine.svg, last accessed on 05/05/2011.

31. Doğan M., Bayramli E., "Effect of Boron-containing Materials on the Flammability and Thermal Degradation of Polyamide 6 Composites Containing Melamine", Journal of Aplied Polymer Science, DOI: 10.1002/app.32637.

32. Liu Y., Wang Q., "Melamine Cyanurate- Microencapsulated Red Phosphorus Flame Retardant Unreinforced and Glass Fiber Reinforced Polyamide 66", Polymer Degredation and Stability, vol. 91, 3103-3109, 2006.

33. ChemWiki,http://chemwiki.ucdavis.edu/Inorganic_Chemistry/Descriptive_Chemistry/Main_Group_Elements/Group_15:_The_Nitrogen_Family/The_Chemistry_of_Phosphorous#Red_Phosphorus_and_Violet_Phosphorus, last accessed on 05/05/2011.

34. Wang H., Meng X., Wen B., Gao X., Zhang S., Yang M., " A Simple Route for the Preparation of Red Phosphorus Microcapsule with Fine Particle Distribution", Materials Letters, vol. 62, 3745-3747, 2008.

35. Davis J., Huggard M., "The Technology of Halogen-free Flame Retardant Phosphorus Additives for Polymeric Systems", Journal of Vinyl & Additive Technology, vol. 2, 69-75, 1996.

36. Levchik G. F., Vorobyova S. A., Gorbarenko V. V., Levchik S. V., Weil E.D., "Some Mechanistic Aspects of the Fire Retardant Action of Red Phosphorus in Aliphatic Nylons", vol. 18, 172- 182, 2000.

37. Schartel B., Kunze R., Neubert D., "Red Phosphorus- Controlled Decompositon for Fire retardant PA66", Journal of Applied Polyme Science, vol. 83, 2060-2071, 2002.

38. Laoutid F., Ferry L., Lopez-Cuesta J. M., Crespy A., "Flame-retardant Action of Red Phosphorus/ Magnesium Oxide and Red Phosphorus/ Iron Oxide Compositions in Recycled PET", Fire and Materials, vol. 30, 343-358, 2006.

39. Chen X., Yu J., He M., Guo S., Luo Z., Lu S., "Effects of Zinc Borate and Microcapsulated Red Phosphorus on Mechanical Properties and Flame Retardancy of Polypropylene/ Magnesium Hydroxide Composites", Journal of Polymer Researches, vol. 16, 357-362, 2009.

40. Levchik S.V., Weil E. D., "A Review of Recent Progress in Phosphorus-based Flame Retardants", Journal of Fire Sciences, vol. 24, 345-364, 2006.

41. Levchik S.V., Weil E. D., "Review Flame Retardancy of thermoplastic polyesters- A Review of the Recent Literature", Polymer International, vol. 54, 11-35, 2005.

42. Braun U., Schartel B., “Flame Retardancy Mechanisms of Aluminium Phosphinate in Combination with Melamine Cyanurate in Glass-Fibre- Reinforced Poly(1,4-butylene terephthalate)”, Macromolecular Materials and Engineering, vol.293, 206-217, 2008.

43. Braun U., Schartel B., Fichera M. A., Jager C., “Flame Retardancy Mechanisms of Aluminium Phosphinate in Combination with Melamine Cyanurate and Zinc borate in Glass-Fibre- Reinforced Polyamide 6,6”, Polymer Degradation and Stability, vol.92, 1528-1545, 2007.

44. Laachachi A., Cochez M., Leroy E., Ferriol M., Lopez-Cuesta J.M., “Fire Retardant Systems in Poly (methyl metacrylate): Interractions Between Metal Oxide Nanoparticles and Phosphinates”, Polymer Degradation and Stability, vol. 92, 61-69, 2007.

45. Gallo E., Braun U., Schartel B., Russo P., Acierno D., “ Halogen-free Flame Retarded Poly (butylene terephtalate) (PBT) Using Metal Oxides/ PBT Nanocomposites in Combinaiton with Aluminium Phosphinate” Polymer Degradation and Stability, vol. 94, 1245-1253, 2009.

46. Vannier A., Duquesne S., Bourbigot S., Alongi J., Camino G., Delobel R., “ Investigaiton of the Thermal Degradation of PET, Zinc Phosphinate, OMPOSS and Their Blends- Identificaiton of the Formed Species”, Thermochimica Acta, vol. 495, 155- 166, 2009.

47. Isıtman N.A., Kaynak C., “Nanoclay and Carbon Nanotubes as Potential Synergists of An Organophosphorus Flame- retardant in Poly (methyl methacrylate)”, Polymer Degradation and Stability, vol. 95, 1523-1532, 2010.

48. Giraud S., Bourbigot S., Rochery M., Vroman I., Tighzert L., Delobel R., Poutch F., "Flame Retarded Polyurea with Microencapsulated Ammonium Phosphate for Textile Coating", Polymer Degredation and Stability, vol.88, 106-113, 2005.

49. Davies P.J., Horrocks A.R., Alderson A., "The Sensitisation of Thermal Decomposition of Ammonium Polyhosphate by Selected Metal Ions and Their Potential for Improved Cotton Fabric Flame Retardancy", Polymer Degredation and Stability, vol.88, 114-122, 2005

50. Ammounyumpolyphosphate, http://www.ul.ie/~childsp/CinA/Issue65/Images/TOC34_8.gif, last accessed on 05/05/2011.

51. Pinfa Flame Retardants, http://www.pinfa.eu/uploads/images/Inorganic _flame _retardants.jpg, last accessed on 05/05/2011.

52. Bourbigot S., Duquesne S., "Fire Retardant Polymers: Recent Developments and Opportunities", Journal of Materials Chemistry, vol. 17, 2283-2300, 2007.

53. Le Bras M., Bourbigot S., Delporte C., Siat C., Le Tallec Y., "New Intumescent Formulations of Fire Retardant Polypropylene-Dissussion of the Free Radical Mechanism of the Formation of Carbonaceous Protective Material during the Thermo Oxidaitve Treatment of the Additives", Fire and Materials, vol. 20, 191-203, 1996.

54. Camino G., Costa L., Trossarelli L., "Study of the Mechanism of Intumescence in Fire Retardant Polymers: Part I- Thermal Degradation of Ammonium Polyphosphate-Pentaerythritol Mixtures", Polymer Degradation and Stability, vol. 6, 243-252, 1984.

55. Camino G., Costa L., Trossarelli L., "Study of the Mechanism of Intumescence in Fire Retardant Polymers: Part II- Mechanism of Action in Polypropylene- Ammonium Polyphosphate- Pentaerythritol Mixtures", Polymer Degradation and Stability, vol. 7, 25-31, 1984.

56. Wu K., Song L., Wang Z., Hu Y., "Microencapsulation of Ammonium Polyphosphate with PVA-melamine-formaldehyde Resin and Its Flame Retardance in Polypropylene", Polymers for Advanced Technologies, vol. 19, 1914-1921, 2008.

57. Nie S., Hu Y., Song L., He Q., Yang D., Chen H., "Synergistic Effect Between a Char Forming Agent (CFA) and Microencapsulated Ammonium Polyphosphate on the Thermal and Flame Retardant Properties of Polypropylene", Polymers for Advanced Technologies, vol 19, 1077-1083, 2008.

58. Tang Y., Hu Y., Xiao J., Wang J., Song L., Fan W., "PA-6 and EVA Alloy/clay Nanocomposites as Char Forming Agents in Poly(propylene) Intumescent Formulations", Polymers for Advanced Technologies, vol. 16, 338-343, 2005.

59. Bourbigot S., Le Bras M., Dabrowski F., Gilman J.W., Kashiwagi T., "PA-6 Clay Nanocomposite Hybrid as Char Forming Agent in Intumescent Formulations", Fire and Materials, vol. 24, 201-208, 2000.

60. Bugajny M., Bourbigot S., Le Bras M., Delobel R., "The Origin and Nature of Flame Retardance in Ethylene-vinyl Acetate Copolymers Containing Hostaflam AP 750", Polymer International, vol. 48, 264-270, 1999.

61. Duquesne S., Samyn F., Bourbigot S., Amigouet P., Jouffret F., Shen K., "Influence of Talc on the Fire Retardant Properties of Highly Filled Intumescent Polypropylene Composites", Polymers for Advanced Technologies, vol. 19, 620- 627, 2008.

62. Samyn F., Bourbigot S., Duquesne S., Delobel R., "Effect of Zinc Borate on the Thermal Degradation of Ammonium Polyphosphate", Thermochimica Acta, vol. 456, 134-144, 2007.

63. Lewin M., "Synergism and Catalysis in Flame Retardancy of Polymers", Polymers for Advanced Technologies, vol. 12; 215-222, 2001.

64. Song P., Fang Z., Lifang Tong L., Jin Y., Lu F., "Effects of Metal Chelates on A Novel Oligomeric Intumescent Flame Retardant System for Polypropylene", Journal of Analytical and Applied Pyrolysis", vol. 82, 286-291., 2008.

65. Wang D., Liu Y., Wang Y., Artiles C.P., Hull T.R., Price D., "Fire Retardancy of A Reactively Extruded Intumescent Flame Retardant Polyethylene System Enhanced by Metal Chelates", Polymer Degradation and Stability, vol. 92, 1592-1598, 2007.

66. Lewin M., Endo M., "Catalysis of Intumescent Flame Retardancy of Polypropylene by Metallic Compounds", Polymers for Advanced Technologies, vol. 14, 3-11, 2003.

67. Fontaine G., Bourbigot S., Duquesne S., "Neutralized Flame Retardant Phosphorus Agent: Facile Synthesis, Reaction to Fire in PP and Synergy with Zinc Borate", Polymer Degradation and Stability, vol. 93, 68-76, 2008.

68. Li Y., Li B., Dai J., Jia H., Gao S., "Synergistic Effects of Lanthanum Oxide on A Novel Intumescent Flame Retardant Polypropylene System", Polymer Degradation and Stability, vol. 93, 9-16, 2008.

69. Wu Z., Shu W., Hu Y., "Synergist Flame Retarding Effect of Ultrafine Zinc Borate on LDPE/IFR System", Journal of Appilied Polymer Science, vol 103, 3667- 3674, 2007.

70. Demir H., Arkış E., Balköse D., Ülkü S., "Synergistic Effect of Natural Zeolites on Flame Retardant Additives", Polymer Degredation and Stability, vol. 89, 478- 483, 2005.

71. Li Q., Jiang P., Wei P., "Studies on the Properties of Polypropylene with A New Silicon-Containing Intumescent Flame Retardant", Journal of Polymer Science: Part B: Polymer Physics, vol. 43, 2548-2556, 2005.

72. Tang Y., Hu Y., Li B., Liu L., Wang Z., Chen Z., Fan W., "Polypropylene/ Montmorillonite Nanocomposites and Intumescent, Flame-Retardant Montmorillonite Synergism in Polypropylene Nanocomposites", Journal of Polymer Science: Part A: Polymer Chemisty , vol. 42, 6163-6173, 2004.

73. Wilkie A. C., Morgan A. B., "Fire Retardancy of Polymeric Materials", CRC Press, New York, 2010.

74. Ishii T., Kokaku H., Nagai A., Nishita T., Kakimoto M., "Calcium Borate Flame Retardation System for Epoxy Molding Compounds", Polymer Engineering and Science, vol. 46, 799-806, 2006.

75. Wang Q., Li J., Winandy J.E., "Chemical Mechanism of Fire Retardance of Boric Acid on Wood", Wood Science Technology, vol. 38, 375-389, 2004.

76. Martin C., Hunt B. J., Ebdon J. R., Ronda J. C., Cadiz V., "Synthesis, crosslinking and Flame Retardance of Polymers of Boron-Containing Difunctional Strenic Monomers", Reactive & Functional Polymers, vol. 66, 1047-1054, 2006.

77. Gao J., Su X., Xia L., "Synthesis and Structure Characterization of Boron-Nitrogen Containing Phenol Formaldehyde Resin", International Journal of Polymeric Materials, vol. 54, 949–961, 2005.

78. Wang D-C., Chang G-W., Chen Y., “Preparation and Thermal Stability of Boron-Containing Phenolic Resin/Clay Nanocomposites”, Polymer Degradation and Stability, vol. 93, 125- 133, 2008.

79. Martin C., Ronda J. C., Cadiz V., “Boron-Containing Novolac Resins as Flame Retardant Materials”, Polymer Degradation and Stability, vol. 91, 747-754, 2006.

80. Seyyidoğlu S**.**, **“**Synthesis and Characterization of Novel Rare Earth Phosphates and Rietveld Structural Analysis of Rare Earth Orthoborates”, PhD Thesis, METU, 2009.

81. Hauf C., Yılmaz A., Kızılyallı M., Kniep R., “ Boronphosphates: Hydrothermal and Microwave-Asisted Synthesis of $Na_5[B_2P_3O_{13}]$”, Journal of solid State Chemistry, vol. 140, 154-156, 1998.

82. Baykal A., Kızılyallı M., Toprak M., Kniep R., “Hydrothermal and Microwave Synthesis of Boron Phosphate, BPO_4”, Turkish Journal of Chemistry, vol. 25, 425-432, 2001.

83. Kılınç M., “Production and Characterization of Boron Based Additives and The Effect of Flame Retardant Additives on PET Based Composites”, PhD Thesis, METU, 2009.

84. Le Bras M., Wilkie C.A., Bourbigout S., DuQuesne S., Jama J., “Fire Retardancy of Polymers: New Applications of Mineral Fillers”, RSC, Cambridge, 2005.

85. Wei P., Hao J., Du J., Han Z., Wang J., “An Investigation on Synergism of An Intumescent Flame Retardant Based on Silica and Alumina”, Journal of Fire Sciences, vol. 21, 17- 28, 2003.

86. Huang H., Tian M., Liu L., He Z., Chen Z., Zhang L., “ Effects of Silicon Additive as Synergists of Mg(OH)2 on the Flammability of Ethylene Acetate Copolymer”, Journal of Applied Polymer Science, vol. 99, 3203-3209, 2006.

87. Alexandre M., Dubois P., “Polymer-Laterred Silicate Nanocomposites: Preparation, Properties and uses of A New Class of Materials, Materials Science and Engineering, vol. 28, 1-63, 2000.

88. Mai Y-W., Yu Z-Z., “Polymer Nanocomposites”, Woodhead Publishing, Boca Ranton, 2006.

89. Mancini L. H., Esposito C. L., “Nanocomposites Preparation, Properties and Performance”, Nova science Publishers, New York, 2008.

90. Ajayan P. M., Schadler L. S., Braun P. V., “Nanocomposite Science and Technology”, Wiley-VCH, Weinheim, 2003.

91. Gupta R. K., Kennel E., Kim K-J., “Polymer Nanocomposites Handbook”, CRC Press, New York, 2008.

92. Kiliaris P., Papaspyrides C.D., “Polymer/Layered Silicate (Clay) Nanocomposites: An Overview of Flame Retardancy”, Progress in Polymer Science, vol. 35, 902- 958, 2010.

93. Kornmann X., “Synthesis and Characterization of Thermoset-Clay Nanocomposites”, Licenciate Thesis, Luleå University of Technology, Sweden 2000.

94. Vaia R. A., Jendt K. D., Kramer E. J., Giannelis E. P., “Kinetics of Polymer Melt Intercalation”, Macromolecules, vol. 28, 8080- 8085, 1995.

95. Braggs Law and Diffraction, http://www.eserc. stonybrook.edu/ProjectJava/Bragg/, last accessed on 05/05/2011.

96. Gilman J. W., “Flammability and Thermal Stability Studies of Polymer Layered Silicate (clay) nanocomposites”, Applied Clay Science, vol. 15, 31-49, 1999.

97. Zanetti M., Camino G., Reichert P., Mülhaupt R., “Thermal Behavior of Poly(propylene) Layered Silicate Nanocomposites”, Macromolecular Rapid Communicaitons, vol. 22, 176-180, 2001.

98. Gilman J.W., Jackson C.L., Morgan A. B., Harris R., Manias E., Giannelis E.P., Wuthenow M., Hilton D., Philips S.H., “Flammability Properties of Polymer-Layered-Silicate Nanocomposites. Polypropylene and Polystyrene Nanocomposites”, Chemical Materials, vol. 12, 1866-1873, 2000.

99. Qin H., Zhang S., Zhao C., Hu G., Yang M., “Flame retardant Mechanism of Polymer/ Clay Nanocomposites Based on Polypropylene”, Polymer, vol. 46, 8386-8395, 2005.

100. Hu Y., Wang S., Ling Z., Zhuang Y., Chen Z., Fan W., “Preparation and Combustion Properties of Flame Retardant Nylon 6/Montmorillonite Nanocomposite”, Macromolecular Materials Engineering, vol. 288, 272-276, 2003.

101. Samyn F., Bourbigot S., Jama C., Bellayer S., “Fire Retardancy of Polymer Clay Nanocomposites. Is There An Influence of the nanomorphology?”, Polymer Degradation and Stability, vol. 93, 2019-2024, 2008.

102. Bourbigot S., Duquesne S., Jama C., “Polymer Nanocomposites: How to Reach Low Flammability”, Macromolecular Symposia, vol. 233, 180-190, 2006.

103. Kashiwagi T., Harris R. H., Zhang X., Briber R. M., Ciprino B. H., Raghavan S. R., Awad W. H., Shields J. R., “Flame Retardant Mechanism of Polyamide 6-Clay Nanocomposites”, Polymer, vol. 45, 881-891, 2004.

104. Jang B. N., Wilkie C. A., “The Effect of Clay on the Thermal Degradation of Polyamide-6 in Polyamide 6/Clay Nanocomposites”, Polymer, vol. 46, 3264-3274, 2005.

105. Morgan A. B., “Flame Retarded Polymer Layerred Silicate Nanocomposites: A Review of Commercial and Open Literature Systems”, Polymers for Advanced Technologies, vol. 17, 206-217, 2006.

106. Schartel B., Bartholmai M., Knoll U., “Some Comments on the main Fire retardancy Mechanisms in Polymer Nanocomposites”, Polymers for Advanced Technologies, vol. 17, 772-777, 2006.

107. Vaia R.A., Price G., Ruth P.N., Nguyen H.T., Lichtenhan J., “Polymer Layered Silicate Nanocomposites as High Performance Ablative Materials”, Applied Clay Science, vol. 15, 67-92, 1999.

108. Bellucci F., Camino G., Frache A., Sarra A., “Catalytic Charring–Volatilization Competition in Organoclay Nanocomposites”, Polymer Degradation and Stability, vol. 92, 425-436, 2007.

109. Song R., Wang Z., Meng X., Zhang B., Tang T., “Influences of Catalysis and Dispersion of Organically Modified Montmorillonite on Flame Retardancy of Polypropylene Nanocomposites”, Journal of Applied Polymer Science, vol. 106, 3488-3494, 2007.

110. Vaccari A., “Clays and Catalysis: A Promising Future”, Applied Clay Science, vol. 14, 161-198, 1999.

111. Jang B. N., Costache M., Wilkie C. A., “The Relationship between Thermal Degradation Behavior of Polymer and The Fire Retardancy of Polymer/Clay Nanocomposites”, Polymer, vol. 46, 10678-10687, 2005.

.

112. Van Krevelen D. W., “Some Basic Aspects of Flame Resistance of Polymeric Materials”, Polymer, vol. 16, 615-620, 1979.

113. Si M., Zaitsev V., Goldman M., Frenkel A., Peiffer D. G., Weil E., “Self-Extinguishing Polymer/Organoclay Nanocomposites”, Polymer Degradation and Stability, vol. 92, 86-93, 2007.

114. Zhang J., Lewin M., Pearce E., Zammarano M., Gilman J.W., “Flame Retarding Polyamide-6 with Melamine Cyanurate and Layered Silicates”, Polymers Advanced Technologies, vol. 19, 928-936, 2008.

115. Ma Z.L., Zhang W. Y., Liu X. Y., “Using PA6 as A Charring Agent in Intumescent Polypropylene Formulations Based on Carboxylated Polypropylene Compatibilizer and Nano-Montmorillonite Synergistic Agent”, Journal of Applied Polymer Science, vol. 101, 739-746, 2006.

116 Tang Y., Hu Y., Wang S., Gui Z., Chen Z., Fan W., “Intumescent Flame Retardant–Montmorillonite Synergism in Polypropylene-Layered Silicate Nanocomposites”, Polymer International, vol. 52, 1396–1400, 2003.

117. Shanmuganathan K., Deodhar S., Dembsey N., Fan Q., Calvert P.D., Warner S.B., “Flame Retardancy and Char Microstructure of Nylon-6/Layered Silicate Nanocomposites”, Journal of Applied Polymer Science, vol. 104, 1540-1550, 2007.

118. Leszczynska A., Njuguna J., Pielichowski K., Banerjee J.R., "Polymer / Montmorillonite Nanocomposites with Improved Thermal Properties. Part I. Factors Influencing Thermal Stability and Mechanisms of Thermal Stability Improvement", Thermochimica Acta, vol.453, 75–96, 2007.

119. Leszczynska A., Njuguna J., Pielichowski K., Banerjee J.R., "Polymer/ Montmorillonite Nanocomposites with Improved Thermal Properties. Part II. Thermal Stability of Montmorillonite Nanocomposites Based on Different Polymeric Matrixes", Thermochimica Acta, vol. 454, 1-22, 2007.

120. Zanetti M., Bracco P., Costa L., "Thermal Degradation Behavior of PE/Clay Nanocomposites", Polymer Degradation and Stability, vol. 85, 657-665, 2004.

121 Gilman J.W., Harris R.H., Shields J.R., Kashiwagi T., Morgan A.B., "A Study of the Flammability Reduction Mechanism of Polystyrene-Layered Silicate Nanocomposite: Layered Silicate Reinforced Carbonaceous Char", Polymers for Advanced Technologies, vol. 17, 263-271, 2006.

122. Lewin M., "Some Comments on the Modes of Action of Nanocomposites in the Flame Retardancy of Polymers" Fire Materials, vol. 27, 1–7, 2003.

123. Lewin M., "Reflections on Migration of Clay and Structural Changes in Nanocomposites", Polymers for Advanced Technologies, vol. 17, 758–763, 2006.

124. Vaia R.A., Ishii H., Giannelis E.P., "Synthesis and Properties of Two Dimensional Nanostructures by Direct Intercalation of Polymer Melts in Layered Silicates", Chemical Materials, vol. 5, 1694-1696, 1993.

125. Zong R.,HuY., Liu N., Li S., Liao G., “Investigation of Thermal Degradation and Flammability of Polyamide-6 and Polyamide-6 Nanocomposites”, Journal of Applied Polymer Science, vol. 104, 2297-2303, 2007.

126. Zanetti M., Luigi Costa L., “Preparation and Combustion Behaviour of Polymer/Layered Silicate Nanocomposites Based upon PE and EVA”, Polymer, vol. 45, 4367–4373, 2004.

127. Zheng X., Wilkie C.A., “Flame Retardancy of Polystyrene Nanocomposites Based on An Oligomeric Organically-Modified Clay Containing Phosphate”, Polymer Degradation and Stability, vol. 81, 539-550, 2003.

128. Mlynarcikova Z., Kaempfer D., Thomann R., Mülhaupt R., Borsig E., Marcincin A., “Syndiotactic Poly(propylene)/Organoclay Nanocomposite Fibers: Influence of the Nano-Filler and the Compatibilizer on the Fiber properties”, Polymers for Advanced Technologies, vol. 16, 362-369, 2005.

129. Horrocks A. R., Kandola B. K., Smart G., Zhang S., Hull T. R., “Polypropylene Fibers Containing Dispersed Clays Having Processing Parameters and Fiber Properties”, Journal of applied Polymer Science, vol. 106, 1707-1717, 2007.

130. Erdem N., Cireli A. A., Erdogan U. H., “Flame Retardancy Behaviors and Structural properties of Polypropylene/Nano-SiO2 Composite Textile Filaments”, Journal of Applied Polymer Science, vol. 111, 2085-2091, 2009.

131. Smart G., Kandola B. K., Horrocks A. R., Nazare S., Marney D., “Polypropylene Fibers Containing Dispersed Clays Having Improved Fire Performance. Part II: Characterization of Fibers and Fabrics from PP-Nanoclay Blends”, vol. 19, 658-670, 2008.

132. Shanmuganathan K., Deodhar S., Dembsey N.A.,Fan Q., Patra P.K., “Condensed-Phase Flame Retardation in Nylon 6- Layered Silicate Nanocomposites: Films, Fibers, and Fabrics”, Polymer Engineering and Science, vol.48, 662-675, 2008.

133. Bourbigot S., Devaux E., Flambard X., “Flammability of Polyamide-6/Clay Hybrid Nanocomposite Textiles”, Polymer Degradation and Stability, vol. 75, 397-402, 2002.

134. Rault F., Campagne C., Rochery M., Giraud S., Devaux E., “Polypropylene multifilament Yarn Filled with Clay and/or graphite: Study of a Potential Synergy”, Journal of Polymer Science Part B: Polymer Physics, vol. 48, 1185-1195, 2010.

135. Rault F., Pleyber E., Campagne C., Rochery M., Giraud S., Bourbigot S., Devaux E., “Effect of Manganese Nanoparticles on the Mechanical, Thermal and Fire Properties of Polypropylene Multifilament Yarn”, Polymer Degradation and Stability, vol. 94, 955-964, 2009.

136. Pavlikova S., Thomann R., Reichert P., Mülhaupt R., Marcincin A., Borsig E., “Fiber Spinning from Poly(propylene)-Organoclay Nanocomposite”, Journal of Applied Polymer Science, vol. 89, 604-611, 2003.

137. Ergungor Z., Cakmak M., Batur C., “Effect of Processing Consitions on the Development of Morphology in Clay Nanoparticle Filled Nylon 6 Fibers”, Macromolecular Symposia, vol. 185, 259-276, 2002.

138. UL-94-Test for Flammability of Plastic Materials for Parts in Devices and Appliances, Northbrook, IL: Underwriters Laboroties Inc., 1997.

139. Laoutid F., Bonnaud L., Alexandre M., Lopez-Cuesta J.M., Dubois Ph., "New Prospects in Flame Retardant Polymer Materials: From Fundementals to Nanocomposites", Materials Science and Engineering R: Reports", vol.63, 100-125, 2009.

140. Shah V., "Handbook of Plastics Testing Technology", John Wiley & Sons, Inc., New York, 1998.

141. Scheirs J., "Compositional and Failure Analysis of Polymers", John Wiley & Sons, Inc., New York, 2000.

142. Schartel B., Bartholmai M., Knoll U., "Some Comments on the Use of Cone Calorimeter Data", Polymer Degradation and Stability, vol. 88, 540-547, 2005.

143. Schartel B., Hull T.R., "Development of Fire-Retarded Materials – Interpretation of Cone Calorimeter Data", Fire and Materials, vol. 31, 327-354, 2007.

144. Lyon R.E., Walters R.N., "Pyrolysis combustion flow calorimetry", Journal of. Analytical. Applied. Pyrolysis, vol. 71, 27-46, 2004.

145. Schartel B., Pawlowski, K. H.; Lyon, R. E., "Pyrolysis combustion flow calorimeter: A tool to assess flame retarded PC/ABS materials?", Thermochimica Acta, vol. 462, 1-14, 2007.

146. Morgan A.B., Galaska M., "Microcombustion calorimetry as a tool for screening flame retardancy in epoxy", Polymers for Advanced Technologies, vol. 19, 530-546, 2008.

147. Yang C.Q., He Q., Lyon R.E:, Hu Y., “Investigation of the Flammability of Different Textile Fabrics Using Micro-scale Combustion Calorimetry”, vol. 95, 108-115, 2010.

148. Micro Combustion Calorimeter, http://www.govmark.com/flammability-fire-testing-instruments/mcc-2-micro scale -combustion-calorimeter.php, last accessed on 05/05/2011

149. Warner S.B., “Fiber Science”, Prentice Hall, New Jersey, 1995

150. Mark H.F., Atlas S.M., Cernia E., “Man-made Fibers Science and Technology”, vol.1, Interscience Publishers, New York, 1967.

151. Salem D.R., “Structure Formation in Polymeric Fibers”, Hanser Publishers, Munich, 2000.

152. Annual Book of ASTM Standards, ASTM D 3822-01: Standard Test Method for Tensile Properties of Single Textile Fibers, 07.01, Philadelphia, 2001.

153. Giles H.F., Wagner J.R., Mount E.M., “Extrusion The Definitive Processing Guide and Handbook”, William Andrew Publishing, New York, 2005.

154. Strong A.B., “Plastics Materials and Processing”, Prentice Hall, New Jersey, 2006

155. Nakajima T., “Advanced Fiber Spinning Technology”, Woodhead Publishing Limited, Cambridge, 2000.

156. Cook J.G., “Handbook of Textile Fibres”, Merrow Publishing, Herts, 1968.

157. Mark H.F., Atlas S.M., Cernia E., “Man-made Fibers Science and Technology”, vol.2, Interscience Publishers, New York, 1968.

158. Lewin M., “Handbook of Fiber Chemistry”, CRC Press, New York, 2006.

159. Mclntyre J.E., “Synthetic Fibres: Nylon, Polyester, Acrylic, Polyolefin”, Woodhead Publishing, CRC Press, 2005.

160. Seyyidoglu S., “High Temperature Chemistry of Some Borophosphates”, MS Thesis, METU, 2003.

161. Ambadas G., Packirisamy S., Ninan K.N., “Synthesis, Characterization and Thermal Properties of Boron and Silicon Containing Preceramic Oligomers”, Journal of Materials Science Letters, vol. 21, 1003-1005, 2002.

162. Özkoç G., “Abs/Polyamide-6 Blends, Their Short Glass Fiber Composites and Organoclay Based Nanocomposites: Processing and Characterization” PhD Thesis, METU, 2007.

163. Tayfun Ü., “Effects of Fillers on Morphological, Mechanical, Flow and Thermal Properties of Bituminous Composites”, MS Thesis, METU, 2006.

164. Dogan M., Yilmaz A., Bayramli E., “Synergistic Effect of Boron Containing Substances on Flame Retardancy and Thermal Stability of Intumescent System”, Polymer Degradation and Stability, vol. 95, 2584-2588, 2010.

165. Levchik S. V., Balabanovich A. I., Levchik G. F., Costa L., “Effect of melamine and its salts on combustion and thermal decomposition of polyamide 6”, Fire and Materials, vol. 21, 75- 83 , 1997.

166. Herrera M., Wilhelm M., Matuschek G., Kettrup A., "Thermoanalytical and pyrolysis studies of nitrogen containing polymers", Journal of Analytical and Applied Pyrolysis, vol. 58, 173- 188, 2001.

167. Nagasawa Y., Yamamoto M., Ozawa K., "Study of fire-retardant polymers using temperature jump/Fourier transform infrared spectroscopy", Thermochimica Acta, vol. 267, 223- 230, 1995.

168. Nagasawa Y., Hotta M., Ozawa K., "Fast thermolysis/FT-IR studies of fire-retardant melamine-cyanurate and melamine-cyanurate containing polymer", Journal of Analytical and Applied Pyrolysis, vol. 33, 253-267, 1995

169. Wang Y.L. Mebel A.M. Wu C. J., Chen Y. T., Lin C. E., Jiang J. C., "IR spectroscopy and theoretical vibrational calculation of the melamine molecule"**,** J. Chem. Soc. Faraday Trans, vol. 93, 3445- 3451, 1997.

170. Gijsman P., Steenbakkers R., Fürst C., Kerses J., "Differences in the flame retardant mechanism of melamine cyanurate in polyamide 6 and polyamide 66", Polymer Degradation and Stability, vol. 78, 219- 224, 2002.

171. Shimasaki C., Watanabe N., Fukushima K., Rengakuji S., Nakamura Y., Ono S., Yoshimura T., Morita H., Takakura M., Shiroishi A., "Effect of the fire-retardant, melamine, on the combustion and the thermal decomposition of polyamide-6, polypropylene and low-density polyethylene", Polymer Degradation and Stability, vol. 58, 171- 1997.

172. Herrera M., Matuschek G., Kettrup A., "Thermal Degradation Studies of Some Aliphatic Polyamides Using Hyphenated Techniques (TG-MS, TG-FTIR)", Journal of Thermal Analysis and Calorimetry, vol. 59, 385-394, 2000.

173. Isıtman N.A., Gunduz H.O., Kaynak C., “Halogen-free Flame retardants that Outperform Halogenated Counterparts in Glass Fiber Reinforced Polyamides”, Journal of Fire Sciences, vol. 28, 87-100, 2010.

174. Cho J.W., Paul D.R., “Nylon 6 nanocomposites by melt compounding”, Polymer vol.42, 1083-1094, 2001.

175. Bakirtzis D., Ramani A., Delichatsios M.A., Zhang J., “Structure of the condensed phase and char of the fire-retarded PBT nanocomposites by TGA/ATR in N_2”, Fire Safety J. vol. 44, 1023-1029, 2009.

176. Kim D. H., Fasulo P.D., Rodgers W. R., Paul D.R, “Structure and properties of polypropylene-based nanocomposites: Effect of PP-*g*-MA to organoclay ratio”, Polymer, vol. 48, 5308-5323, 2007.

177. Kim D.H., Fasulo P.D., Rodgers W.R., Paul D. R., “Effect of the ratio of maleated polypropylene to organoclay on the structure and properties of TPO-based nanocomposites. Part I: Morphology and mechanical properties”, Polymer, vol. 48, 5960-5978, 2007.

178. Perrin-Sazarin F., Ton That M.T., Bureau M.N, Denault J., “Micro- and nano-structure in polypropylene/clay nanocomposites”, Polymer, vol. 46, 2005,11624-11634.

179. Mosnacek J.,. Basfar A. A, Shukri T. M.,. Bahattab M. A, “Poly(ethylene vinyl acetate) (EVA)/ low density polyethylene (LDPE)/ammonium polyphosphate (APP) composites cross-linked by dicumyl peroxide for wire and cable applications”, Polymer Journal, vol. 40, 2008, 460-464.

180. Moffat J.B., Neeleman J.F., “Infrared spectroscopic studies of boron phosphate and adsorbed species: I. Effects of evacuation at elevated temperatures and the adsorption of water”, Journal of Catalysis, vol. 34, 1974, 376.

181. Zhang X., Yang M., Zhao Y., Zhao S., Dong X., Liu X., Wang D., Xu D.J., “Polypropylene/montmorillonite composites and their application in hybrid fiber preparation by melt-spinning”, Journal of Applied Polymer Science, vol. 92, 2004, 552.

182. Joshi M., Viswanatham V.J., “High-performance filaments from compatibilized polypropylene/clay nanocomposites”, Journal of Applied Polymer Science, vol. 102, 2006, 2164.

183. Kim K.J., Lee J.S., Prabu A.A., Kim T.H., “Preparation and characterization of nylon 6/Organoclay Nanocomposite Filament Fibers”, Polymer Composites, vol. 30, 2009, 265.

CURRICULUM VITAE

PERSONAL INFORMATION

Name & Surname: Mehmet Doğan

Nationality: Turkish

Date and Place of Birth: 01.02. 1979-Şarkışla

EDUCATION

Degree	**Institution**	**Year**
M.Sc.	METU, Polymer Science and Technology	2006
B.Sc.	Ege Unv., Textile Engineering	2001
High School	Kayseri Sümer Lisesi	1996

WORK EXPERIENCE

Place	**Position**	**Year**
METU, Dept. of Polym. Sci. Tech	Teaching Asistant	2003-2011
E.U, Dept. of Textile Eng.	Teaching Asistant	2001-2003

FOREIGN LANGUAGES

Advanced English

HONORS

2004 -2005 Academic year METU Graduate Courses Performance Award

PROJECTS

1) **M. Doğan,** S. Erdoğan, E. Bayramlı " Bor içeren güç tutuşur poliamid-6 ve polipropilen liflerin üretilmesi", Boren Ç0209-2009, Şubat 2009-Şubat 2011
2) **M. Doğan,** E. Bayramlı, " Tabii Kauçuk dolgu alma kabiliyetinin arttırılması", TOFAŞ Türk Otomobil A.Ş., ODTÜ Biltir Merkezi, Haziran 2008- Aralık 2009.
3) **M. Doğan,** E. Bayramlı, "Polipropilene güç tutuşurluk özelliği kazandırma", Arçelik A.Ş., ODAGEM Ostim Ortak Arş. Gel. Merkezi A.Ş., Temmuz 2010-Ocak 2011.

PUBLICATIONS

Books:

1. S. Kiralp, P. Camurlu, G Ozkoc, **M. Dogan,** T. Baydemir, S. Erdogan, "Plastikler", ODTU yayıncılık (2006).

Publications

1. **M. Dogan,** E. Bayramli, "Effect of polymer additives and process temperature on the physical properties of bitumen-based composites", Journal of Applied Polymer Science, 113, 2331-2338 (2009).
2. **M. Dogan,** E. Bayramli, "Effect of boron containing materials on the flammability and thermal degradation of polyamide-6 composites containing melamine", Journal of Applied Polymer Science, 118, 2722-2727 (2010).

3. **M. Dogan,** A. Yilmaz, E. Bayramli, “Synergistic effect of boron containing substances on flame retardancy and thermal stability of intumescent polypropylene composites”, Polymer Degradation and Stability, 95, 2584-2588 (2010).

4. **M. Dogan,** E. Bayramli, “Synergistic effect of boron containing substances on flame retardancy and thermal stability of clay containing intumescent polypropylene nanoclay composites”, Polymers for Advanced Technologies, (2010), DOI: 10. 1002/pat. 1650

5. **M. Dogan,** A. Yilmaz, E. Bayramli, “Effect of boron containing materials on flammability and thermal degradation of polyamide-6 composites containing melamine cyanurate, Polymers for Advanced Technologies, 22, 560-566 (2011).

6. **M. Dogan,** D.D. Oral, B. Yilmaz, M. Savu, S. Karahan, E. Bayramli, “Physical properties and cure characteristics of natural rubber/nanoclay composites with two different compatibilizers”, Journal of Applied Polymer Science, 121, 1530-1535 (2011).

7. N.A. Isıtman, **M. Dogan,** E. Bayramlı, C. Kaynak, “Fire retardant properties of intumescent polypropylene composites filled with calcium carbonate”, Polymer Engineering and Science, 51, 875-883 (2011)

Oral Presentations:

1. **M. Dogan**, U. Tayfun, E. Bayramli, 1. Ulusal Polimer Bilim ve Teknoloji Kongresi ve Sergisi, “Polimer katkılı bitüm bazlı kompozitlerin hazırlanması ve karakterizasyonu”, Ankara, Türkiye (2006)

Poster Presentations:

1. **M. Dogan,** E. Bayramli, PPS 24, “Effect of polymer additives on the physical properties of bitumen based composites”, Salerno, Italy (2008).

2. **M. Dogan,** E. Bayramli, U. Tayfun, PPS 24, “Effects of fillers on morphological, mechanical, flow and thermal properties of bituminous composites”, Salerno, Italy (2008)

3. **M. Doğan,** E. Bayramlı, EPF’09, “Effect of boron containing substances on flammability and thermal degradation of flame retarded polyamide-6 composites containing melamine cyanurate”, Graz, Austria (2009)

4. **M. Doğan,** E. Bayramlı, 3. Ulusal Polimer Bilim ve Teknoloji Kongresi ve Sergisi, “Polipropilen Kompozitlerde Nano-kil ve Borlu bileşiklerin güç tutuşurluk ve termal stabilite üzerine sinerjik etkileri”, Kocaeli, Türkiye (2010)

5. **M. Doğan,** E. Bayramlı, 24. Ulusal Kimya Kongresi, “Kırmızı Fosfor İçeren Poliamid-6 Kompozitlerinde Borlu Bileşiklerin Güç Tutuşurluk ve Termal Stabilite Üzerine Sinerjik Etkileri”, Zonguldak, Türkiye (2010)

6. **M. Dogan,** E. Bayramlı, PPS-26 İstanbul regional meeting, “Synergistic Effect of boron containing substances on flame retardancy and thermal stability of intumescent polypropylene composites”, Istanbul, Turkey (2010).